LIVER REGENERATION BY SMALL HEPATOCYTE-LIKE PROGENITOR CELLS AFTER HEPATOTOXIC AND NECROTIC INJURY IN FISCHER 344 RATS

Daniel Hunter Best

A dissertation submitted to the faculty of the University of North Carolina at Chapel Hill in partial fulfillment of the requirements for the degree of Doctor of Philosophy in the Department of Pathology.

Chapel Hill
2007

Approved by:

William B. Coleman, Ph.D.

C. Robert Bagnell, Ph.D.

Frank C. Church, Ph.D.

David A. Gerber, M.D.

Gregory J. Tsongalis, Ph.D.

ABSTRACT

Daniel Hunter Best: Liver Regeneration by Small Hepatocyte-like Progenitor Cells After Hepatotoxic and Necrotic Injury in Fischer 344 Rats
(Under the direction of William B. Coleman)

Liver regeneration after surgical partial hepatectomy (PH) in animals exposed to the mito-inhibitory agent retrorsine is completed through the outgrowth and expansion of small hepatocyte-like progenitor cells (SHPCs). Although the SHPC-mediated regenerative response has been well characterized in the retrorsine/PH model of liver injury, the role that these cells play in other forms of liver injury has not been investigated. The experimental objectives of the current studies were: (i) to characterize SHPC responses in hepatotoxic and necrotic models of liver injury, (ii) to determine the progenitor cell of origin of SHPCs, and (iii) to identify factors involved in the activation of SHPCs after liver injury. SHPCs are not observed after PH in retrorsine-exposed rats treated with the mito-inhibitory agent 2-acetamidofluorene, but are observed after PH in retrorsine-exposed rats treated with the biliary toxin 4,4'-diaminodiphenylmethane. Together, these observations suggest strongly that oval cells do not represent progenitor cells of SHPCs, but that SHPCs represent another liver progenitor cell population that resides in the hepatic parenchyma and responds to certain forms of liver injury. In addition, these investigations found that SHPCs respond to restore liver mass and structure when retrorsine-exposed rats are treated with the pericentral necrotizing agent carbon tetrachloride. This observation shows that SHPCs are capable of regenerating liver damaged by surgical resection as well as chemically-induced necrotic

injury. Finally, these studies establish that treatment of retrorsine-exposed rats with the cytokine inhibitor dexamethasone blocks SHPC proliferation after PH and that this blockade can be overcome by administration of recombinant IL6 protein. These observations suggest that SHPCs are activated for proliferation in a cytokine-dependent manner similar to other regenerative cell populations in liver (mature hepatocytes, oval cells), and that IL6 may function as the master regulatory molecule for activation of progenitor cell responses after liver injury. Together, these investigations provide evidence that a hierarchy of cellular responses exists in the mammalian liver in which the form of regenerative response occurring after liver injury reflects (i) the type of liver injury, and (ii) the progenitor cell populations that are capable of proliferating.

ACKNOWLEDGEMENTS

First, I would like to thank my mentor Bill for providing a learning environment that encourages independence while simultaneously providing support and guidance. Without Bill's never-ending patience and willingness to answer even the most elementary of questions, I would have never completed my first year of graduate school, much less this dissertation.

I would also like to thank my mother and father for constantly providing support in my endeavors and always encouraging me to follow my dreams, regardless of how far-fetched or lofty they were.

Furthermore, I wish to acknowledge the members of my committee—Drs. David Gerber, Frank Church, Greg Tsongalis, and Robert Bagnell—for their cogent insight and advice regarding my project and this document. To Dr. Bagnell, the Director of the Microscopy Services Lab, I am especially grateful for his teaching me about the use of numerous tools that were absolutely essential for the completion of the work described in this dissertation.

I would also like to acknowledge Genelle Butz for teaching me how to perform not only surgical partial hepatectomies, but several other techniques that I performed on a daily basis throughout my graduate training. Additionally, I would like to thank all of the people that have made my time at UNC enjoyable: the Mack lab guys, the Church lab ladies, Josh, and all of the Biology 11L students that taught me as much as I ever taught them. Finally, I would like to thank Jen for always helping me to see the bright side of things. Your enduring

support and friendship have meant a great deal to me and it has been a privilege to work with you.

Most of all I would like to express my deepest gratitude to my best friend and wife, Julie. Without your constant support, encouragement, optimism, and love I would never have finished graduate school. Words can not express how deeply grateful I am to have you in my life. This dissertation is every bit as much your accomplishment as it is mine.

TABLE OF CONTENTS

LIST OF TABLES

LIST OF FIGURES

LIST OF ABBREVIATIONS

2-AAF	2-acetamidofluorene
3’-Me-DAB	3’-methyl-4-dimethylaminobenze
AFP	alpha-fetoprotein
BrdU	5-bromo-2’-dexoyuridine
CCl_4	carbon tetrachloride
ck19	cytokeratin 19
CYP450	cytochrome P450
DAPM	4,4’-diaminodiphenylmethane
DEN	diethylnitrosamine
DEX	dexamethasone
DIPIN	1,4-bis[N,N’-di(ethylene)-phosphamide]-piperazine
DMSO	dimethyl sulfoxide
DPPIV	dipeptidylpeptidase IV
EGF	epidermal growth factor
ELISA	enzyme-linked immunosorbent assay
F344	Fischer 344
GaIN	D-galactosamine
H&E	hematoxylin and eosin
HBsAg-tg	hepatitis B surface antigen transgenic
HGF	hepatocyte growth factor
HNF4	hepatocyte nuclear factor 4
IL6	interleukin-6

JAK	janus kinase
MAPK	mitogen-activated protein kinase
PA	pyrrolizidine alkaloid
PBS	phosphate buffered saline
PH	surgical partial hepatectomy
SHPC(s)	small hepatocyte-like progenitor cells
TGFα	transforming growth factor alpha
TGFβ	transforming growth factor beta
TNF-α	Tumor necrosis factor-alpha
TNFR-I	Tumor necrosis factor receptor-I

I. INTRODUCTION

THE BIOLOGY OF NORMAL LIVER

The mammalian liver is the largest visceral organ of the body, accounting for 2-5% of the body weight of adults (1) and is one of the most functionally diverse organ systems (2). The liver has several important functions that are essential for organismal homeostasis, including catabolic, metabolic, and absorptive functions (1, 2). For example, the liver is involved in the synthesis of body fat, amino acids, plasma proteins that aid in blood clotting (i.e. prothrombin, fibrinogen), growth factors that aid in development, and bile that plays a crucial role in intestinal digestion (2-4). Likewise, the liver is important for storage of several important vitamins and minerals (i.e. iron), as well as glycogen synthesis and gluconeogenesis (2, 3). Finally, the liver is important for detoxification of various substances, including drugs, alcohol, and ammonia (2, 3). Over 75% of the cellular mass of the normal liver is composed of mature (fully differentiated) hepatocytes and biliary epithelial cells, and these cells perform the majority of liver functions (1). In addition, the liver contains several other cell types, including sinusoidal endothelial cells and kupffer cells. Although these cells make up a relatively small percentage of the cellular mass of the liver, they are important in active transport of nutrients, regulation of blood pressure, waste removal, production of cytokines, and many other biological activities (1).

Structurally, the liver is organized into millions of functional units termed hepatic lobules (1, 3, 4). The hepatic lobule is roughly hexagonal in shape and is composed of hepatocytes arranged in plates that surround a central vein, with the portal vein, bile duct, and the hepatic artery grouped together as a triad and located at the corners of the hexagonal structure **(FIGURE 1.1)** (3). This structural arrangement facilitates interaction of hepatocytes with the blood as it moves through the liver. Nutrient-rich blood from the gastrointestinal tract enters the liver via the portal circulation. This blood mixes with oxygen-rich blood from the hepatic artery and then percolates through the sinusoids in direct contact with the hepatocyte cell surface. Intimate contact between the hepatocytes and blood is essential to the various absorptive, metabolic, protective, and synthetic functions of the liver (3).

NORMAL LIVER REGENERATION

Mature (fully differentiated) hepatocytes of the liver are metabolically active, but are mitotically quiescent, and only enter the cell cycle when liver function is impaired by hepatotoxic injury or tissue mass is lost to surgical resection (5). Still, the liver is an extremely resilient organ and possesses an enormous capability to regenerate tissue mass and functional capacity following liver injury (5-9). In an otherwise normal liver, loss of tissue mass results in the activation and proliferation of quiescent mature hepatocytes present in the remaining liver tissue, leading to restoration of liver mass and function (7). Liver regeneration after surgical partial hepatectomy (PH) has been extensively studied (10). In this model, approximately 67% (two-thirds) of the liver is surgically removed resulting in a strong priming stimulus for the residual hepatocytes (10). After injury, hepatocytes are primed for cell division through an increase in the levels of cytokines (namely IL6 and TNF-

FIGURE 1.1. *Structural features of the adult mammalian liver*. The adult mammalian liver is organized into lobules that are defined by the presence of a central vein (A,B) at the center and portal triads (C,D) in the periphery. Long black arrows indicate the central vein, long white arrows indicate the portal vein, short black arrows indicate the bile duct, and short white arrows indicate the hepatic artery. Original objective lens magnification 10x for panels (A,C) and 20x for panels (B,D).

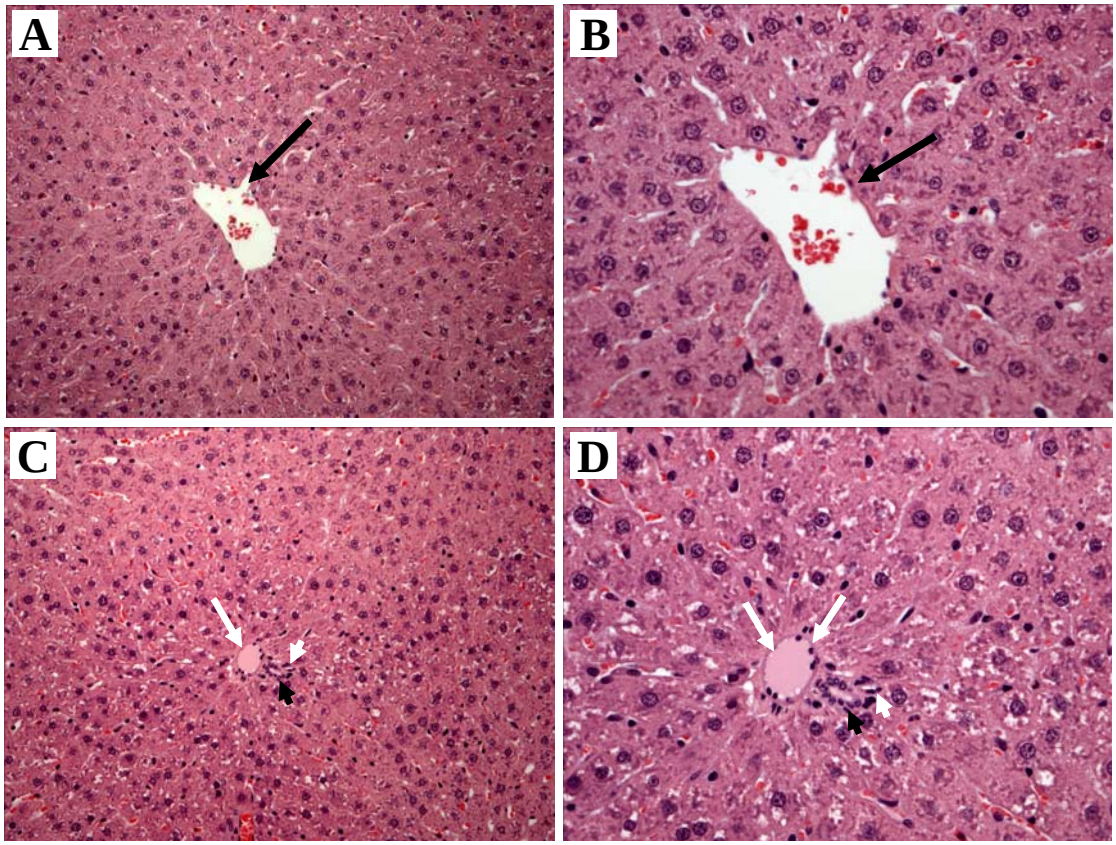
A
B
C
D

α) in the serum (9, 11-14). Once primed, these hepatocytes rapidly enter the cell cycle and restore the lost tissue mass over a period of approximately one week through multiple rounds of cell proliferation (5-9). The term regeneration, as it is commonly applied to liver, is a misnomer. The resected lobes of the liver are not replaced. Rather the residual liver tissue expands to restore the proper liver/body weight ratio through compensatory hyperplasia (6, 7, 9, 15). During this process the typical hepatocyte divides approximately 1.7 times (16). However, this is not the limit of hepatocyte replication potential as these cells are capable of dividing upwards of one hundred times (17). Thus, mature (fully differentiated) hepatocytes represent the primary response to liver deficit and secondary (reserve) progenitor cell populations (such as oval cells) do not respond when hepatocytes are capable of proliferating (18).

EXPERIMENTAL MODELS OF HEPATOCELLULAR INJURY

In several models of hepatocellular injury mature hepatocytes are incapable of proliferating due to exposure to mito-inhibitory agents such as 2-acetamidofluorene (2-AAF) **(FIGURE 1.2)** or retrorsine **(FIGURE 1.3)**. Under these circumstances, the liver is regenerated through the outgrowth and expansion of reserve (stem-like) progenitor cell populations, such as oval cells or small hepatocyte-like progenitor cells (SHPCs) (19). In order for these reserve progenitor cell populations to be activated two important criteria must be met: (i) injury to liver that results in a growth stimulus, and (ii) blockade of mature hepatocyte proliferation (20).

Over the last 50 years several experimental models have been developed to study the cellular responses of the adult mammalian liver to various forms of injury (20). These

FIGURE 1.2. *The chemical structure 2-AAF*. 2-AAF (N-hydroxy-2-acetamidofluorene, CAS #53-95-2) is a DNA alkylating agent with mito-inhibitory effects on mature hepatocytes.

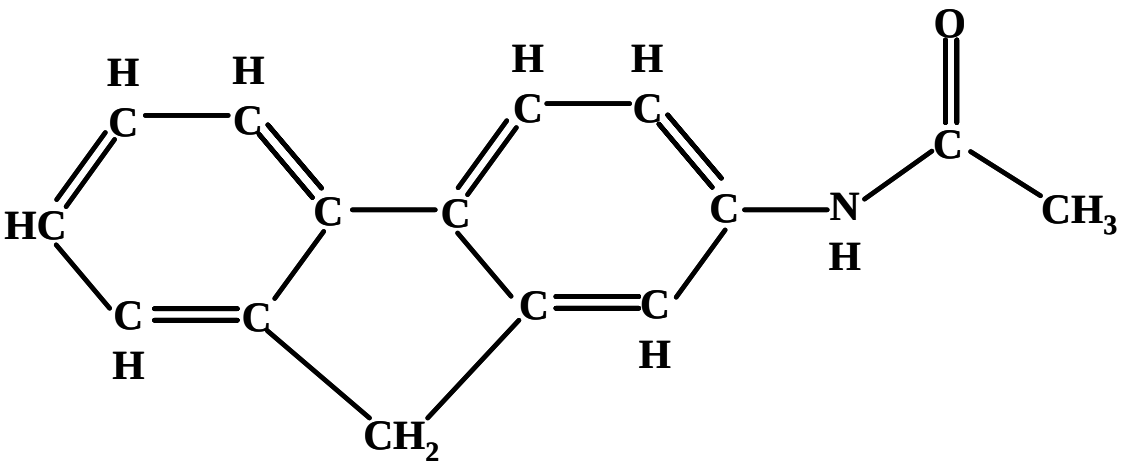

2-AAF

FIGURE 1.3. *The chemical structure of retrorsine.* Retrorsine (12, 18-dihydroxysenecionan – 11, 16-dione; β-Longilobine, CAS #480-54-6) is a naturally occurring pyrrolizine alkaloid.

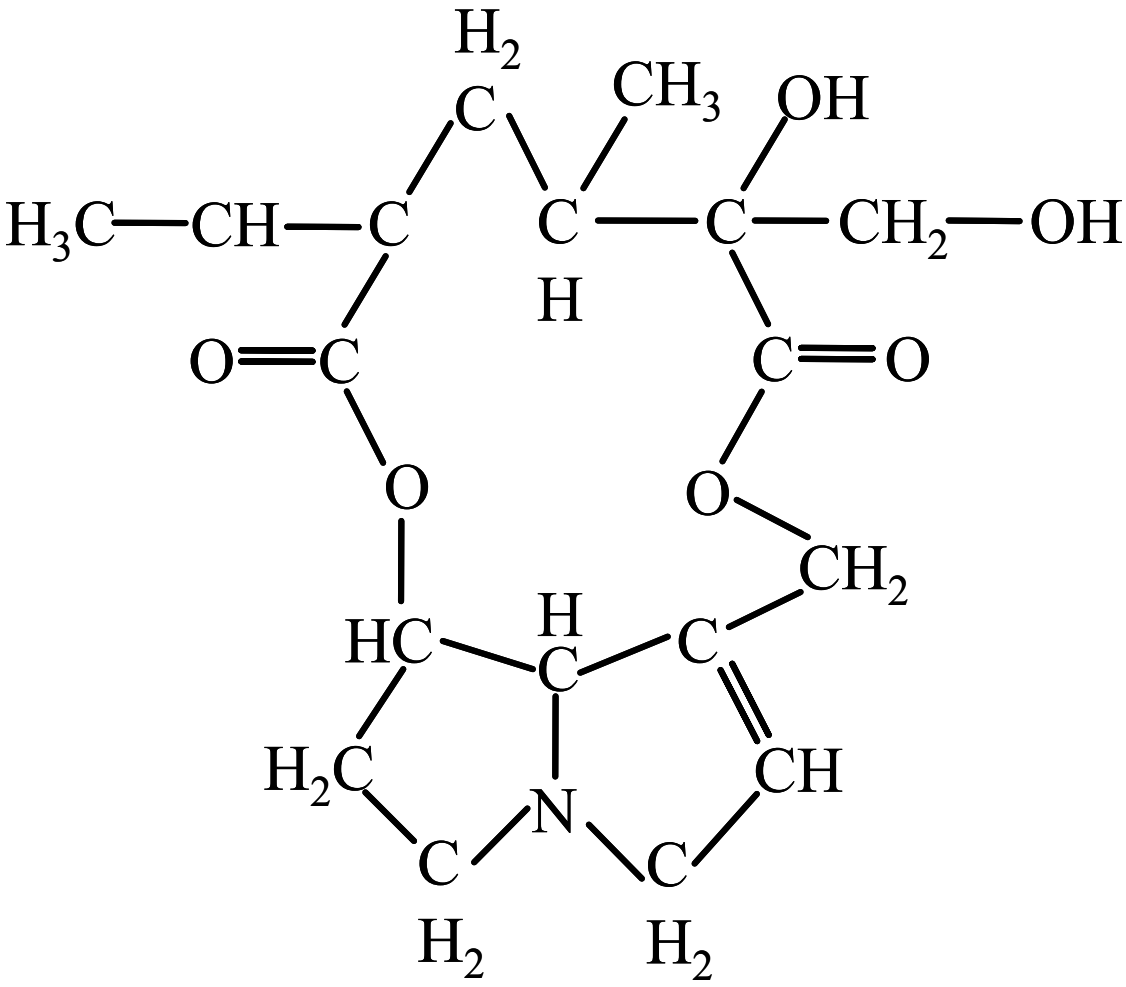

Retrorsine

models include both carcinogenic (such as 2-AAF, DIPIN) and non-carcinogenic (such as galactosamine) mechanisms of injury and many are known to elicit responses from specific liver progenitor cell populations (15, 19, 21). This introduction will focus on injury models that result in the activation of reserve progenitor cells (i.e. oval cells, SHPCs).

The Azo-dye Model of Hepatocellular Injury

The azo-dye model of liver injury was first introduced by Inaoka *et al.* in 1967 (22) and has been primarily used as a model to study oval cell mediated response to injury and hepatocarcinogenesis (20, 23). In this model rats are fed a diet containing the carcinogenic azo-dye 3'-methyl-4-dimethylaminoazobenzene (3'-Me-DAB). Treatment with this toxin results in DNA adduct formation in the mature hepatocytes of rat liver (24, 25). These adducts impair DNA replication and cell division by mature hepatocytes, preventing these cells from contributing to liver repair in any significant manner (22, 23). As a result, oval cells are observed shortly after the onset of carcinogenesis in this model (23). Oval cells appear approximately 1 week following treatment with 3'-Me-DAB, proliferate for a period of weeks, and ultimately replace the damaged hepatocytes and restore liver structure 10 weeks after the initial treatment (20, 23).

The Choline-deficient Diet Model of Hepatocellular Injury

The choline-deficient diet has been used for quite some time to induce a strong oval cell proliferative response (26). In the basic version of this model animals are fed a choline deficient diet supplemented with 0.05-0.1% (in rats) or 0.15% (in mice) ethionine for 2-3 weeks (21, 26, 27). This treatment results in fatty infiltration (steatosis), cell necrosis, and marked oval cell proliferation (26). Oval cells are observed in large numbers approximately

4 weeks after initiation of choline-deficient diet with a return to the normal structure of the liver around 10 weeks post-initiation (26). However, additional studies have been performed using a modified version of this model whereby animals are fed the choline-deficient diet that also contains the mito-inhibitory agent 2-AAF (28, 29). In this model oval cells are observed within a few days after the onset of the experimental period and restore the structure of liver in a more rapid fashion than that observed in animals treated with a choline-deficient diet in the absence of 2-AAF (20, 26, 28, 29).

The (Modified) Solt-Farber Model of Hepatocellular Injury

The original Solt-Farber model of liver injury was used to study the early stages of chemical carcinogenesis by combining an initiating agent [diethylnitrosamine (DEN)], with a hepatocyte growth inhibiting agent (such as 2-AAF), followed by growth stimulus (such as surgical PH) (30). This model was later modified to exclude the initiating agent in order to study the contributions of various cell types to liver regeneration (31). The modified Solt-Farber model (also known as the 2-AAF model of liver injury) has since become one of the most commonly studied models of hepatocellular injury. In this model hepatocyte proliferation is blocked by 2-AAF treatment for 7 days (31, 32). Following this treatment period cell division is stimulated through surgical PH, followed by 4 additional days of 2-AAF treatment (31, 32). Hepatocytes do not divide in this model as 2-AAF treatment results in DNA adduct formation that prevents proper cell division (33). Instead, mature hepatocytes either undergo apoptosis or remain in a growth arrested state in the liver parenchyma (34). Liver injury in animals treated with 2-AAF results in massive oval cell proliferation that begins within 2-3 days following PH, peaks about one week later, and restores liver mass and structure by 16-days post-PH (20, 31, 32). It is important to note that

it was through the use of the modified Solt-Farber model of liver injury in combination with BrdU administration that investigators were able to directly demonstrate that a precursor-product relationship exists among oval cells and hepatocytes (31, 35, 36).

The D-galactosamine Model of Hepatocellular Injury

D-galactosamine (GaIN) is a non-carcinogenic agent capable of causing substantial necrosis of the liver parenchyma and specifically targets mature hepatocytes (37, 38). In this model, animals are given a single injection of GaIN that results in massive necrosis of the liver parenchyma and delayed onset of proliferation in surviving mature hepatocytes (37, 38). As a result of delayed hepatocyte proliferation, oval cells proliferate in large numbers in this model. These cells appear approximately 24 hours after GaIN administration and continue to proliferate even after residual basophilic hepatocytes begin to proliferate (around 72 hours after GaIN administration) until liver structure is restored around 10 days after GaIN treatment (20, 37, 38). However, in addition to the proliferation of mature (basophilic) hepatocytes and oval cells, a third cell population of phenotypically 'small' hepatocytes are observed in the livers of GaIN-treated animals. These cells are observed approximately 5 days after GaIN administration and eventually differentiate into mature hepatocytes (37). It is likely that these cells represent an intermediate cell type representing the differentiating progeny of oval cells as they transition into mature hepatocytes. However, it is possible that these small hepatocytes are a distinct progenitor cell population, similar or identical to the SHPCs observed in the regenerating liver of retrorsine-exposed rats (39).

The DIPIN Model of Hepatocellular Injury

DIPIN (1,4-bis[N,N'-di(ethylene)-phosphamide]-piperazine) is an alkylating agent that results in the irreversible crosslink of DNA in mature hepatocytes of the mouse liver (40). In this model of liver injury, animals are treated with a single dose of DIPIN combined with surgical partial hepatectomy (40). Mature hepatocytes are damaged by DIPIN resulting in necrosis and apoptosis, and liver mass is restored through the outgrowth and expansion of oval cells (20, 40). Oval cells appear in the livers of these animals approximately 1 week after PH and continue proliferating for the weeks following (20, 40). In this model the replacement of the damaged liver parenchyma is not completed until greater than 4 months after the initial injury (20, 40).

The Retrorsine Model of Hepatocellular Injury

Retrorsine is a mito-inhibitory pyrrolizidine alkaloid that is damaging to mature hepatocytes (39, 41, 42). In this model, animals are treated with two doses of retrorsine and then subsequently subjected to surgical PH (39). When retrorsine-exposed hepatocytes are stimulated to proliferate they become megalocytes and subsequently undergo apoptosis (39, 41, 43, 44). Oval cells are never observed in this model and mature hepatocytes are incapable of dividing (39). As a result, the liver mass of retrorsine-exposed rats is regenerated through the outgrowth and expansion of SHPCs (39). These cells emerge as small clusters 1-3 days after PH, proliferate to lobule size by 14-days post-PH, and differentiate into mature hepatocytes by 30-days post-PH resulting in normalization of liver mass and structure (39).

PROGENITOR CELLS IN LIVER REGENERATION

In the past, the presence of a stem cell population in the adult liver has been the topic of debate. The controversy surrounding liver stem cells was largely due to the lack of cellular turnover in the liver like that observed in other organs that are known to contain a classic stem-cell-fed lineage system (i.e. colon, bone marrow) (45-47). The presence of a liver stem cell was further questioned because mature hepatocytes are capable of restoring lost tissue mass after surgical resection or injury, making an undifferentiated progenitor cell appear unnecessary. However, mounting evidence over the past several years has led to the acceptance of the presence of cell population(s) with stem-like properties in the livers of adult rodents (48). These cells include (i) propagable multipotential stem-like cells (such as WB-F344, RLE-13, and others derived from liver epithelial cells) capable of differentiating into cells of both hepatic and extrahepatic tissues (20), (ii) bipotential stem-like cells (such as oval cells) capable of differentiating into mature hepatocytes and biliary epithelia (6, 15), and (iii) unipotential stem-like cells (such as SHPCs) capable of differentiating into mature hepatocytes (48).

Oval Cells

Oval cells, so called because histologically these cells appear with a large ovoid nuclei **(FIGURE 1.4)**, were first identified in animals exposed to carcinogenic azo-dyes (22), but have since been observed in animals treated with the mito-inhibitory agent 2-AAF (28, 49), D-galactosamine (37), fed a choline-deficient diet (26), treated with DIPIN (40), and have been observed in animals exposed to the necrotic agents allyl alcohol and carbon tetrachloride **(FIGURE 1.5)** in combination with other toxins (50). Although there is some degree of variation among the oval cell responses observed in these models of liver injury, the general course of events in oval cell mediated liver regeneration is the same. Shortly

FIGURE 1.4. *Oval cells, small hepatocyte-like progenitor cells, and hepatic megalocytes.* (A,B,C) Oval cells (indicated with white arrows) appear histologically with scant cytoplasm and large ovoid nuclei. (D,E) Small hepatocyte-like progenitor cells (indicated by long black arrows) are histologically similar to mature hepatocytes but are much smaller. (F) SHPCs are easily identified due to their contrasting size with the surround hepatocyte megalocytes (giant cells, indicated by short black arrows). Original objective lens magnification: 10x (A,D), 20x (B,E,F), and 40x (C).

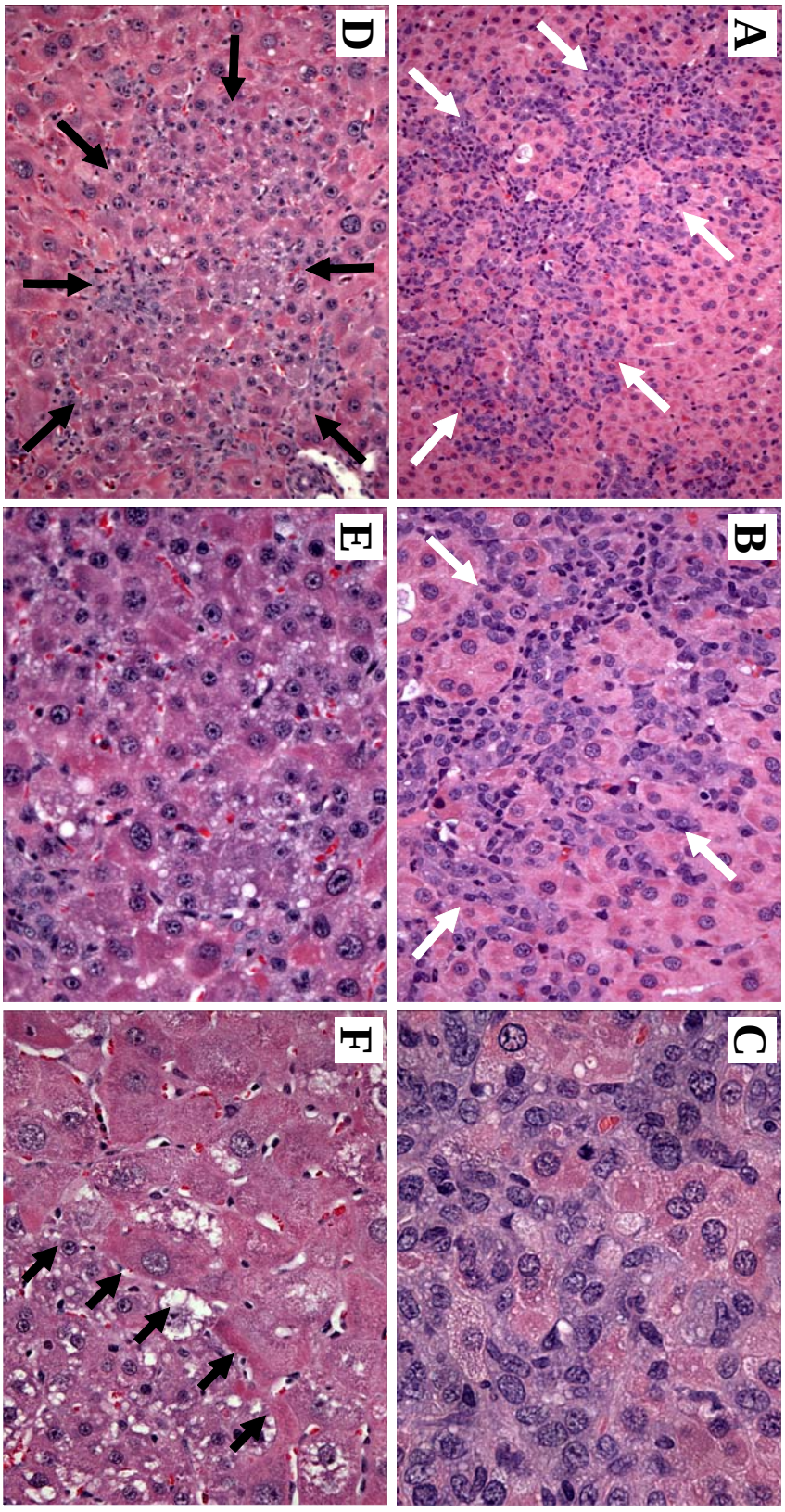
D
A
E
B
F
C

FIGURE 1.5. *The chemical structure of carbon tetrachloride.* Carbon tetrachloride (CCl_4, CAS #56-23-5) is a liquid compound that is highly toxic to several mammalian tissues including liver where it causes the targeted necrosis of the centrilobular zone of the parenchyma.

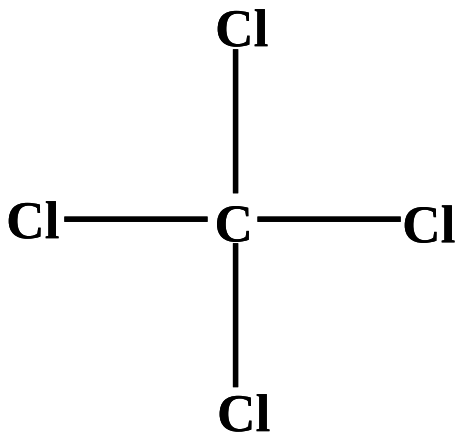

Carbon Tetrachloride

after liver injury oval cells are primed for proliferation through an increase in serum cytokine (IL6, TNF-α) levels, emerge from the periportal regions of the liver parenchyma, and expand into the centrilobular parenchyma (15, 21, 51-53). After several days of continued proliferation these cells begin to differentiate into immature hepatocytes that ultimately mature and replace the damaged parenchyma (15). This process has been most extensively studied in animals treated with 2-AAF. Several investigators performed elegant studies characterizing the time course for liver regeneration after PH in 2-AAF-treated rats (28, 31, 35, 54-57) and many of these studies demonstrated that a precursor/product relationship exists among oval cells and hepatocytes in animals treated with 2-AAF (31, 35). Using the 2-AAF model investigators have phenotypically characterized oval cells over the course of regeneration. When oval cells first appear they are positive for various cytokeratins (i.e. cytokeratin 19) (21) and α-fetoprotein (AFP) (58, 59), a known marker for less differentiated cell types as well as additional markers of biliary cells (connexin 43 and α6 integrin) (56). However, when these cells differentiate into immature hepatocytes they stop expressing these markers and initiate expression of hepatocyte specific markers (α1 integrin, connexin 32, HNF4) (56). The tissue niche of the progenitors of oval cells has long been suggested to reside in the portal triad in close association with the biliary epithelium. Recently, a group of investigators demonstrated that the destruction of bile ducts with the toxin 4,4'-diaminodiphenylmethane **(FIGURE 1.6)** results in a complete blockade of oval cell proliferation (60). This observation forms the basis for the conclusion that oval cells originate in the bile ducts (perhaps from a biliary epithelial cell population?) of the liver.

Small Hepatocyte-like Progenitor Cells

Small hepatocyte-like progenitor cells, named for their histological appearance **(FIGURE 1.4)**, have only been observed after liver injury in animals that have been exposed to the pyrrolizidine alkaloid retrorsine (39, 61, 62). Retrorsine is a naturally occurring mito-inhibitory agent that results in a long-lasting DNA crosslinks in the hepatocytes of the mammalian liver (39, 41). As a result of these crosslinks mature hepatocytes stimulated to divide by surgical resection or exposure to necrotic agents are incapable of dividing properly and instead undergo megalocytosis (39, 41). The liver of retrorsine-exposed rats is regenerated through the outgrowth and expansion of SHPCs (39). The time course for SHPC-mediated liver regeneration after PH in retrorsine-exposed animals has been described in great detail in studies by Gordon *et al.* (39). In this model SHPCs emerge approximately 3-days after PH and continue to proliferate and expand to reach lobule size by 14-days post-PH (39). During this period of SHPC expansion the hepatocytic megalocytes undergo apoptosis (63). Because of this apoptosis the liver weights of retrorsine-exposed animals remain low through 14-days post-PH even though there is a high level of cellular regeneration occurring (39). It is not until 21 days after PH that an increase in liver weight is observed and shortly thereafter (30-days post-PH) regeneration is completed (39). The timing and kinetics of the SHPC-mediated regenerative response is clearly different from that observed in liver regeneration mediated by mature hepatocytes or oval cells (19). Although SHPCs are histologically similar to mature hepatocytes, they are phenotypically less mature and express markers of oval cells/fetal hepatoblasts (OC.2, OC.5) and mature hepatocytes (albumin, transferrin) (39). Taken together these data suggest that the SHPCs are a distinct population of liver progenitor cells capable of regenerating the liver when the proliferation of mature hepatocytes is blocked. However, the origin of the SHPCs remains unknown (19).

POTENTIAL ORIGINS OF THE SMALL HEPATOCYTE-LIKE PROGENITOR CELLS

The cellular origins of SHPCs is the subject of debate and some investigators have suggested that SHPCs and oval cells might represent the same (or closely related) population of cells (6). There are many potential sources for SHPCs in the adult liver **(FIGURE 1.7)**. Several recent studies have attempted to address the cellular origins of SHPCs. These studies produced extremely varied results. Avril *et al*. employed a retroviral-based model to genetically label mature hepatocytes with the β-galactosidase gene in retrorsine-exposed Sprague-Dawley rats before PH to determine the contribution of mature hepatocytes to the formation of SHPC clusters in this model of liver injury (61). This study showed that a significant number of SHPC clusters express β-galactosidase and based upon this evidence concluded that mature hepatocytes are the source of SHPCs (61). However, this study failed to rule out the potential contributions of other cell types. For example, the investigators never specify the percentage of biliary epithelial cells and other extrahepatic cells that were labeled with β-galactosidase gene using this retroviral-based method (19). Therefore, it is impossible to determine if oval cells or some other cell type contributed to the formation of SHPC clusters in these animals (19). A more recent study by Vig *et al.* used a hepatitis B surface antigen (HBsAg-tg) mouse model of chronic liver injury to study the origins of the SHPCs (62). This study used three dimensional mapping techniques to demonstrate that livers of retrorsine-exposed HBsAg-tg mice exhibit SHPC proliferation, and that these clusters were both surrounded and infiltrated by proliferating oval cells (62). However, the investigators note that not all of the SHPCs observed are positive for oval cell markers and conclude that other cell types may possibly contribute to the formation of these cell clusters (62). The original model of retrorsine-induced liver injury is based upon acute injury and

FIGURE 1.6. *The chemical structure of DAPM.* DAPM (diamino diphenylmethane or methylene dianiline, CAS #101-77-9) is a is an aromatic diamine that results in the targeted destruction of the bile ducts of rat liver with no significant effect on hepatocytes.

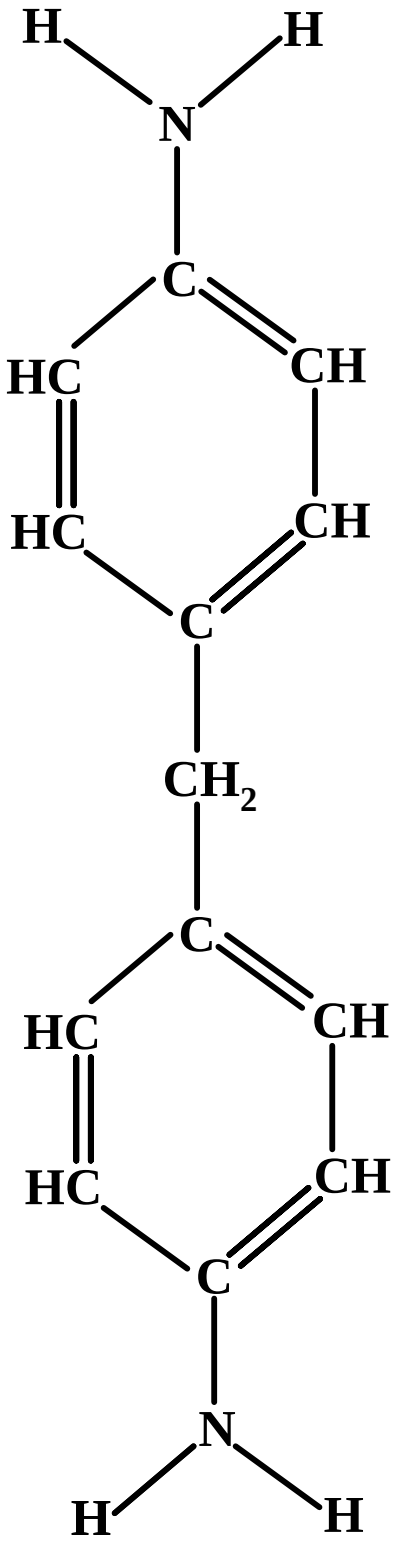

DAPM

FIGURE 1.7. *Potential origins of the small hepatocyte-like progenitor cells.* It is well established that oval cells are derived from a periportal stem cell population. However, the origin of SHPCs is not known and several cell populations could potentially be the progenitor cell giving rise to these cells. These potential progenitor cell populations include a non-hepatocytic retrorsine-resistant cells located in the liver parenchyma, a population of retrorsine-resistant mature hepatocytes, or oval cells. (Adapted from Coleman *et al.* (19)).

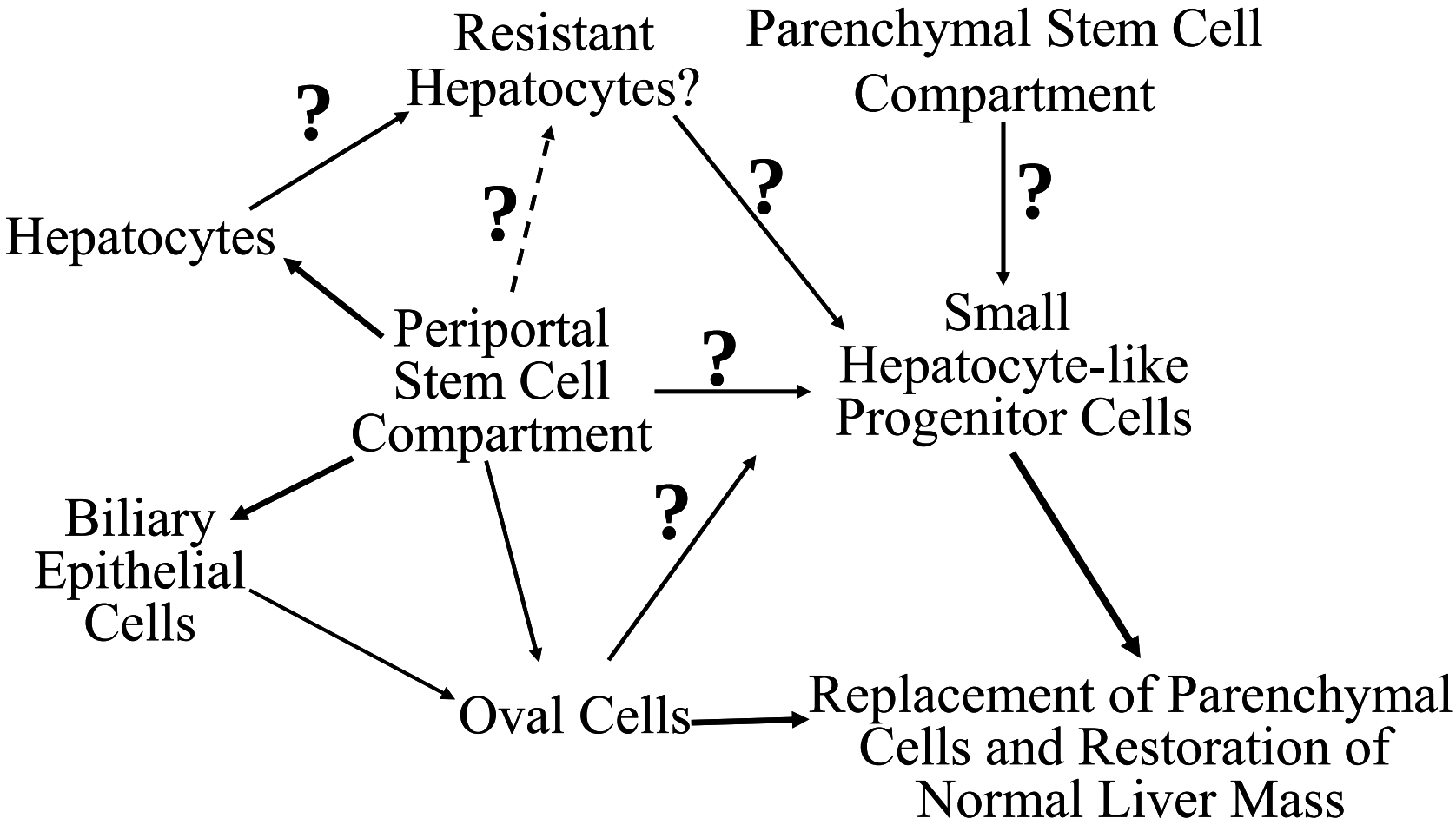
Resistant
Hepatocytes?
Parenchymal Stem Cell
Compartment
?
?
?
?
Hepatocytes
Periportal
Stem Cell
Compartment
?
Small
Hepatocyte-like
Progenitor Cells
Biliary
Epithelial
Cells
?
Oval Cells
Replacement of Parenchymal
Cells and Restoration of
Normal Liver Mass

regeneration in rats (39). Thus, it is difficult to determine if the cell clusters observed in the chronic HBsAg-tg mouse model are the same cell type (i.e. SHPCs) observed in retrorsine/PH (RP) rats. Moreover, it is known that oval cells differentiate into phenotypically 'small' hepatocytes before becoming mature hepatocytes (56). Thus, it is possible that the cells observed in this model are not SHPCs, but new hepatocyte progeny of proliferating oval cells. Combined, these published studies leave several unanswered questions about the origins of the SHPCs. Are the SHPCs derived from a population of retrorsine-resistant hepatocytes? Are these cells the progeny of oval cells? Do these cells represent an independent reserve progenitor cell population?

GOALS OF THIS DISSERTATION

Although it is well established that SHPCs emerge, proliferate, and regenerate the liver in the retrorsine/PH model, the origin of the SHPCs and the role that these cells play in the repair of tissue mass in other models of liver injury has not been investigated. The overall goal of this dissertation is to further our understanding of the contributions of SHPCs in the regeneration of the adult mammalian liver. The specific goals of the current study are to (i) to characterize the SHPC responses in both hepatotoxic and necrotic models of liver injury, (ii) to determine the progenitor cell of origin of the SHPC, and (iii) to determine the factors involved in the activation of SHPCs for proliferation after liver injury. The studies performed in this dissertation directly investigate the possibility that oval cells are the progenitor cell of origin of the SHPCs. Additionally, these studies address the possibility that the progenitor cell of origin of SHPCs are localized to a specific region of the liver

parenchyma. Finally, these studies investigate the possibility that cytokines (such as IL6, TNF-α) are involved in the priming of SHPCs for proliferation after injury.

II. EXPERIMENTAL PROCEDURES

ANIMALS

Male Fischer 344 German-strain DPPIV-deficient rats were used in all studies. Rats were either bred in-house or purchased from Charles River Laboratories (Wilmington, MA) and maintained in the AAALAC accredited animal facilities of the University of North Carolina at Chapel Hill. Animals were kept on a 12 hour light/dark schedule and were given water and chow *ad libitum*. All animals subjected to surgical manipulation were anesthetized using a cocktail of ketamine (60 mg/kg) and xylazine (5 mg/kg), and were given butorphanol (2.1 mg/kg) as a post-operative analgesic. Additionally, an intraperitoneal injection of 3 cc phosphate buffered saline (PBS) solution (1.54 mM KH_2PO_4, 155.17 mM NaCl, 2.71 mM NaH_2PO_4-$7H_2O$; pH 7.2) was administered post-operatively to increase survivability among surgically manipulated animals. All studies involving animals were conducted in accordance with federal and state guidelines put forth by the NIH and the Institutional Animal Care and Use Committee of the University of North Carolina at Chapel Hill.

EXPERIMENTAL GROUPS AND TREATMENT

Administration of Retrorsine

Retrorsine (12,18-dihydroxysenecionan-11,16-dione; β-Longilobine) was purchased from Sigma Chemical Company (St. Louis, MO). Male 6-week-old littermate Fischer 344 rats included in the retrorsine-treated + partial hepatectomy (RP) (n=27) and retrorsine only (Ret. Only) (n=15) groups received two intraperitoneal injections of retrorsine (30 mg/kg) at ages 6 and 8 weeks. Animals in the control (no treatment) + partial hepatectomy (CP) group were not treated. Partial hepatectomy was performed when rats reached 13 weeks of age, essentially as originally described (10). The retrorsine working solution was prepared by adding the solid to distilled water at a concentration of 10 mg/ml and then titrated to pH 2.5 using 1N HCl to dissolve the powder. The retrorsine solution was neutralized using 1N NaOH and brought to a final concentration of 6 mg/ml retrorsine using distilled water. The working solution was used immediately following preparation. All animals included in the RP and retrorsine only groups, and select animals in the CP group included in these studies were originally treated and surgically manipulated for studies by Gordon *et al.* (39).

Administration of 2-acetamidofluorene

N-2-acetamidofluorene (2-AAF) was administered using slow-release pellets obtained from Innovative Research Inc. (Sarasota, FL) (13, 50, 59, 60). At the outset of the experiment, male littermate Fischer 344 rats were randomized into retrorsine treatment (n=46) and control (n=113) groups. The animals were then further divided into the following groups: (i) 2-acetamidofluorene treatment + PH (2-AAF/PH), (ii) 2-acetamidofluorene treatment + retrorsine treatment + partial hepatectomy (2-AAF/RP), (iii) 2-acetamidofluorene treatment only (2-AAF only), (iv) placebo treatment + partial hepatectomy (Placebo/PH), (vii) placebo treatment only (placebo only). In addition, animals in these groups were compared to RP rats (n=27) from previously reported studies (39). Retrorsine-treated

animals received two doses of retrorsine (30 mg/kg) at ages 6 and 8 weeks, as described above. Four weeks following the second retrorsine treatment (at twelve weeks of age), all animals were implanted with either a 50 mg 21-day controlled release 2-AAF (Catalog # A-102) or a placebo pellet (Catalog # C-111). The experimental pellets deliver a daily dose of approximately 10 mg/kg 2-AAF. Placebo pellets are comprised of cholesterols, lactose, celluloses, phosphates, and stearates. These pellets are identical to the 2-AAF pellets in composition, but exclude the active compound. Animals in groups receiving surgical manipulation were subjected to PH one week following pellet implantation (at 13 weeks of age), essentially as originally described (10). Due to significant mortality in the 2-AAF/PH and 2-AAF/RP groups, only 130 (70%) rats survived the experimental protocol and these rats are included in the results presented. Animals were euthanized and liver tissue was harvested from all animal groups at 3, 7, 10, 14, and 21 days post-PH (n=3-7 animals per time point, except for 21 day time point in 2-AAF/RP and 2-AAF groups which suffered high rates of mortality, where n=2). **FIGURE 2.1** illustrates the treatment timeline for each group in this study.

Administration of 4,4'-diaminodiphenylmethane

4,4'-diaminodiphenylmethane (DAPM) was purchased from Sigma Chemical Company (St. Louis, MO) and prepared by dissolving in dimethylsulfoxide (DMSO) at a concentration of 50 mg/ml, as previously described (64). At the outset of the experiment, rats were randomized into retrorsine treatment (n=45) and control (n=91) groups. Subsequently, animals were further divided into the following groups: (i) DAPM treatment + retrorsine treatment + partial hepatectomy (DAPM/RP), (ii) 4,4'-diaminodiphenylmethane treatment + partial hepatectomy (DAPM/PH), (iii) 4,4'-diaminodiphenylmethane treatment

FIGURE 2.1. *Experimental design timeline for 2-AAF study.* A timeline indicating the age of animals (weeks) at the various times of treatment in this study is provided. R indicates the time points for retrorsine injection (30 mg/kg each). 2-AAF indicates the time of insertion of a 21 day time-release 2-acetamidofluorene pellet (50 mg). Placebo indicates insertion of 21 day time-release placebo pellet (50 mg). (A) Retrorsine treatment + Partial Hepatectomy (RP). (B) Retrorsine treatment only (Retrorsine Only). (C) 2-AAF treatment + Partial Hepatectomy (2-AAF/PH). (D) 2-AAF treatment + Retrorsine treatment + Partial Hepatectomy (2-AAF/RP). (E) 2-AAF treatment only (2-AAF only). (F) Placebo treatment + Partial Hepatectomy (Placebo/PH). (G) Placebo treatment only (Placebo only).

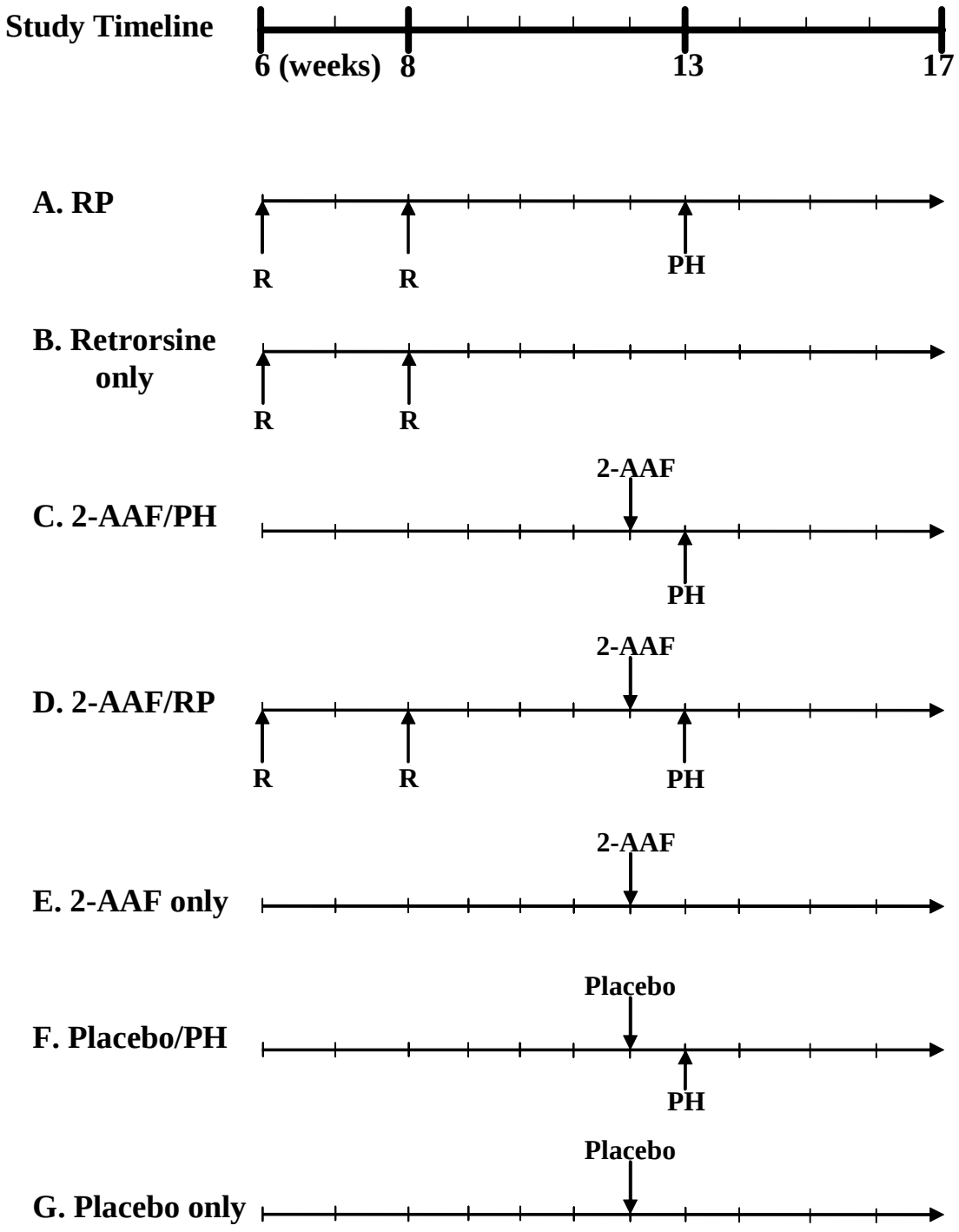
Study Timeline
6 (weeks)
8
13
17
A. RP
R
R
PH
B. Retrorsine only
R
R
2-AAF
C. 2-AAF/PH
PH
2-AAF
D. 2-AAF/RP
R
R
PH
2-AAF
E. 2-AAF only
Placebo
F. Placebo/PH
PH
Placebo
G. Placebo only

only (DAPM only), (iv) dimethylsulfoxide (vehicle) treatment + partial hepatectomy (DMSO/PH), and (v) dimethylsulfoxide (vehicle) treatment only (DMSO only). In addition, animals in these groups were compared to RP rats (n=27) from previously reported studies (39). Retrorsine-treated animals received two doses of retrorsine (30 mg/kg) at ages 6 and 8 weeks, as described above. At 13 weeks of age, animals were injected with either DAPM or DMSO (vehicle) and PH was performed 24 hours later, essentially as originally described (10). Animals in the DAPM only and DMSO only groups were not surgically manipulated. The treatment protocol was well tolerated. A total of 108 (79%) rats survived the experimental protocol and these rats are included in the results presented. Animals were euthanized and liver tissue was harvested at 3, 7, 10, 14, 21, and 30 days post-PH (n=3-6 animals per time point). **FIGURE 2.2** illustrates the treatment timeline for each group in this study.

Administration of Carbon Tetrachloride

Carbon Tetrachloride (CCl_4) was purchased from Sigma Chemical Company (St. Louis, MO) and prepared by diluting the solution with corn oil (1:1 vol/vol) resulting in a final concentration of 797 mg/mL, as previously described (50). At the outset of the experiment animals were divided into retrorsine treatment (n=53) and control (n=48) groups. Subsequently, animals were further divided into the following groups: (i) retrorsine treatment + carbon tetrachloride treatment (Ret/CCl_4), (ii) carbon tetrachloride treatment only (CCl_4 only), or (iii) corn oil (vehicle) treatment only (Corn oil only). Retrorsine-treated animals received two doses of retrorsine (30 mg/kg) at ages 6 and 8 weeks, as described above. At 13 weeks of age the animals were injected with a single dose of either CCl_4 (1500 mg/kg or 1.88 ml/kg) or corn oil (vehicle) (1.88 ml/kg). Due to significant mortality in the Ret/CCl_4 and

FIGURE 2.2. *Experimental design timeline for DAPM study.* A timeline indicating the age of animals (weeks) at the various times of treatment is given. R indicates the times of retrorsine injection (30 mg/kg each). DAPM indicates the time of 4, 4-diaminodiphenylmethane injection (50 mg/kg). DMSO indicates the time of dimethyl sulfoxide injection (1 ml/kg). (A) Retrorsine + Partial Hepatectomy (RP) (B) DAPM treatment + Partial Hepatectomy (DAPM/PH). (C) DAPM treatment + Retrorsine treatment + Partial Hepatectomy (DAPM/RP). (D) DMSO + Partial Hepatectomy (DMSO/PH). (E) DAPM treatment only (DAPM only). (F) DMSO treatment only (DMSO Only).

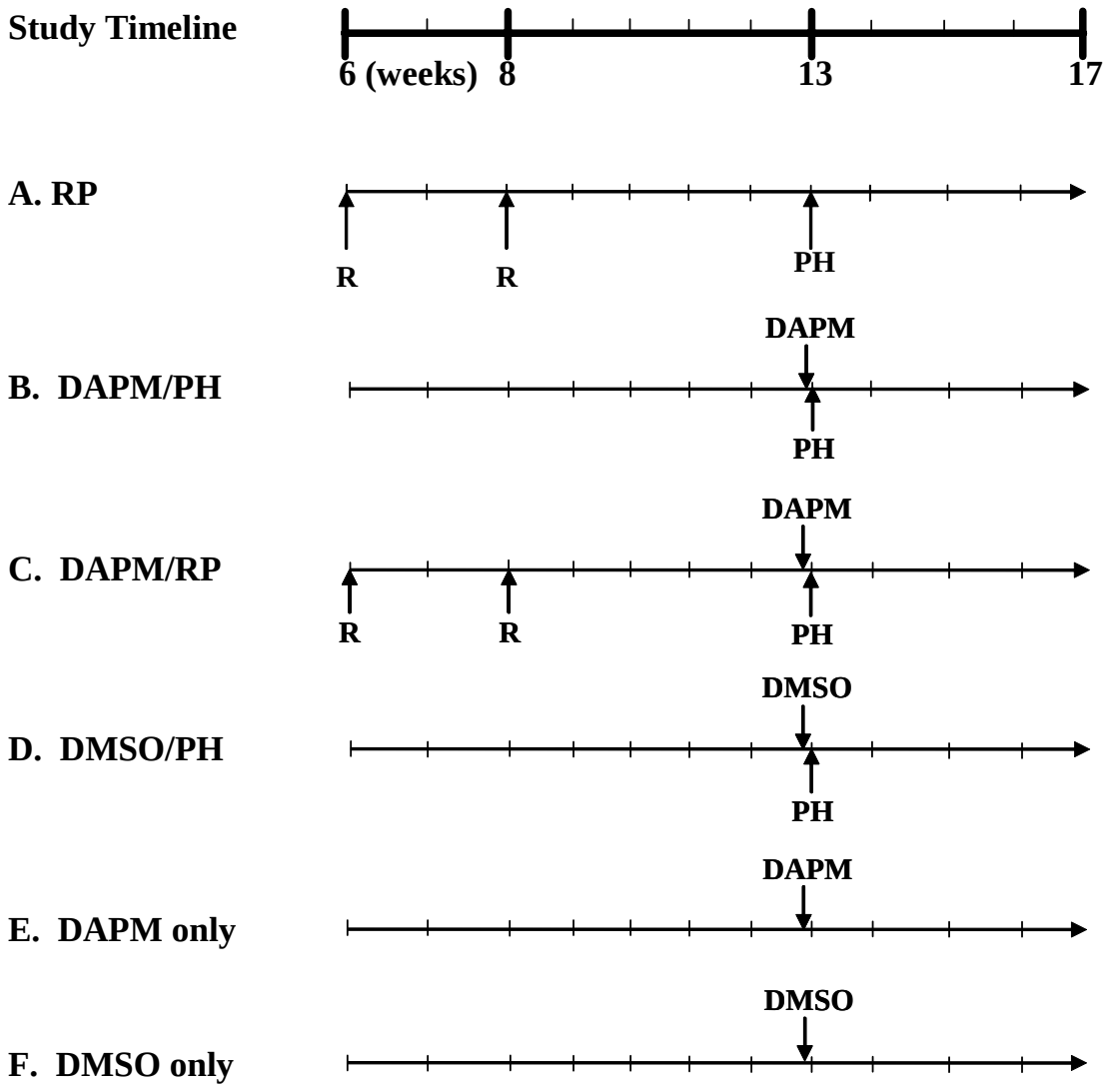
Study Timeline
6 (weeks)
8
13
17
A. RP
R
R
PH
B. DAPM/PH
DAPM
PH
C. DAPM/RP
DAPM
R
R
PH
D. DMSO/PH
DMSO
PH
E. DAPM only
DAPM
F. DMSO only
DMSO

CCl_4 groups, only 45 (45%) rats survived the experimental protocol and these rats are included in the results presented. Animals were euthanized and liver tissue was harvested at 3, 7, 14, 21, and 30 days post-injection (n=3 animals per time point). **FIGURE 2.3** illustrates the treatment timeline for each group in this study.

Administration of Dexamethasone

Dexamethasone (DEX) (9α-Fluoro-16α-methyl-11β, 17α, 21-trihydroxy-1,4-prenadiene-3,20-dione) was purchased from Sigma Chemical Company (St. Louis, MO). A working solution of DEX was prepared by dissolving the solid in a small volume of 100% ethanol and then bringing the solution to a final concentration of 0.6 mg/ml using distilled water. The working solution was used immediately after preparation. At the outset of the experiment, rats were randomized into retrorsine treatment (n=82) and control (n=70) groups. In addition, these animals were compared to RP animals (n=27) and CP animals (n=13) from previously reported studies (39). Animals in retrorsine treatment group were treated with retrorsine (30 mg/kg) at 6 and 8 weeks of age, as described above. Five weeks following the second retrorsine treatment, retrorsine-exposed and age-matched control rats were further randomized into the following groups: (i) no treatment + partial hepatectomy (CP), (ii) multiple dexamethasone treatments + retrorsine treatment (MDR), (iii) dexamethasone treatment + retrorsine treatment + partial hepatectomy (DRP), (iv) multiple dexamethasone treatments + partial hepatectomy (MDCP), (v) multiple dexamethasone treatments + retrorsine treatment + partial hepatectomy (MDRP), (vi) multiple dexamethasone treatments + retrorsine treatment + partial hepatectomy + interleukin-6 treatment (MDRP/IL6). Animals receiving surgical manipulation were subjected to PH essentially as originally described (10). DEX-treated animals in both the retrorsine and control groups were either

FIGURE 2.3. *Experimental design timeline for CCl_4 study.* Schematic at the top of the figure is a timeline indicating the age of animals (weeks) at the various times of treatment in this study. R indicates the times of retrorsine injection (30 mg/kg each). CCl_4 indicates the time of carbon tetrachloride injection (1500 mg/kg). (A) Retrorsine treatment + Carbon Tetrachloride treatment (Ret/CCl_4). (B) Carbon Tetrachloride only (CCl_4 only). (C) Corn Oil (Vehicle) only (corn oil only).

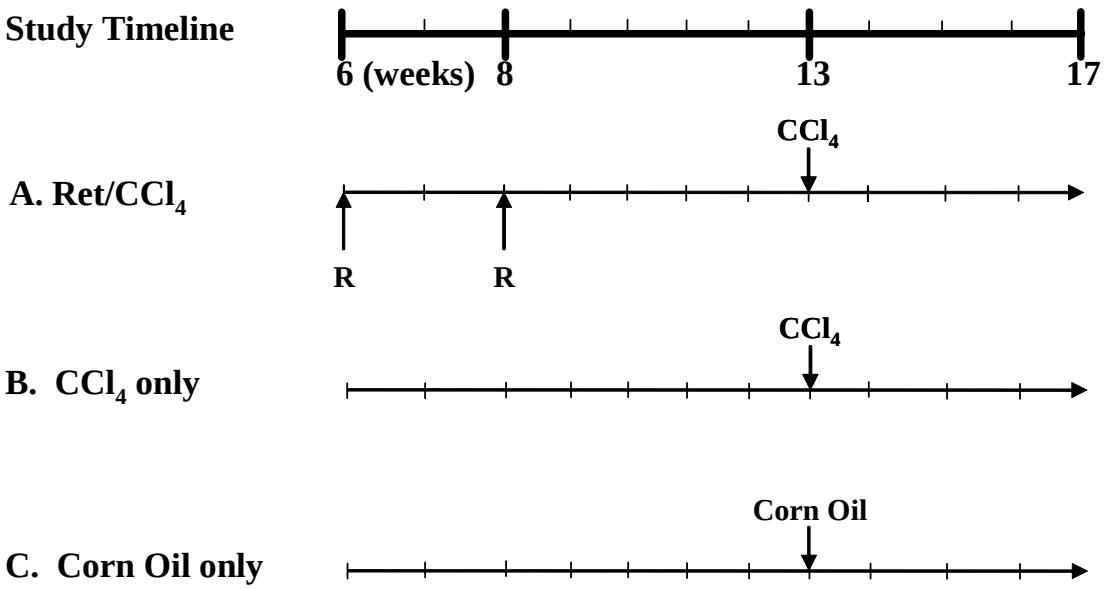
Study Timeline
6 (weeks)
8
13
17
A. Ret/CCl4
CCl4
R
R
B. CCl4 only
CCl4
C. Corn Oil only
Corn Oil

given a single (intraperitoneal) dose of DEX (2 mg/kg) at the time of PH or multiple (n=5) DEX treatments (2 mg/kg each) at 24h and 1h before PH and 1, 2, and 3 days post-PH. Due to significant mortality in the MDRP and MDCP groups, only 101 (66%) rats survived the experimental protocol and these rats are included in the results presented. Blood samples were collected from the abdominal aorta of select animals in the CP, MDCP, MDRP groups at 1, 12, and 48 hours after PH (n=3 for each time point and group except MDRP 24 and 48 hour time points where n=4) and incubated at room temperature for 2 hours to allow coagulation to occur. Coagulated blood samples were centrifuged at 1000 x g for 20 minutes to pellet red blood cells and platelets. Following centrifugation, serum was collected and stored at -20°C. Serum IL6 levels were quantified by the enzyme-linked immunosorbent assay (ELISA) at ELISA Tech (Aurora, CO). Samples were analyzed in triplicate using the rat IL6 DuoSet ELISA development kit and Quantitkine® Rat IL6 Immunoassay Kit (R & D Systems, Minneapolis, MN). An IL6 standard curve was generated using samples of known concentration ranging from 40 to 5000 pg/mL. This curve was used to calculate the concentration of IL6 in experimental serum samples. Liver tissues were harvested from surviving rats at 7, 14, 21, and 30 days after PH (n=3-7 per time-point) or at the equivalent time points for control animals. **FIGURE 2.4** illustrates the treatment timeline for each group in this study.

Administration of Interleukin-6

Rat interleukin-6 (IL6) recombinant protein was purchased from R&D Systems. IL6 was provided as a 0.586 mg/mL stock solution. The IL6 working solution was prepared by diluting the stock solution with a PBS solution (1.54 mM KH_2PO_4, 155.17 mM NaCl, 2.71 mM NaH_2PO_4-$7H_2O$; pH 7.2) to yield a concentration of 100 μg/ml. The working solution

FIGURE 2.4. *Experimental design timeline for DEX study*. Schematic at the top of the figure is a timeline indicating the age of animals (weeks) at the various times of treatment in this study. R indicates the times of retrorsine administration (30 mg/kg each). DEX with a horizontal arrow indicates multiple (n=5) DEX treatments (2 mg/kg each), whereas DEX with a vertical arrow indicates a single 2 mg/kg dose of DEX (see methods). (A) Control (no retrorsine) + partial hepatectomy (CP). (B) Retrorsine treatment + partial hepatectomy (RP). (C) Multiple dexamethasone treatments + retrorsine (designated MDR). (D) Dexamethosone + retrorsine + partial hepatectomy (DRP). (E) Control (no retrorsine) + multiple dexamethasone treatments + partial hepatectomy (MDCP). (F) Multiple dexamethasone treatments + retrorsine + partial hepatectomy (MDRP). (G) Multiple dexamethasone treatments + retrorsine + partial hepatectomy + IL6 (MDRP/IL6).

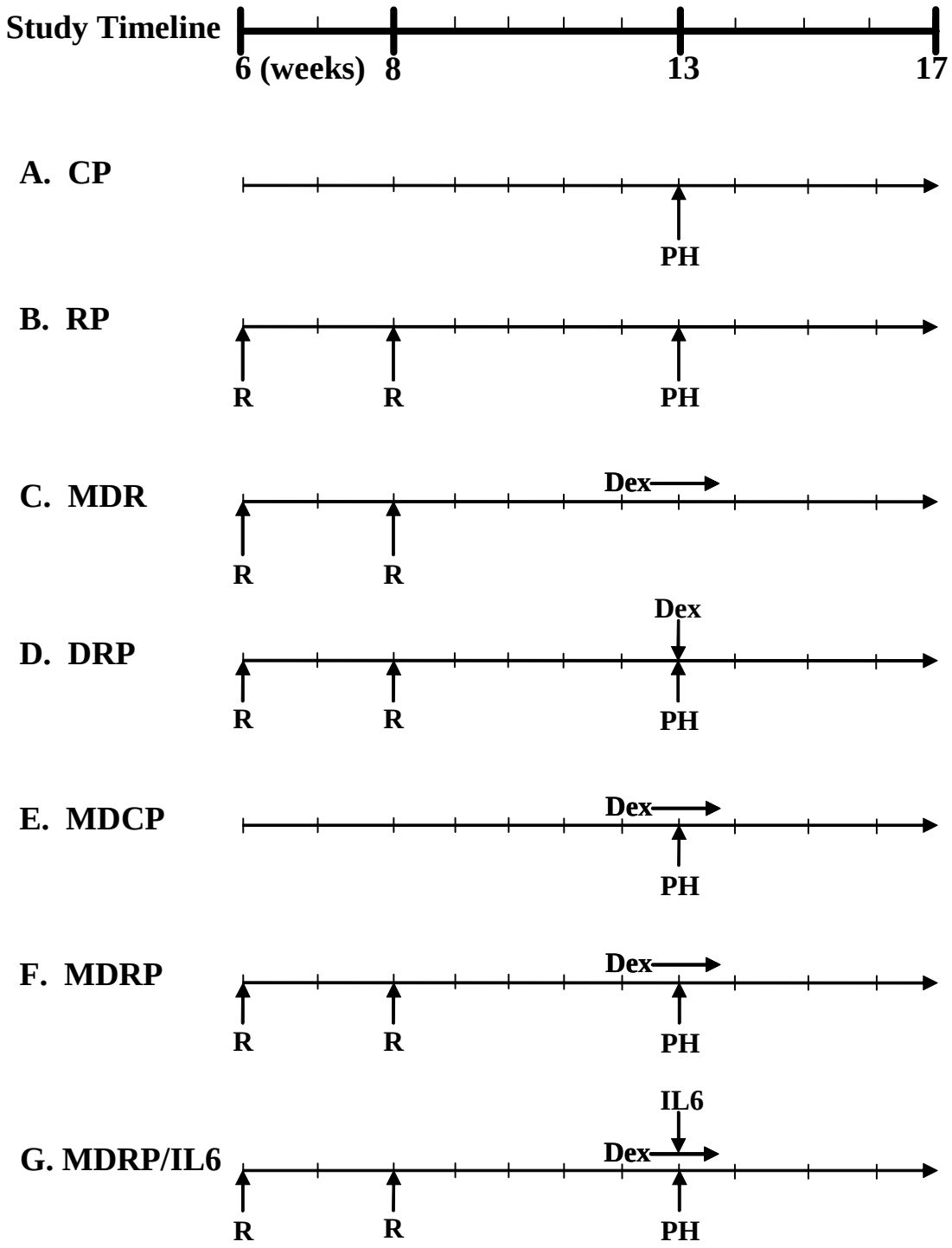
Study Timeline
6 (weeks)
8
13
17
A. CP
PH
B. RP
R
R
PH
C. MDR
Dex
R
R
D. DRP
Dex
R
R
PH
E. MDCP
Dex
PH
F. MDRP
Dex
R
R
PH
G. MDRP/IL6
IL6
Dex
R
R
PH

was used immediately after preparation. Animals receiving IL6 were injected with 10 μg of protein in the tail vein.

Administration of Bromodexoyuridine

BrdU (5-bromo-2'-dexoyuridine) was purchased from Sigma Chemical Company (St. Louis, MO). BrdU-treated animals received a single intraperitoneal dose of BrdU (100 mg/kg) at 6-days post-PH. The BrdU working solution was prepared by dissolving the solid in PBS (1.54 mM KH_2PO_4, 155.17 mM NaCl, 2.71 mM NaH_2PO_4-$7H_2O$; pH 7.2) at 33.3 mg/mL. This solution was heated using hot tap water and vortexed vigorously to dissolve the solid. The working solution was administered immediately following preparation.

TISSUE HARVEST AND PREPARATION

Liver tissue was harvested at various time points following PH or CCl_4 exposure. Animals were anesthetized using a cocktail containing ketamine (60 mg/kg) and xylazine (5 mg/kg) and liver tissues were resected. Euthanasia of the animals resulted from exsanguination secondary to removal of the liver. Animal weights and liver tissue weights were recorded for each animal at the time of PH (or treatment) and at necropsy. Liver tissues were fixed in 10% neutral buffered formalin. Formalin-fixed liver tissue was sent to Histo-Scientific Research Laboratories (Mt. Jackson, VA) for routine paraffin embedding and sectioning. Five μm sections were cut and H&E stained slides and unstained slides prepared. In addition, sections for immunohistochemical analysis were prepared from selected tissue samples.

IMMUNOHISTOCHEMICAL ANALYSIS

Colorimetric immunoperoxidase analysis was carried out on paraffin-embedded tissue sections using standard procedures. Liver tissues were deparaffinized in xylene, dehydrated through a gradient of ethanol solutions, and rehydrated in PBS (1.54 mM KH_2PO_4, 155.17 mM NaCl, 2.71 mM NaH_2PO_4-$7H_2O$; pH 7.2). Endogenous peroxidase activity was quenched by incubation in a 0.3% H_20_2 solution (in 100% methanol) for 10 minutes. Antigen retrieval was achieved by placing the tissues in a heated 10 mM citrate buffer (DakoCytomation, Carpinteria, CA) and steaming for 30 minutes. Non-specific antibody binding was blocked using a serum-free protein block (DakoCytomation). Primary antibodies were diluted in antibody diluent with background reducing components (DakoCytomation). Detection of primary antibodies was accomplished using the DakoCytomation Labelled Streptavidin-Biotin2, Horseradish Peroxidase (LSAB2®, HRP) system (DakoCytomation). Detection of the secondary antibodies was accomplished with a peroxidase substrate containing diaminobenzidine (DakoCytomation). Tissue sections were counterstained with Mayer's hematoxylin (Sigma Chemical Company). Primary antibodies were purchased from Santa Cruz Biotech (Santa Cruz, CA), Abcam (Cambridge, MA), or DakoCytomation. Mouse anti-rat BrdU antibody (Abcam, Catalog #ab9557-500) and mouse anti-human cytokeratin 19 antibody (DakoCytomation, Catalog #M0772) were used at a dilution of 1:25. Goat anti-rat α-fetoprotein antibody (Santa Cruz Biotech, Catalog #sc-8108) was used at a dilution of 1:100.

MORPHOMETRIC ANALYSIS

Morphometric analysis was performed by digitally scanning H&E stained slides using an Aperio Scanscope T2 Virtual Microscope System (Vista, CA) at a resolution of 0.4667 μm/pixel. Images were analyzed using Aperio Imagescope v6.25 software. SHPC clusters were identified in the H&E sections based upon cell morphology and arrangement. Using the various tools provided by the Imagescope v6.25 software, SHPC clusters were enumerated and measured (area). All data obtained using Imagescope v6.25 was normalized to the cross sectional area of the tissue section, measured using Image J v1.36 software (National Institutes of Health, Bethesda, MD).

STATISTICAL ANALYSIS

All statistical analyses reported were performed using either Kaleidograph v4.0 software (Synergy Software, Reading, PA) or Graphpad Prism v4.03 (GraphPad Software, San Diego, CA). Determination of significance in quantitative data was accomplished using the Student's two-tailed t-test for unpaired data with unequal variance. Statistical significance of survival curve data was determined by the Kaplan-Meier log-rank test.

III. RESULTS

LIVER REGENERATION AFTER PH IN 2-AAF-TREATED RETRORSINE-EXPOSED RATS

Rationale

The 2-AAF/PH model of liver injury is commonly used to study the role of oval cells in liver regeneration. In this model, the mito-inhibitory effects of 2-AAF inhibit mature hepatocytes from dividing in response to proliferative stimulus (such as PH), and the liver is regenerated through the emergence and proliferation of oval cells (6, 15). Oval cells appear 1-3-days post-PH, proliferate extensively, and then differentiate into new hepatocyte clusters between 7 and 14-days after PH, depending on the dose of 2-AAF administered (56). Oval cell-derived new hepatocyte clusters are histologically similar to SHPCs, leading some investigators to suggest that there may be a precursor-product relationship between oval cells and SHPCs (6, 19, 62). We investigated this possibility by combining the retrorsine/PH model of liver injury and regeneration with exposure to the mito-inhibitory agent 2-AAF. Given that liver regeneration after PH in rats exposed to 2-AAF occurs through the outgrowth and expansion of oval cells, it can be inferred that oval cells are resistant to the mito-inhibitory effects of 2-AAF. Likewise, SHPCs are resistant to the mito-inhibitory effects of retrorsine. However, based on the differences in cytochrome P450s that are required for the metabolism of retrorsine and 2-AAF (65, 66), it is plausible that retrorsine-resistant SHPCs may be susceptible to 2-AAF poisoning. Determination that SHPCs are

sensitive to 2-AAF poisoning would provide significant new evidence that oval cells do not represent progenitor cells for SHPCs.

Regenerative responses after PH in rats exposed to retrorsine alone and retrorsine in combination with 2-AAF.

At 3-days following PH, RP animals have liver weights and liver/body weight ratios comparable to that observed in 2-AAF/PH animals (P>0.05 for RP versus 2-AAF/PH) **(FIGURE 3.1B-C)**. RP animals have low liver weights and liver/body weight ratios through 14-days post-PH, and then show a moderate increase in liver weight at 21-days post-PH **(FIGURE 3.1B-C)**. Animals in the 2-AAF/RP group have liver weights that are not significantly different (P>0.05) from those observed in RP animals for the first 14-days post-PH **(FIGURE 3.1B)**. The lack of increasing liver weights among these animals during the first 14-days post-PH does not reflect a lack of regenerative activity. Rather, retrorsine-injured hepatocytes undergo megalocytosis following PH, and then apoptosis as new cells are generated in response to liver deficit (39). Animals in the 2-AAF/RP group show a dramatic increase in liver weight between 14 and 21-days post-PH and have liver weights that are indistinguishable from placebo/PH control animals at 21-days post-PH (P>0.05 for 2-AAF/RP versus placebo/PH) **(FIGURE 3.1B)**. In contrast, 2-AAF/PH animals have low liver weights through 7-days post-PH, with a moderate increase in liver size at 10-days post-PH, and becoming indistinguishable (P>0.05 for 2-AAF/PH versus placebo/PH) from control (placebo/PH) by 14-days post-PH **(FIGURE 3.1B)**. Likewise, 2-AAF/PH animals demonstrate an increase in liver/body weight ratio by 14-days post-PH and attain a control liver/body weight ratio by 21-days post-PH (P>0.05 for 2-AAF/PH versus placebo/PH) **(FIGURE 3.1C)**. Together, these results suggest that the timing and kinetics of liver

FIGURE 3.1. *Treatment with 2-AAF blocks the SHPC regenerative response but not liver regeneration in retrorsine-exposed rats.* The effects of 2-AAF treatment on (A) average body weight, (B) average liver weight, and (C) average liver/body weight ratios are shown. Each bar represents the mean calculated from all surviving animals in the various experimental groups (± SEM, n=3-7 per time point for all groups, except for 21 day 2-AAF/RP and 2-AAF/PH where n=2). The asterisks denote statistically significant differences ($P<0.05$) in liver weight (B) or liver/body weight ratios (C) for the designated comparisons. NS denotes no significant difference ($P>0.05$) for the designated comparison.

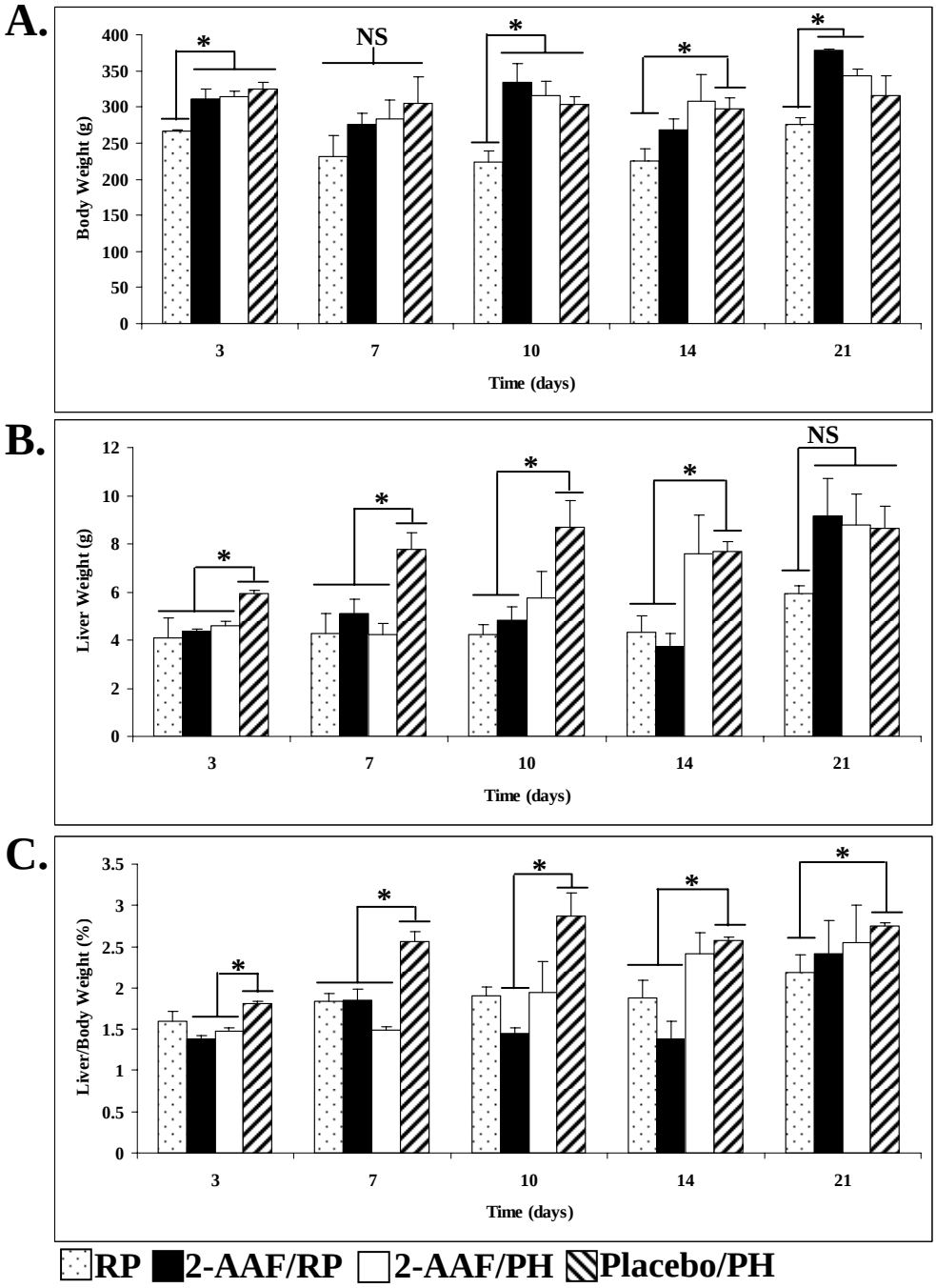
A.
Body Weight (g)
400
350
300
250
200
150
100
50
0
*
NS
*
*
*
3
7
10
14
21
Time (days)
B.
Liver Weight (g)
12
10
8
6
4
2
0
*
*
*
*
NS
3
7
10
14
21
Time (days)
C.
Liver/Body Weight (%)
3.5
3
2.5
2
1.5
1
0.5
0
*
*
*
*
*
3
7
10
14
21
Time (days)
RP
2-AAF/RP
2-AAF/PH
Placebo/PH

regeneration after PH in retrorsine-exposed animals treated with 2-AAF is similar to that observed in 2-AAF/PH animals.

Analysis of H&E stained liver sections showed that the nature of the regenerative responses observed in RP and 2-AAF/RP animals differ significantly. Liver tissue harvested from RP animals at 3-days post-PH contain emerging SHPC clusters and modest numbers of oval cells **(FIGURE 3.2A)**. At this same time point post-PH, oval cells begin to appear in large numbers in animals treated with 2-AAF, but SHPCs are not observed **(FIGURE 3.2B-C)**. By 7-days post-PH, livers from RP animals show a robust SHPC response with numerous proliferating cell clusters and very little oval cell proliferation **(FIGURE 3.2E)**. In contrast, livers harvested at this time point from 2-AAF/RP and 2-AAF/PH rats exhibit marked proliferation of oval cells, but SHPCs are not observed **(FIGURE 3.2F-G)**. At 10-days post-PH, RP animals exhibit large numbers of proliferating SHPC clusters **(FIGURE 3.2I)**, while SHPCs are not observed in livers harvested from 2-AAF/RP **(FIGURE 3.2J)** and 2-AAF/PH animals **(FIGURE 3.2K)**. At 14-days post-PH a population of phenotypically 'small' hepatocytes appear in the 2-AAF/RP and 2-AAF/PH animals **(FIGURE 3.2N-O)**. These hepatocytes are found in close proximity to proliferating oval cells suggesting that these cells are the differentiated progeny (i.e. new hepatocytes) of oval cells **(FIGURE 3.2N-O)**. Livers from RP animals at this time-point did not contain significant numbers of oval cells, but contained large numbers of expanding SHPC clusters **(FIGURE 3.2M)**. Neither SHPC clusters nor oval cells are observed at any time point after PH in placebo-treated animals **(FIGURE 3.2D, H, L, and P)**. Likewise, SHPC clusters and oval cells are not observed in 2-AAF only, placebo only, and retrorsine only animals that were not surgically manipulated **(FIGURE 3.3)** (39). The differences between progenitor cell responses observed

FIGURE 3.2. *SHPCs do not respond to liver deficit in retrorsine-exposed animals treated with 2-AAF*. Livers from animals receiving retrorsine treatment and PH contain expanding SHPC clusters at (A) 3-days, (E) 7-days, (I) 10-days, and (M) 14-days post-PH. In contrast, livers from animals receiving both retrorsine and 2-AAF contain large numbers of oval cells at (B) 3-days, (F) 7-days, and (J) 10-days post-PH, and new hepatocyte formation is observed at (N) 14-days post-PH. Likewise, livers from animals receiving only 2-AAF contain large numbers of proliferating oval cells at (C) 3-days, (G) 7-days, or (K) 10-days post-PH, and formation of some new hepatocyte clusters can be observed (O) 14 days after PH. Animals receiving placebo treatment do not exhibit oval cells or SHPC clusters at (D) 3-days, (H) 7-days, (L) 10-days, or (P) 14-days post-PH. Short white arrows indicate SHPC clusters, long black arrows indicate oval cells, and short black arrows indicate new hepatocyte clusters. (Original objective lens magnification 10x).

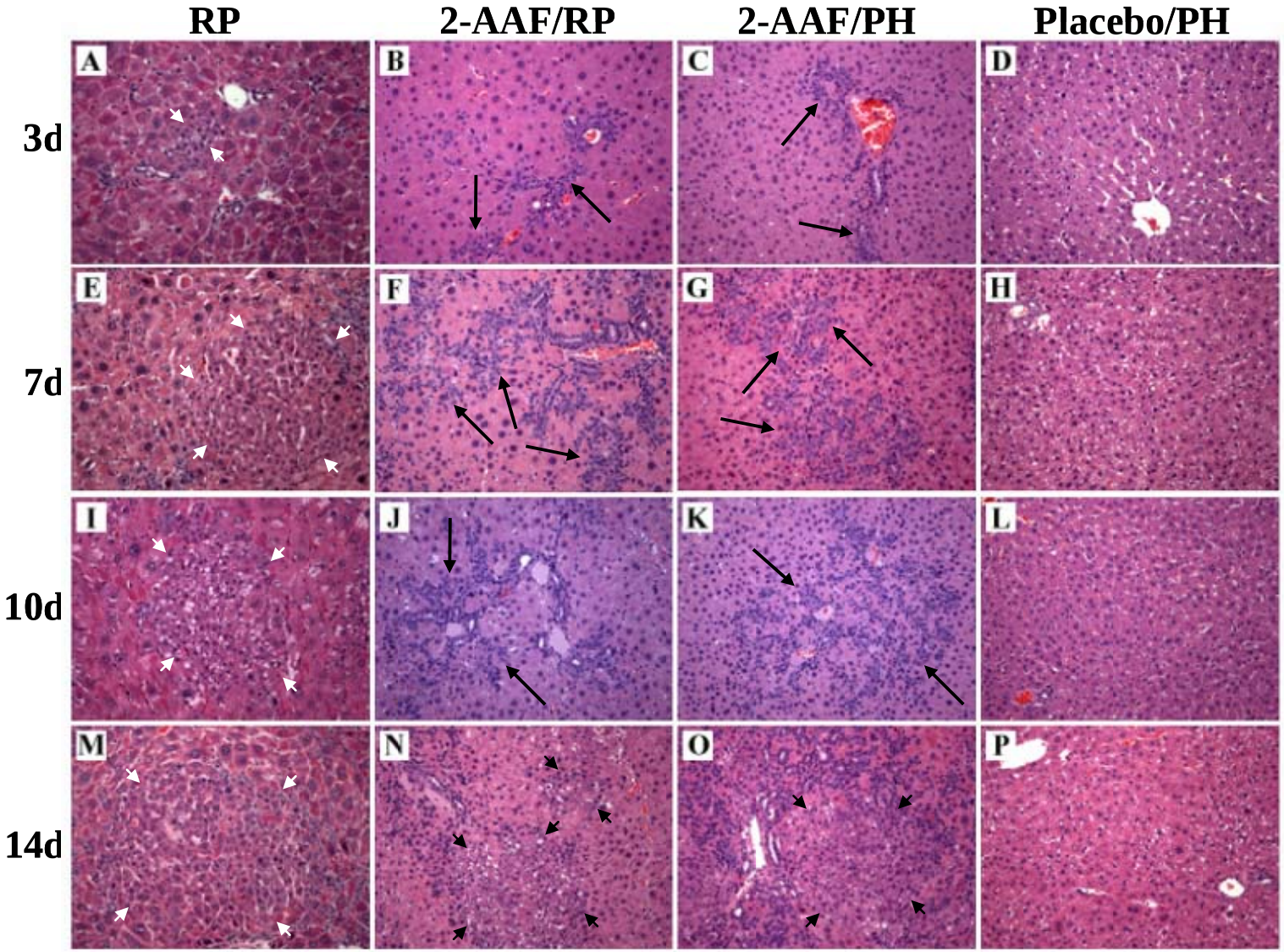
RP
2-AAF/RP
2-AAF/PH
Placebo/PH
3d
7d
10d
14d
A
B
C
D
E
F
G
H
I
J
K
L
M
N
O
P

FIGURE 3.3. *Cellular responses in 2-AAF control groups*. SHPCs are never observed at any time after implantation of 2-AAF (A-D) or placebo (E-H) pellets. (Original objective lens magnification 10x).

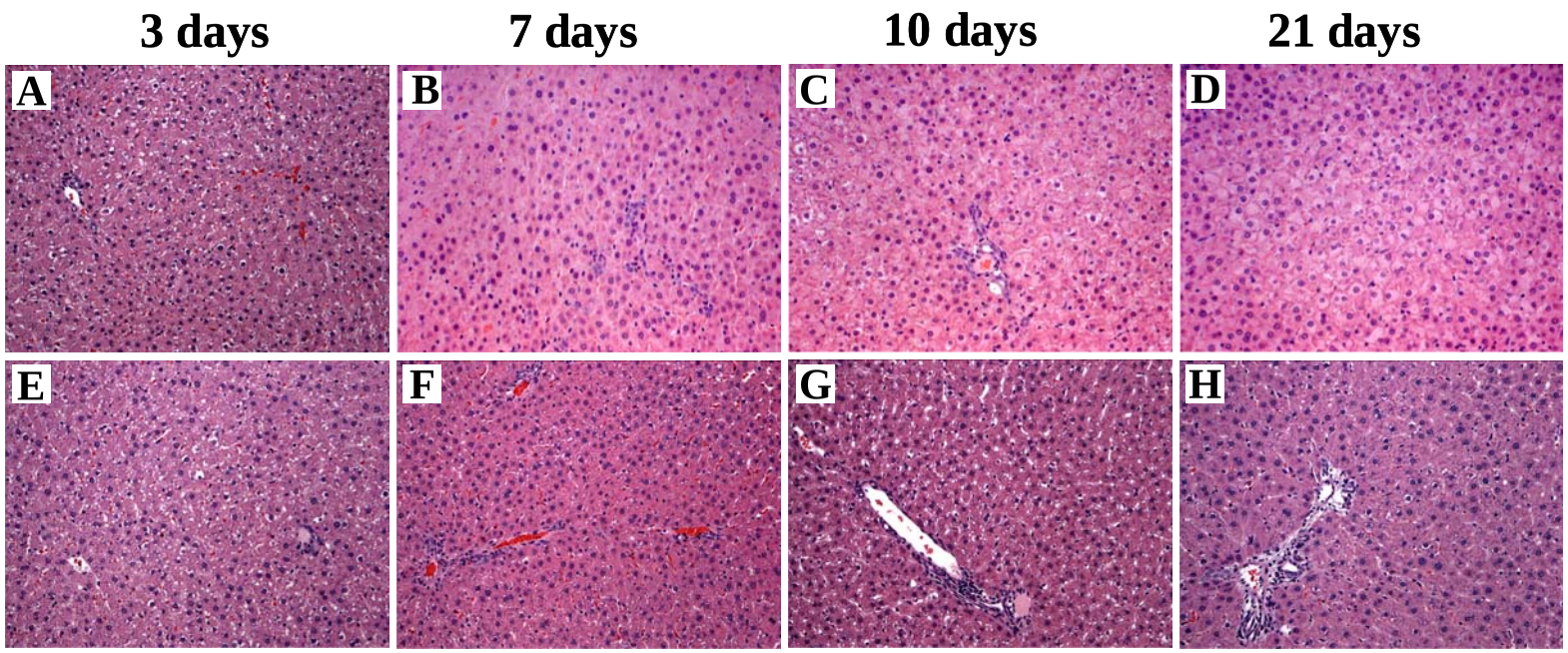
3 days
7 days
10 days
21 days
A
B
C
D
E
F
G
H

during liver regeneration in RP and 2-AAF/RP animals suggest that although the SHPCs (and their progenitors) are resistant to the mito-inhibitory effects of retrorsine, they may be susceptible to 2-AAF poisoning.

Immunohistochemical analysis of 2-AAF-treated retrorsine-exposed rat liver.

Immunostaining of the oval cell and biliary tract marker cytokeratin 19 (ck19) clearly labeled proliferating oval cells (along with biliary epithelia) in 2-AAF/PH and 2-AAF/RP rats at 7-days post-PH **(FIGURE 3.4A, C)**. At 14-days post-PH in 2-AAF/PH animals, ck19-positive oval cells surround new hepatocyte clusters **(FIGURE 3.4B)**. The new hepatocytes were weakly positive for ck19 **(FIGURE 3.4B)**. This observation suggests that the new hepatocytes represent the progeny of proliferating/differentiating oval cells, as observed by others (56). Likewise, ck19-positive oval cells surround new hepatocyte clusters in livers of 2-AAF/RP animals at 14-days post-PH **(FIGURE 3.4D)**. In contrast, ck19 immunostaining of livers from RP animals at 7 days and 14-days post-PH decorated the modest oval cell response, but failed to reveal ck19-positive oval cells in close proximity to SHPC clusters **(FIGURE 3.4E-F)**. Rather ck19 immunostaining exclusively labeled biliary tracts in these animals **(FIGURE 3.4E-F)**. These results provide additional evidence that the oval cell response in RP rats is modest and that identifiable oval cells do not obviously feed into SHPC clusters.

BrdU labeling demonstrates that new hepatocyte clusters observed in 2-AAF-treated animals are the progeny of oval cells.

To investigate the potential lineage relationship between oval cells and hepatocytes observed in 2-AAF-exposed animals, BrdU (100 mg/kg i.p.) was administered to 2-AAF/RP

FIGURE 3.4. *Immunostaining with oval cell marker cytokeratin 19.* Cytokeratin 19 (ck19) staining in 2-AAF/PH animals at (A) 7-days post-PH labels biliary epithelial cells and oval cells. and (B) 14-days post-PH labels biliary epithelial cells, oval cells and new hepatocyte clusters. Likewise, ck19 immunostaining in 2-AAF/RP animals at (C) 7-days and (D) 14-days post-PH labels biliary epithelial cells and oval cells surrounding new hepatocyte clusters. Ck19 immunostaining in RP animals at (E) 7-days and (F) 14-days post-PH only labels biliary tracts in these animals. White arrows indicate ck19 positive biliary tracts, black arrows indicate new hepatocyte clusters. (Original objective lens magnification 10x).

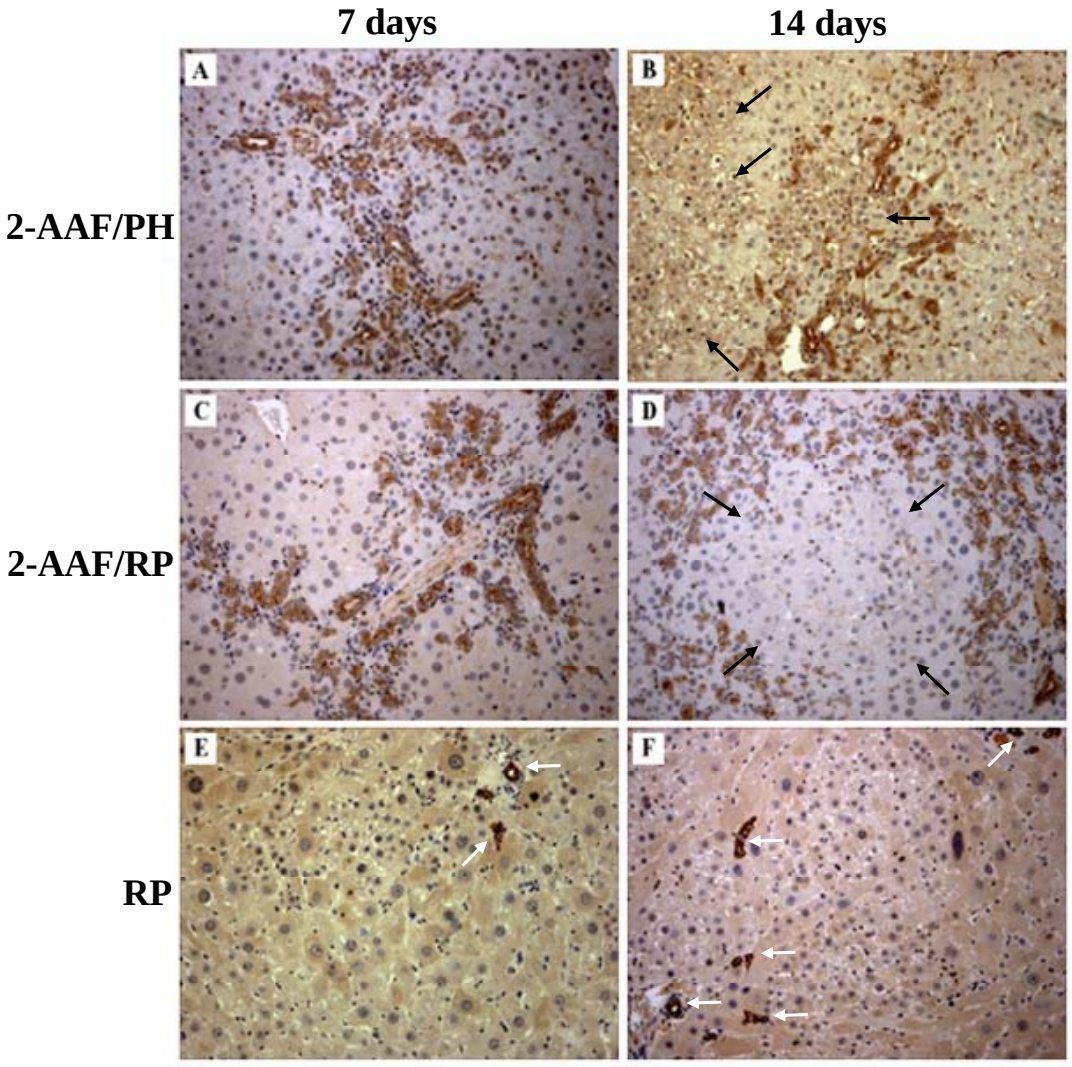
7 days
14 days
2-AAF/PH
2-AAF/RP
RP
A
B
C
D
E
F

FIGURE 3.5. *Bromodeoxyuridine labeling demonstrates a precursor-product relationship between oval cells and new hepatocyte clusters in 2-AAF-treated animals.* Treatment with BrdU at 6-days post-PH specifically labels oval cells in liver tissue collected at 7-days post-PH from 2-AAF treated animals: (A) 2-AAF/PH and (C) 2-AAF/RP. By 14-days post-PH in animals, BrdU-positive oval cells give rise to new hepatocytes clusters (B). A similar result is seen at 14-days post-PH in 2-AAF/RP rats (D). Colon taken from a BrdU-treated rats serves as a positive control (E) and colon taken from an untreated rat (no BrdU) serves as a negative control (F). (Original objective lens magnification 10x).

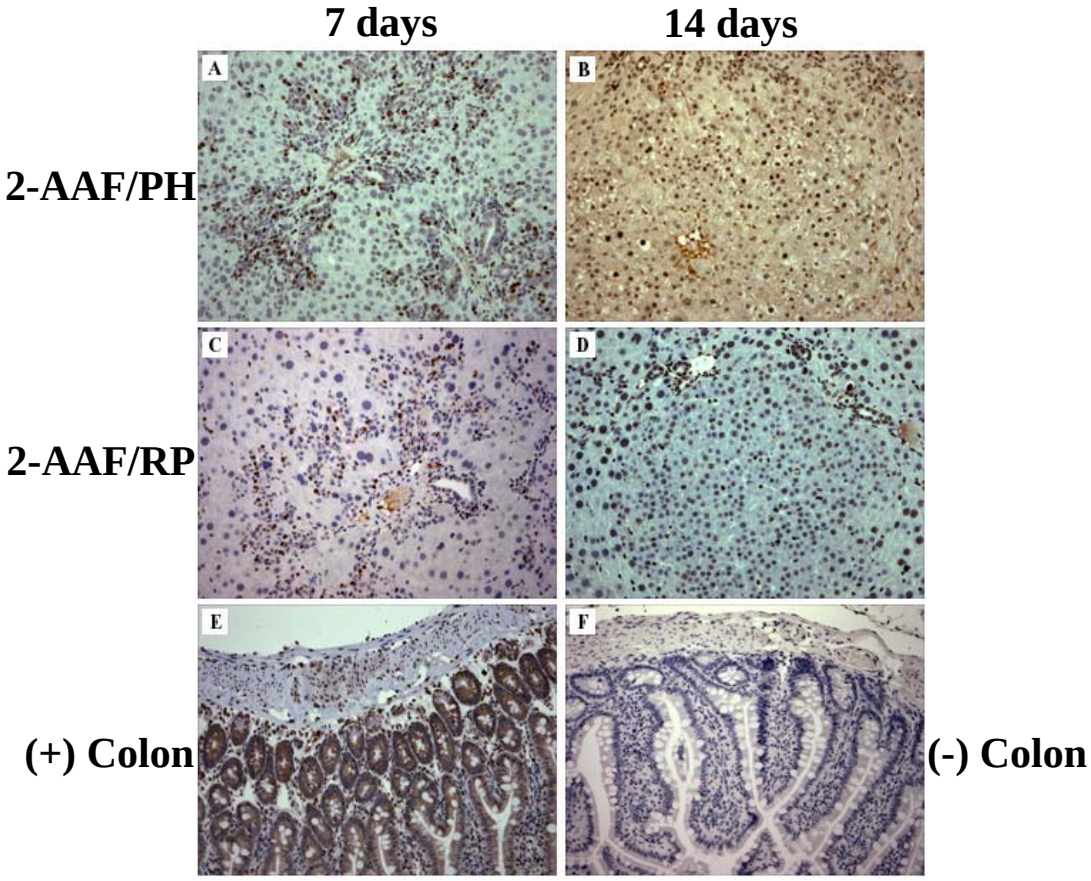
7 days
14 days
2-AAF/PH
2-AAF/RP
(+) Colon
(-) Colon
A
B
C
D
E
F

and 2-AAF/PH rats 6-days after PH. As previously described (31, 36, 57), treatment with BrdU 6-days post-PH exclusively labels oval cells in animals receiving 2-AAF before PH **(FIGURE 3.5A, C)**. At 14-days post-PH, BrdU-positive cells are observed in 100% of the newly formed hepatocyte clusters in 2-AAF/PH **(FIGURE 3.5B)** and 2-AAF/RP animals **(FIGURE 3.5D)**. These results demonstrate that new hepatocyte clusters observed in 2-AAF/PH and 2-AAF/RP animals are the progeny of proliferating/differentiating oval cells.

Treatment with 2-AAF after PH blocks SHPC cluster expansion.

To directly address the possibility that SHPCs are susceptible to the mito-inhibitory effects of 2-AAF poisoning, rats were treated with the standard RP protocol followed by the addition of 2-AAF after the initiation of SHPC proliferation **(FIGURE 3.6)**. One week following PH, rats were treated with either a placebo (n=5) or a 2-AAF (n=6) controlled time release pellet and livers were collected 7 days later (14-days post-PH). Morphometric analysis of H&E stained tissue from these animals demonstrated that SHPC clusters in animals receiving 2-AAF ceased to expand after administration of 2-AAF, suggesting that the proliferation of SHPC was inhibited by 2-AAF exposure **(FIGURE 3.6D and TABLE 3.1)**. The size of SHPC clusters observed in RP + 2-AAF animals at 14-days post-PH were indistinguishable ($P>0.05$) from those observed in RP animals at 7-days post-PH **(FIGURE 3.6D and TABLE 3.1)**. In contrast, SHPC clusters in RP + placebo animals expand reflecting the continued proliferation of SHPCs, and by 14-days post-PH are approximately two-fold larger than those observed in RP + 2-AAF animals **(TABLE 3.1 and FIGURE 3.6E)**. There were no differences ($P>0.05$ for RP versus RP + placebo at 14-days post-PH) in the size of SHPC clusters observed in RP animals receiving placebo pellets and RP animals (in the absence of placebo) at 14-days post-PH **(TABLE 3.1)**. These data directly demonstrate that

FIGURE 3.6. *Treatment with 2-AAF after PH in retrorsine-exposed rats blocks SHPC expansion.* A timeline indicating the age of animals (weeks) at the various times of treatment in this study is provided. R indicates the time points for retrorsine injection (30 mg/kg each). 2-AAF indicates the time of insertion of a 21 day time-release 2-acetamidofluorene pellet (50 mg). Placebo indicates insertion of 21 day time-release placebo pellet (50 mg). (A) Retrorsine + parital hepatectomy + 2-AAF treatment 7-days post-PH (RP + 2-AAF). (B) Retrorsine + partial hepatectomy + placebo treatment 7-days post-PH (RP + Placebo). H&E stained liver harvested from at 14-days post-PH from (D) RP + 2-AAF animals exhibit SHPC clusters comparable in size to those observed in (C) RP animals at 7-days post-PH. However, livers taken from (E) RP + Placebo animals at 14-days post-PH exhibit SHPC clusters comparable to (F) RP animals at 14-days post-PH. Arrows indicate SHPC clusters. (Original objected lens magnification 10x).

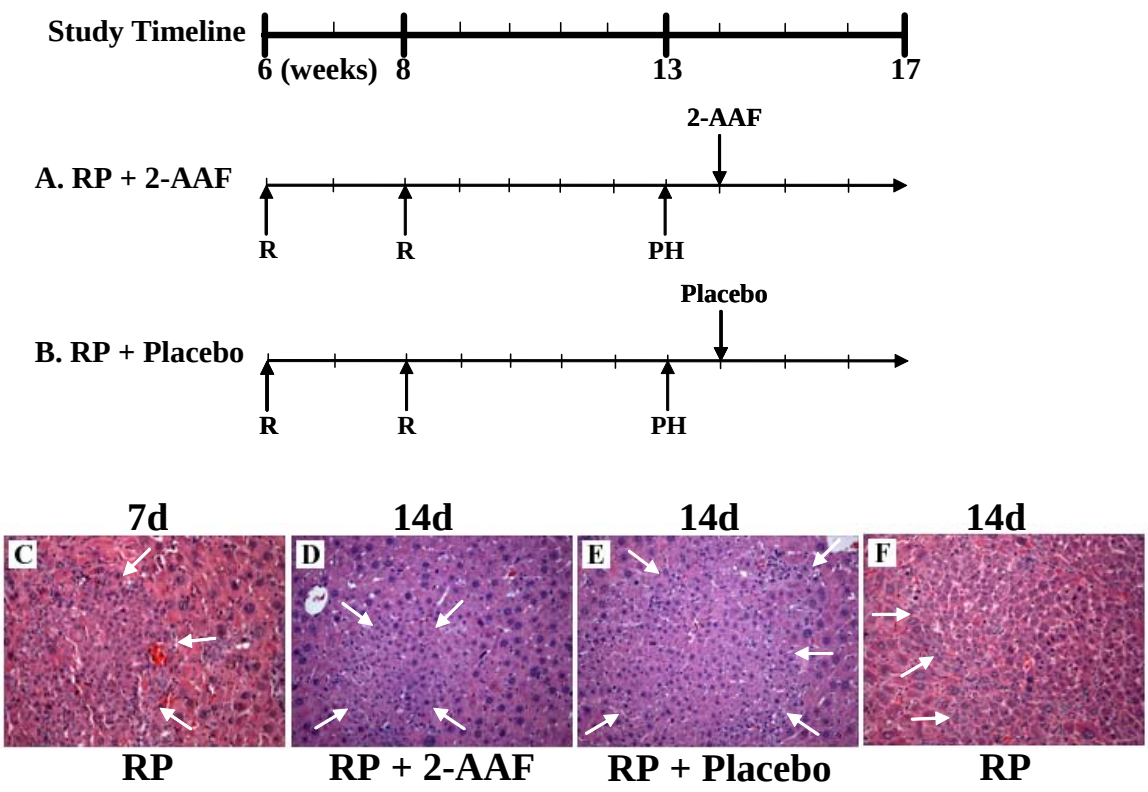
Study Timeline
6 (weeks)
8
13
17
2-AAF
A. RP + 2-AAF
R
R
PH
Placebo
B. RP + Placebo
R
R
PH
7d
14d
14d
14d
C
D
E
F
RP
RP + 2-AAF
RP + Placebo
RP

Table 3.1. *Treatment with 2-AAF 7d post-PH Blocks Expansion of SHPCs in Retrorsine-Exposed Rats*

	SHPC Cluster Area (μm^2)
RP 7-days Post-PH*	$4.82 \times 10^4 \pm 1.76 \times 10^3$ (n=100)
RP + 2-AAF 14-days Post-PH***	$4.39 \times 10^4 \pm 2.87 \times 10^3$ (n=100)
RP + Placebo 14-days Post-PH**	$8.00 \times 10^4 \pm 3.81 \times 10^3$ (n=100)
RP 14-days Post-PH****	$8.65 \times 10^4 \pm 4.12 \times 10^3$ (n=100)

*P=0.2059 for RP + 2-AAF 14-days post-PH versus RP 7-days post-PH
**P<0.0001 for RP + Placebo 14-days post-PH versus RP at 7-days post-PH
***P<0.0001 for RP + Placebo versus RP + 2-AAF at 14-days post-PH
****P=0.2462 for RP + Placebo versus RP at 14-days post-PH

SHPCs are susceptible to 2-AAF poisoning and suggest that SHPCs are not the progeny of 2-AAF resistant oval cells.

LIVER REGENERATION AFTER PH IN DAPM-TREATED RETRORSINE-EXPOSED RATS

Rationale

A precursor-product relationship between oval cells and SHPCs has been suggested by several investigators (6, 62). Oval cells are resistant to the mito-inhibitory effects of 2-AAF poisoning, whereas retrorsine-resistant SHPCs are susceptible to this toxin, providing strong evidence that SHPCs are not the progeny of oval cells. To further investigate the possibility that oval cells are progenitors of SHPCs, F344 rats were treated with retrorsine and DAPM, a biliary toxin, 24 hours prior to PH. Oval cells reside in the bile ducts of the liver (40, 60, 67). Thus, it is possible to eliminate the oval cell-mediated regenerative response by destroying the bile ducts of the liver using a biliary specific toxin. Several investigators have shown that DAPM treatment leads to the targeted destruction of the bile ducts of F344 rats (60, 64). Therefore, the appearance of SHPCs in the livers of retrorsine-exposed rats treated with DAPM after PH would provide strong evidence that these cells are not derived from oval cells.

DAPM treatment produces bile duct injury in retrorsine-exposed rats.

Treatment of rats with a singe dose of DAPM results in the targeted destruction of bile ducts **(FIGURE 3.7)**, as previously reported (60, 64). The destruction of bile duct structures is rapid, with evidence of severe bile duct damage by 24-hours after DAPM treatment **(FIGURES 3.7A, 3.8A)**. DAPM-induced bile duct damage persists through 3-days

FIGURE 3.7. *DAPM selectively destroys bile ducts in rats.* DAPM causes the selective destruction of bile ducts by 24 hours after administration in control rats that receive DAPM only (A,E), DAPM/PH (B,F), and DAPM/RP (C,G). Bile duct injury is not observed in animals receiving (D,H) DMSO (vehicle) only. (Original objective lens magnification 20x for panels (A-D), 40x for panels (E-H)).

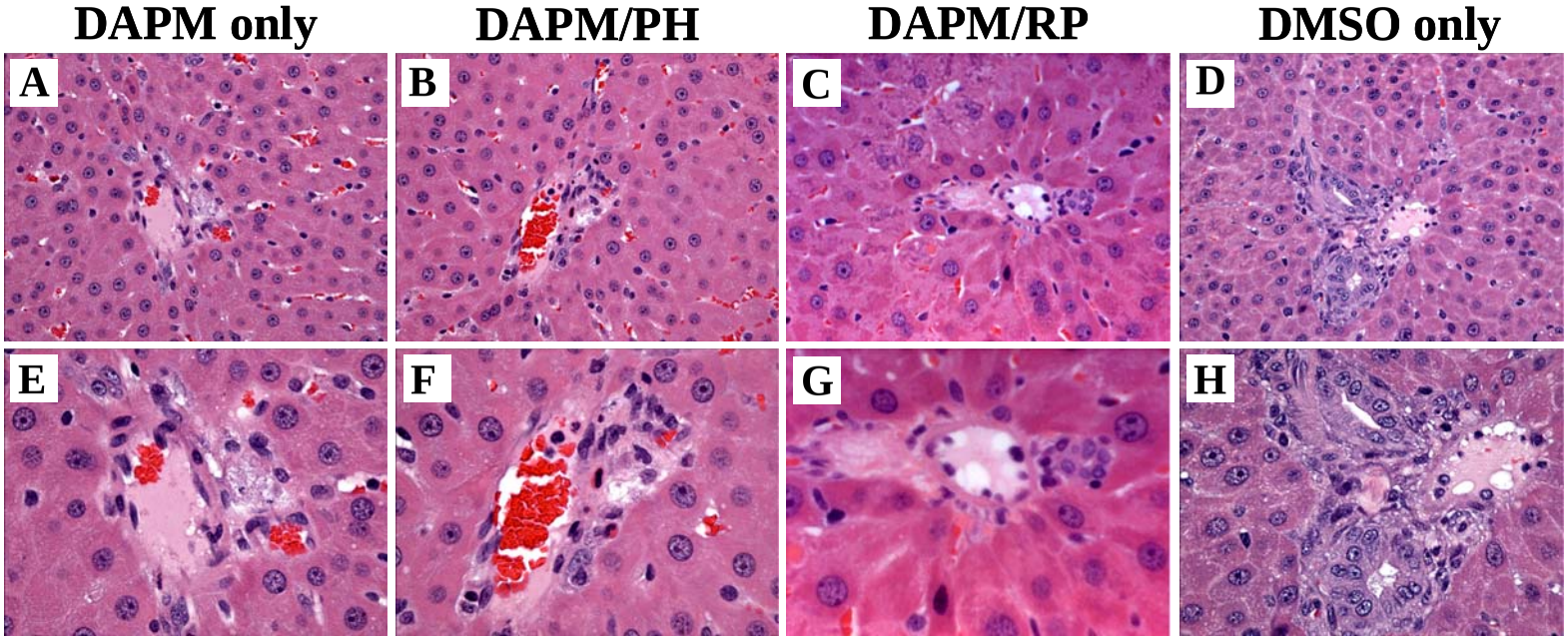
DAPM only
DAPM/PH
DAPM/RP
DMSO only
A
B
C
D
E
F
G
H

FIGURE 3.8. *Time-course for recovery of bile ducts following DAPM-induced injury.* (A) At 24 hours after DAPM administration, bile ducts are severely damaged in the livers of DAPM only rats. (B) By 3-days after DAPM administration, immune cells are recruited to regions of cellular necrosis. (C) At 7-days post-DAPM, bile duct structure is restored and appears normal. Bile duct damage is not observed in DMSO-treated control animals at (D) 24 hours, (E) 3 days, and (F) 7-days post-DMSO administration. Arrows indicate damaged bile ducts. (Original objective lens magnification 20x).

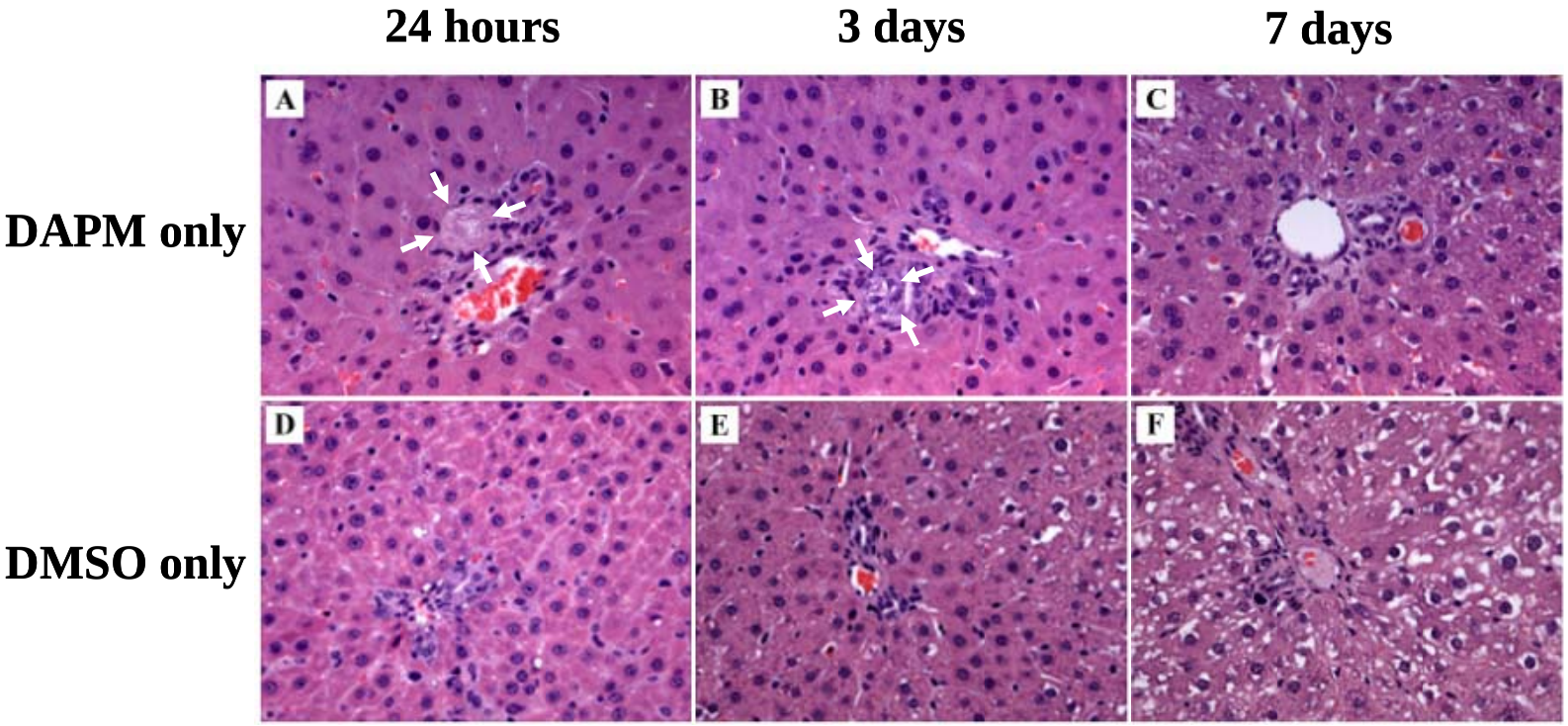
24 hours
3 days
7 days
DAPM only
DMSO only
A
B
C
D
E
F

post-injection **(FIGURE 3.8B)** before recovery of biliary cell types was observed. For several days following DAPM administration (in DAPM only animals), remnants of bile duct structures can be observed in damaged portal tracts **(FIGURE 3.8A-B)**, and immune cells recruited in areas of injury populate the necrotic lesions **(FIGURE 3.8B)**. Morphologically normal bile duct structures can be observed in portal tracts 7-days after DAPM injection in DAPM only treated animals **(FIGURE 3.8C)**. In DAPM/PH animals, DAPM-induced bile ductular damage occurs rapidly, with evidence of bile duct injury at 24-hours post-injection **(FIGURE 3.7)**. However, recovery of biliary epithelial cells and bile duct structures is achieved over a shorter time course compared to DAPM only animals. In DAPM/PH rats, restoration of morphologically normal bile duct structures is observed by 3-days post-PH, corresponding to 4-days post-DAPM administration **(FIGURE 3.9K)**. Likewise, in DAPM/RP rats bile duct damage is noted at 24-hours after DAPM administration **(FIGURE 3.7)**, evidence of bile duct repair is observed at 3-days post-PH (4-days post-DAPM treatment), and normalization of bile duct structure is observed by 7-days post-PH **(FIGURE 3.9A-B)**. No bile duct injury is observed in DMSO-treated control animals at any time point after injection **(FIGURE 3.8D-F)**. Similarly, retrorsine treatment alone (in the absence of DAPM) does not produce notable bile duct injury (39).

Liver regeneration after partial hepatectomy in retrorsine-exposed rats following DAPM treatment.

At 3-days post-PH, animals in all groups exhibit similar body weights, liver weights, and liver/body weight ratios **(FIGURE 3.10)**. These similarities persist through 7-days post-PH among animals in the RP and DAPM/RP treatment groups. At 7-days post-PH, these animals have liver weights (P=0.561 for RP versus DAPM/RP) and liver/body weight ratios

FIGURE 3.9. *Destruction of bile ducts by DAPM does not block the SHPC regenerative response in retrorsine-exposed rats.* Livers from DAPM/RP rats contain SHPCs at (A) 3-days post-PH. These clusters expand through (B) 7-days, (C) 10-days, (D) 14-days, and (E) 30-days post-PH. This response is indistinguishable from that observed in the livers of RP animals at (F) 3-days, (G) 7-days, (H) 10-days, (I) 14-days, and (J) 30-days post-PH. SHPC clusters are never observed in DAPM/PH (K-O) or DMSO/PH (P-T) control animals at any time point after PH. Arrows indicate SHPC clusters. (Original objective lens magnification 10x).

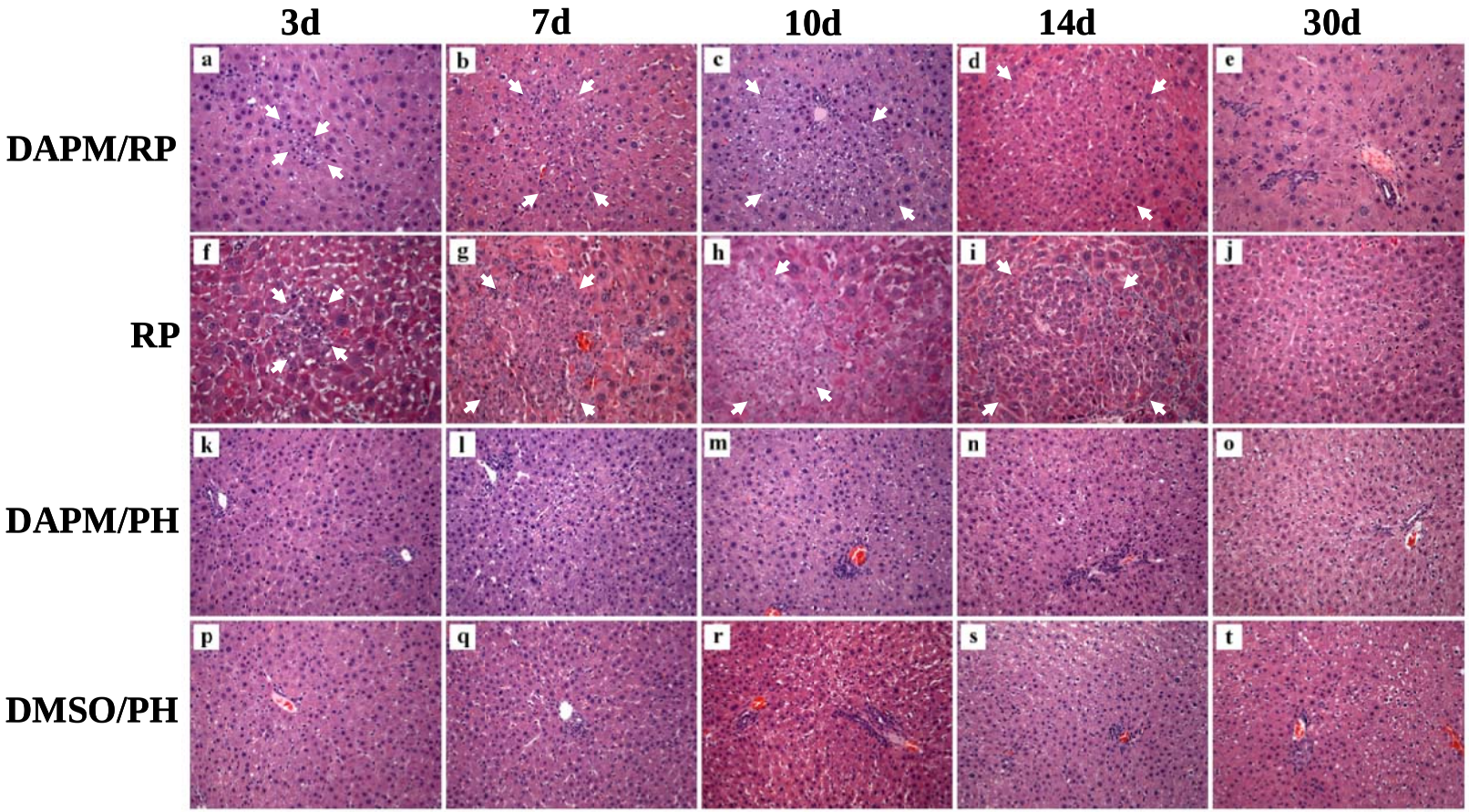
3d
7d
10d
14d
30d
DAPM/RP
RP
DAPM/PH
DMSO/PH
a
b
c
d
e
f
g
h
i
j
k
l
m
n
o
p
q
r
s
t

FIGURE 3.10. *DAPM treatment does not block liver regeneration in retrorsine-exposed rats.* The effects of DAPM treatment on (A) average body weight, (B) average liver weight, and (C) average liver/body weight ratios are shown. Each bar represents mean calculated from all surviving animals in the various experimental groups (± SEM, n=3-10 per time point for all groups). Asterisks denote significant differences ($P<0.05$) in DAPM/RP and RP weights and liver/body weight ratios. NS denotes no significant difference in DAPM/RP and RP weights and liver/body weight ratios.

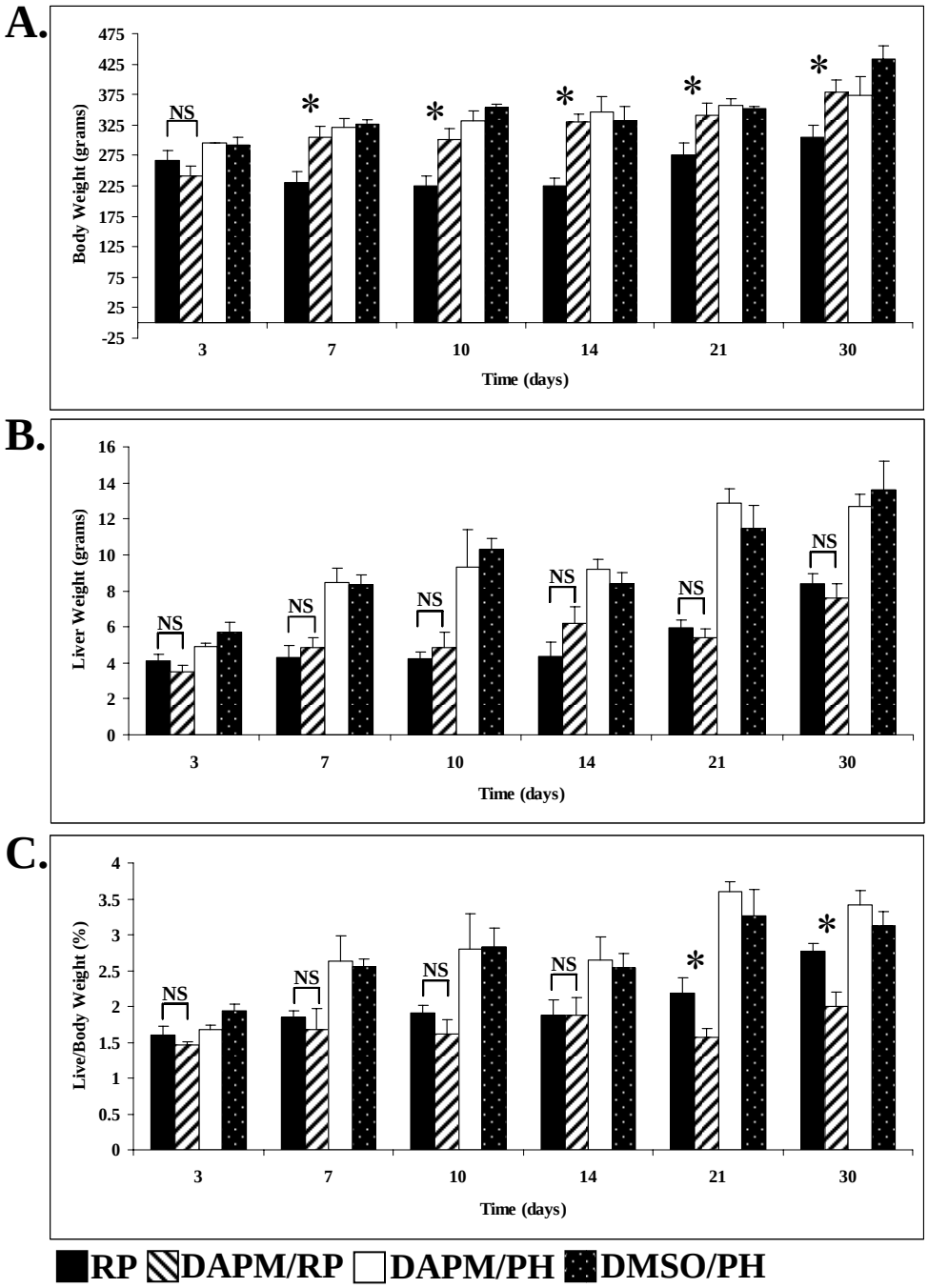
A.
Body Weight (grams)
475
425
375
325
275
225
175
125
75
25
-25
NS
*
3
7
10
14
21
30
Time (days)
B.
Liver Weight (grams)
16
14
12
10
8
6
4
2
0
NS
3
7
10
14
21
30
Time (days)
C.
Live/Body Weight (%)
4
3.5
3
2.5
2
1.5
1
0.5
0
NS
*
3
7
10
14
21
30
Time (days)
RP
DAPM/RP
DAPM/PH
DMSO/PH

(P=0.275 for RP versus DAPM/RP) that are not significantly different from one another. However, control (DMSO/PH and DAPM/PH) animals have significantly increased (P<0.05) liver weights and liver/body weight ratios compared to RP and DAPM/RP animals at this time point **(FIGURE 3.10B-C)**, reflecting a robust regenerative response in these animals. This trend continues through 10 and 14-days post-PH **(FIGURE 3.10B-C)**. Liver regeneration in DMSO/PH and DAPM/PH animals is mediated by proliferation of mature hepatocytes and is completed over a short period of time. However, at 10 and 14-days post-PH the liver weights and liver/body weight ratios for DAPM/RP and RP rats are lower than those observed in control animals **(FIGURE 3.10B-C)**. The low liver weights are not due to a lack of cellular regeneration, but reflect loss of tissue mass related to apoptosis of retrorsine-injured hepatocytes (megalocytes) in retrorsine-exposed liver (63). By 21-days post-PH, an increase in the liver weights of retrorsine-exposed animals is observed **(FIGURE 3.10B)**. At this time point, animals in the DAPM/RP group have liver weights comparable to that observed in RP rats (P=0.453 NS), but have liver/body weight ratios that are significantly (P=0.032) lower than that observed in RP rats **(FIGURE 3.10C)**. This difference in liver/body weight ratio between RP and DAPM/RP animals is due to the higher average body weight observed in DAPM/RP animals (versus RP animals), while the liver weights observed in these two treatment groups are indistinguishable at this time point **(FIGURE 3.10)**. Control animals at 21-days post-PH have significantly higher (P<0.05) body weights, liver weights, and liver/body weight ratios than those observed in the retrorsine-treated animals **(FIGURE 3.10)**. At the end of the 30-day post-PH time period, animals in the RP and DAPM/RP groups have significantly (P<0.05) lower liver weights and liver/body weight ratios than

those observed in DAPM/PH and DMSO/PH control groups, suggesting that regeneration is not complete and may be ongoing in these retrorsine-exposed animals **(FIGURE 3.10B-C)**.

Examination of H&E stained liver tissue harvested from DAPM/RP rats reveals a SHPC-mediated regenerative response similar to that observed in RP rats **(FIGURE 3.9)**. Livers harvested from RP animals contain SHPC clusters that are easily recognized by 3-days post-PH **(FIGURE 3.9F)**. These cell clusters expand through 7 and 10-days post-PH, reach lobule size by 14-days post-PH, and eventually replace the injured hepatocytes and restore the liver mass **(FIGURE 3.9G-J)**. Similarly, SHPC clusters are seen in liver tissues harvested from DAPM/RP animals at 3-days post-PH **(FIGURE 3.9A)**. These cell clusters expand through 7-days and 10-days post-PH **(FIGURE 3.9B-C)** and reach lobule size by 14-days post-PH **(FIGURE 3.9D)**. Moreover, SHPC clusters in the livers of DAPM/RP rats ultimately replace damaged hepatocytes resulting in the normalization of the liver parenchyma by 30-days post-PH **(FIGURE 3.9E)**. Thus, the cellular regenerative response observed in DAPM/RP animals is indistinguishable from that seen in RP animals. Oval cells are never observed after PH in DAPM/RP rats, reflecting the effectiveness of the DAPM treatment. Likewise, SHPC clusters are never observed in DAPM/PH, DMSO/PH, DAPM only, and DMSO only control rats **(FIGURES 3.7 AND 3.9)**. In addition, SHPCs are not observed in animals treated with retrorsine only in the absence of PH or after PH in control animals that do not receive retrorsine (39). Together, these observations suggest that liver regeneration in DAPM/RP rats is mediated by an oval cell-independent SHPC response and is histologically identical to that observed in RP rats.

Immunostaining of oval cell/biliary tract marker cytokeratin 19 in DAPM-treated retrorsine-exposed rats.

Oval cells originate from cells located in the portal tracts (possibly biliary epithelial cells) and expansively proliferate in several models of liver injury and regeneration (6, 15, 20, 60). DAPM-induced destruction of bile ducts effectively eliminates the oval cell reaction after PH in these models of liver injury secondary to bile duct injury (60). In the current study, oval cells were never observed in H&E stained liver sections of DAPM-treated animals **(FIGURE 3.9)**. To verify the absence of an oval cell response following DAPM treatment in experimental rats, tissues from DAPM/RP animals were immunostained for ck19. At 3 and 7-days post-PH, residual (DAPM-damaged) biliary tracts are decorated by antibodies to ck19 in DAPM/RP animals, but proliferating oval cells are not observed **(FIGURE 3.11A-B)**. In contrast, liver harvested from a rat that was treated with 2-AAF shows a robust ck19-positive oval cell response following PH, as reported by others (68-70). At 7-days post-PH in 2-AAF-treated animals, oval cells are clearly present in H&E stained liver tissue **(FIGURE 3.11C)**. Ck19 immunostaining of liver tissue from these animals clearly labels proliferating oval cells **(FIGURE 3.11D)**. Together, these results demonstrate that oval cells are not present after PH in DAPM-treated retrorsine-exposed animals, suggesting strongly that oval cells are not the source of the SHPCs.

Morphometric analysis of SHPC clusters in DAPM/RP rats.

To determine if the magnitude of SHPC responses observed in DAPM/RP and RP rats are similar, morphometric analyses on H&E stained liver sections from these animals at 7 and 14-days post-PH were performed. At 7-days post-PH there is no significant difference in the number (P=0.359) or size (P=0.286) of the SHPCs clusters observed in DAPM/RP and RP animals **(TABLE 3.2)**. Likewise, at 14-days post-PH there is no significant difference in the number (P=0.122) or size (P=0.268) of SHPC clusters observed in RP and DAPM/RP

FIGURE 3.11. *Immunostaining for cytokeratin 19 suggests a lack of oval cell activation in DAPM treated animals.* Immunostaining of cytokeratin 19 (ck19) in DAPM/RP animals at 3-days post-PH (A) labels bile duct remnants. At 7-days post-PH (B), ck19 immunostaining labels the recovered/normalized biliary tissue and portal tracts. No ck19-postive oval cells are observed in the liver parenchyma at either of these time points (A,B). In contrast, liver tissue harvested from a 2-AAF/PH rat at 7-days post-PH contain large numbers of oval cells in (H&E stained section, C), and these oval cells are clearly decorated by ck19 (D). (Original objective lens magnification 10x).

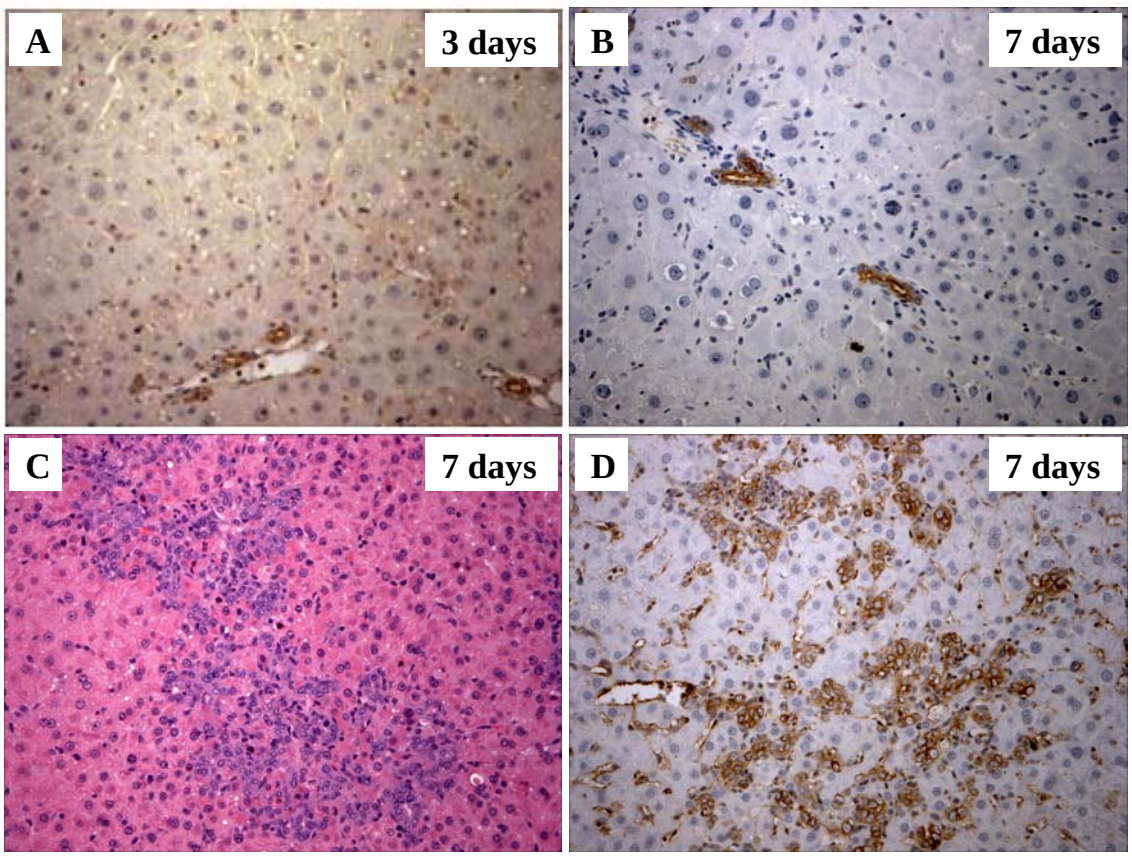
A
3 days
B
7 days
C
7 days
D
7 days

Table 3.2. *Number and Size of SHPC Clusters in Liver Sections from DAPM-treated Retrorsine-exposed Animals*

	7-days Post-PH		14-days Post-PH	
	Number of Clusters[1]	Size of Clusters[2]	Number of Clusters	Size of Clusters
RP	$82 \pm 2^{*}_{(n=3)}$	$4.8 \times 10^4 \pm 1.8 \times 10^{3\#}_{(n=100)}$	$95 \pm 14^{**}_{(n=5)}$	$8.7 \times 10^4 \pm 4.1 \times 10^{3\#\#}_{(n=100)}$
DAPM/RP	$60 \pm 20_{(n=4)}$	$5.2 \times 10^4 \pm 3.4 \times 10^3{}_{(n=100)}$	$117 \pm 12_{(n=3)}$	$9.3 \times 10^4 \pm 4.6 \times 10^3{}_{(n=100)}$

[1]Numbers of SHPC clusters represent mean ± standard error of the mean (n=number of animals/tissue sections analyzed). The number of SHPC clusters in each section was normalized to the cross-sectional area of the liver section analyzed.

[2]Size of clusters (given in μm^2) represents mean ± standard error of the mean (n=number of clusters analyzed per animal, between 3-5 animals analyzed per treatment group).

*P=0.359 (NS) for RP versus DAPM/RP at 7-days post-PH. **P=0.122 (NS) for RP versus DAPM/RP at 14-days post-PH.

#P=0.286 (NS) for RP versus DAPM/RP at 7-days post-PH. ##P=0.268 (NS) for RP versus DAPM/RP at 14-days post-PH.

animals **(TABLE 3.2)**. These data are consistent with the suggestion that the SHPC-mediated regenerative responses observed in RP rats and DAPM/RP rats are indistinguishable.

LIVER REGENERATION AFTER CCL_4 TREATMENT IN RETRORSINE-EXPOSED RATS

Rationale

The results of our studies strongly suggest that SHPCs are not derived from oval cells or any other biliary cell type and that the stem cell niche may not be restricted to the periportal aspect of the hepatic lobule. In fact, Gordon *et al.* observed that emerging SHPC clusters arise in all three zones of the hepatic lobule (39). These observations combine to suggest that SHPCs may represent a parenchymal stem-like cell with distribution to all three zones of the liver lobule. To begin to address this possibility, we treated retrorsine-exposed rats with the necrotizing agent CCl_4. In rats, administration of CCl_4 results in the targeted destruction of pericentral and centrilobular hepatocytes (50). Therefore, if the SHPCs (or their progenitors) are localized or restricted to the pericentral or centrilobular zones of the parenchyma then the SHPC-mediated regenerative response will be diminished or blocked after CCl_4 treatment in retrorsine-exposed rats.

Effects of carbon tetrachloride treatment on liver in retrorsine-exposed rats.

As reported previously (71), CCl_4 administration produced significant liver damage in the form of pericentral necrosis, but loss of liver tissue mass was not observed. Liver tissue harvested 24-hours after CCl_4 injection contains significant necrosis of the liver parenchyma with loss of approximately 59 ± 2% of hepatocytes **(FIGURE 3.11)**. This extent of liver injury is observed in 100% of animals exposed to CCl_4. CCl_4-mediated injury was highly specific

FIGURE 3.12. *Effects of carbon tetrachloride treatment on rat liver.* H&E stained liver tissue harvested 24-hours post-CCl_4 shows that approximately 60% of the parenchyma has undergone necrosis and that the CCl_4-induced damage is specific to the pericentral zone of the liver (A,B). Necrotic tissue is easily observed surrounding the central vein (C), while the area around the portal triad remains intact (D). Pericentral hepatocytes exhibit damage and loss of structural integrity (E). In contrast, periportal hepatocytes appear normal (D). Original objective lens magnification: 4x (A,B), 10x (C,D), and 20x (E,F).

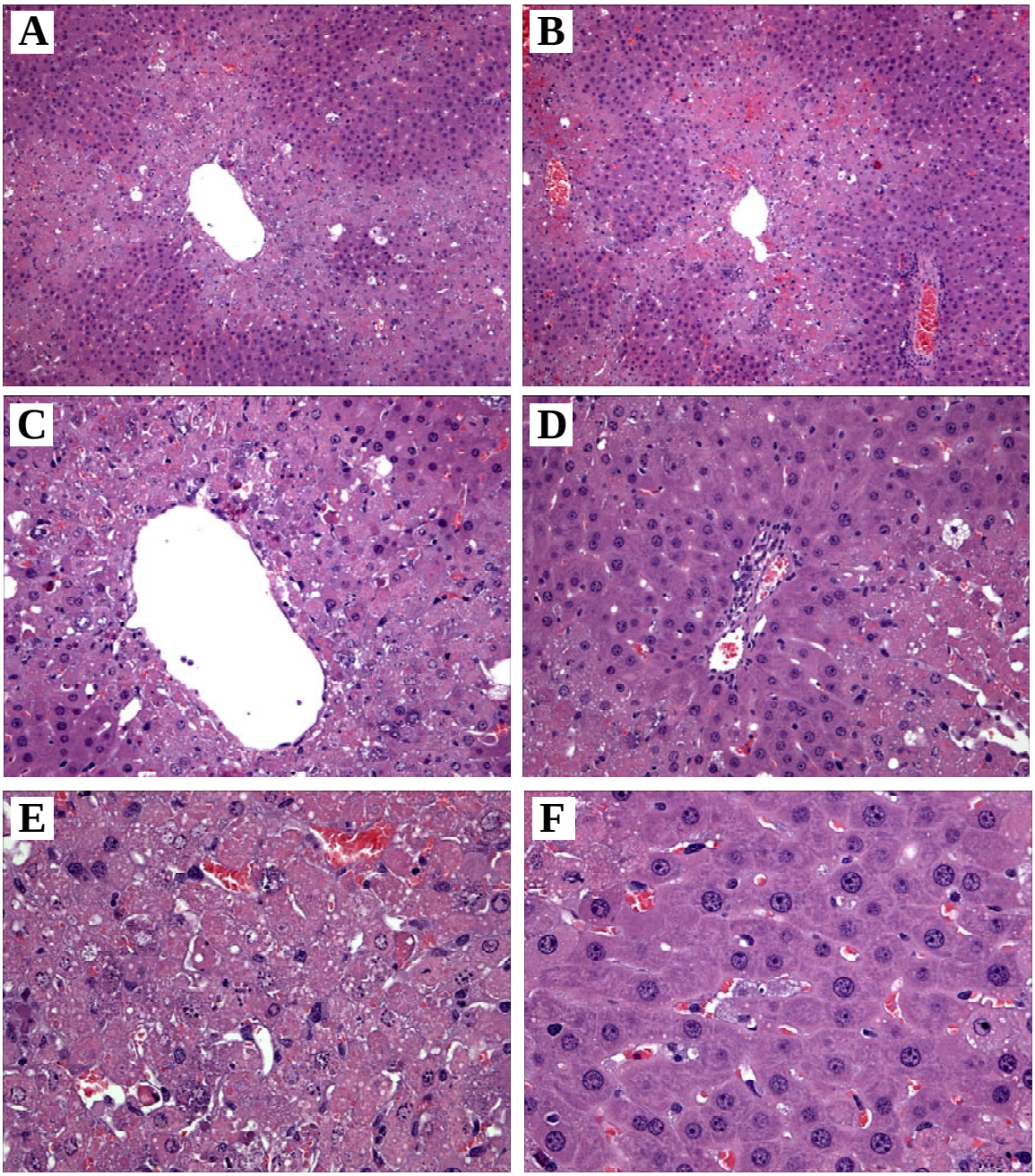
A
B
C
D
E
F

FIGURE 3.13. *Liver regeneration after carbon tetrachloride treatment in retrorsine-exposed rats.* The effects of CCl_4 treatment on (A) average body weight, (B) average liver weight, and (C) average liver/body weight ratios are shown. Each bar represents mean calculated from all surviving animals in the various experimental groups (± SEM, n=3 per time point). Asterisks denote statistically significant differences ($P<0.05$) among groups compared. NS denotes no statistically significant differences observed.

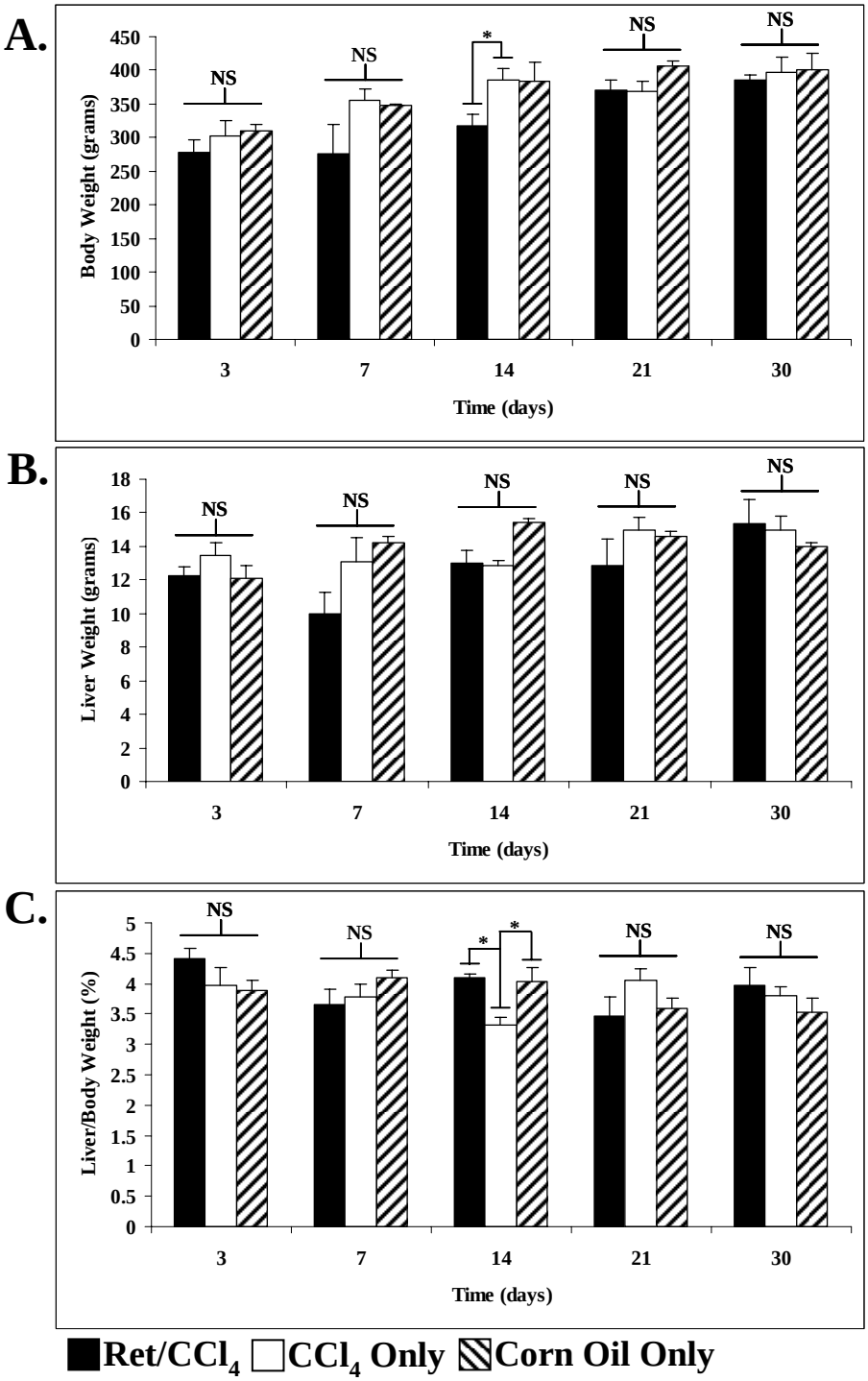
A.
Body Weight (grams)
450
400
350
300
250
200
150
100
50
0
NS
NS
*
NS
NS
3
7
14
21
30
Time (days)
B.
Liver Weight (grams)
18
16
14
12
10
8
6
4
2
0
NS
NS
NS
NS
NS
3
7
14
21
30
Time (days)
C.
Liver/Body Weight (%)
5
4.5
4
3.5
3
2.5
2
1.5
1
0.5
0
NS
NS
*
*
NS
NS
3
7
14
21
30
Time (days)
Ret/CCl4
CCl4 Only
Corn Oil Only

to pericentral and centrilobular hepatocytes, with virtually no damage to hepatocytes in the periportal zone **(FIGURE 3.11)**. However, necrosis is never observed in animals treated with corn oil (vehicle) only **(FIGURE 3.12)**, nor is it observed in animals receiving retrorsine only (39).

Regenerative responses to carbon tetrachloride treatment in retrorsine-exposed rat liver.

Ret/CCl_4 animals have body weights, liver weights, and liver/body weight ratios that are similar (P>0.05) to those observed in CCl_4 and corn oil only (control) rats at all time points after injection with the exception of the 14-day post-CCl_4 time point when significant differences are observed among groups in body weight and liver/body weight ratios **(FIGURE 3.13)**. Analysis of liver tissue from Ret/CCl_4 rats reveals that the regenerative response in these animals is similar to that observed after PH in RP rats (39). At 3-days after CCl_4 injection, SHPC clusters are found in retrorsine-exposed rats **(FIGURE 3.13A)**, continue to expand through 7-days and 14-days post-CCl_4 **(FIGURE 3.13B-C),** and have begun to differentiate into mature hepatocytes by 30-days post-CCl_4 **(FIGURE 3.13E)**. In RP rats, SHPCs emerge by 3-days post-PH **(Figure 3.8F)**, expand through 7-days and 10-days post-PH, reach lobule size by 14-days post-PH, and eventually replace the injured hepatocytes and restore the liver mass by 30-days post-PH **(FIGURE 3.8G-J)**. Thus, the SHPC responses are nearly identical in Ret/CCl_4 and RP rats, suggesting that the cellular reaction to liver injury is mediated by the same cells. SHPCs are never observed at any time point after injection in CCl_4 only **(FIGURE 3.13E-H)**, nor are they observed at any time after injection in animals receiving vehicle (corn oil) only **(FIGURE 3.13I-L)** or in rats that were treated with retrorsine only (39). These results suggest that SHPCs can respond to various forms of injury in retrorsine-exposed rats, involving both necrosis and surgical resection.

FIGURE 3.14. *Destruction of the centrilobular zone of the liver by carbon tetrachloride does not block the SHPC regenerative response in retrorsine-exposed rats.* SHPCs appear in Ret/CCl_4 rat liver at (A) 3-days post-CCl_4, continue to expand through (B) 7-days and (C) 14-days post-CCl_4, with completion restoration of parenchymal structure by (D) 30-days post-CCl_4. (E-H) SHPCs are never observed at any time point after injection in CCl_4 only rats. Likewise, SHPCs are never observed in vehicle (corn oil) only rats (I-L). Arrows indicate SHPC clusters. (Original objective lens magnification 10x).

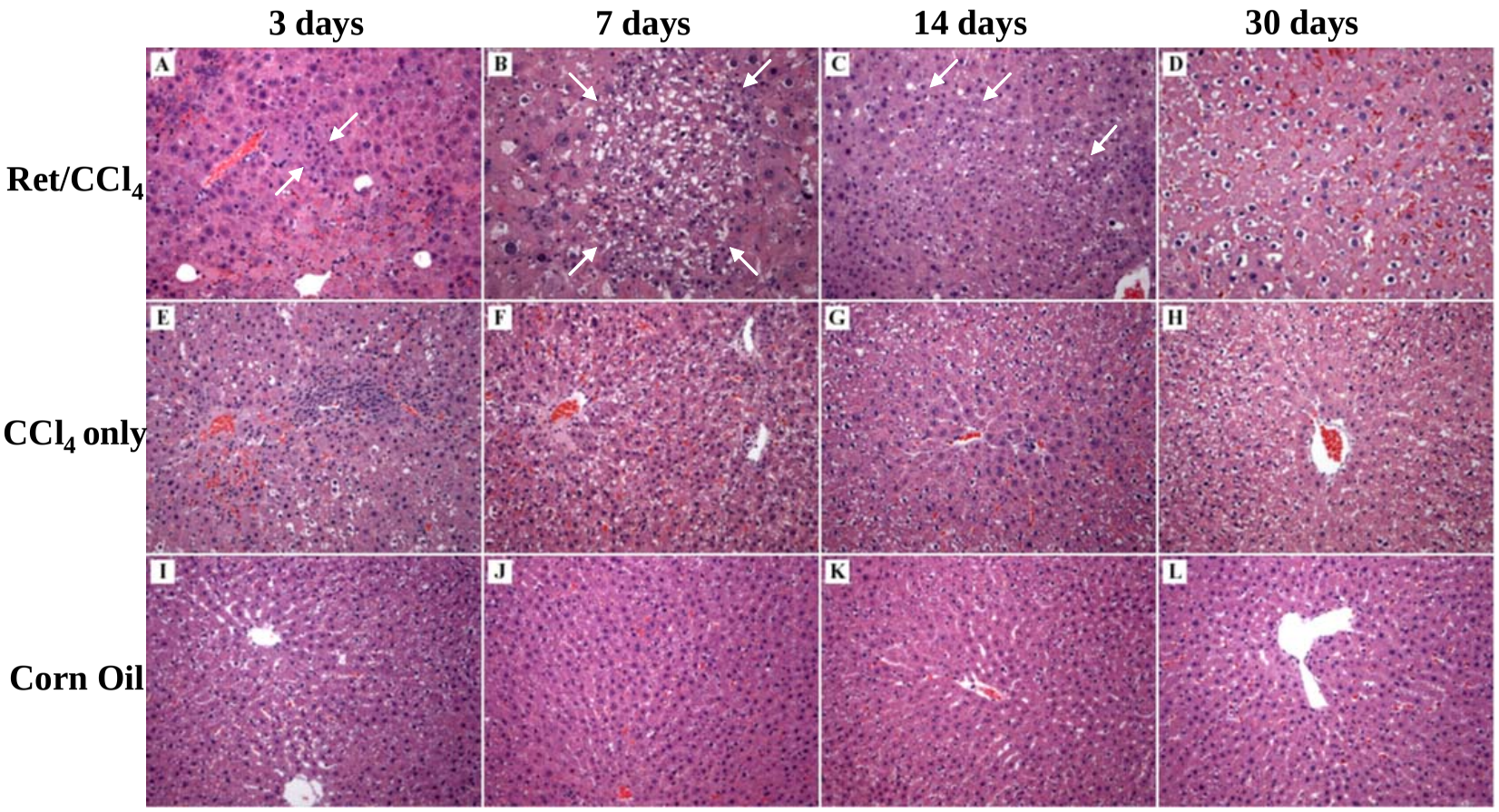
3 days
7 days
14 days
30 days
Ret/CCl4
CCl4 only
Corn Oil
A
B
C
D
E
F
G
H
I
J
K
L

FIGURE 3.15. *Immunohistochemical analysis of carbon tetrachloride-treated retrorsine-exposed rat liver.* Cytokeratin 19 immunostaining labels few parenchymal cells but strongly labels the biliary tracts at (A) 3-days post-CCl_4. Decoration of the biliary tracts continues through (B) 7 days and (C) 14-days post-CCl_4. α-fetoprotein immunostaining labels SHPCs at all time points but also decorates injured hepatocytes and megalocytes, (D-F). (Original objective lens magnification 10x).

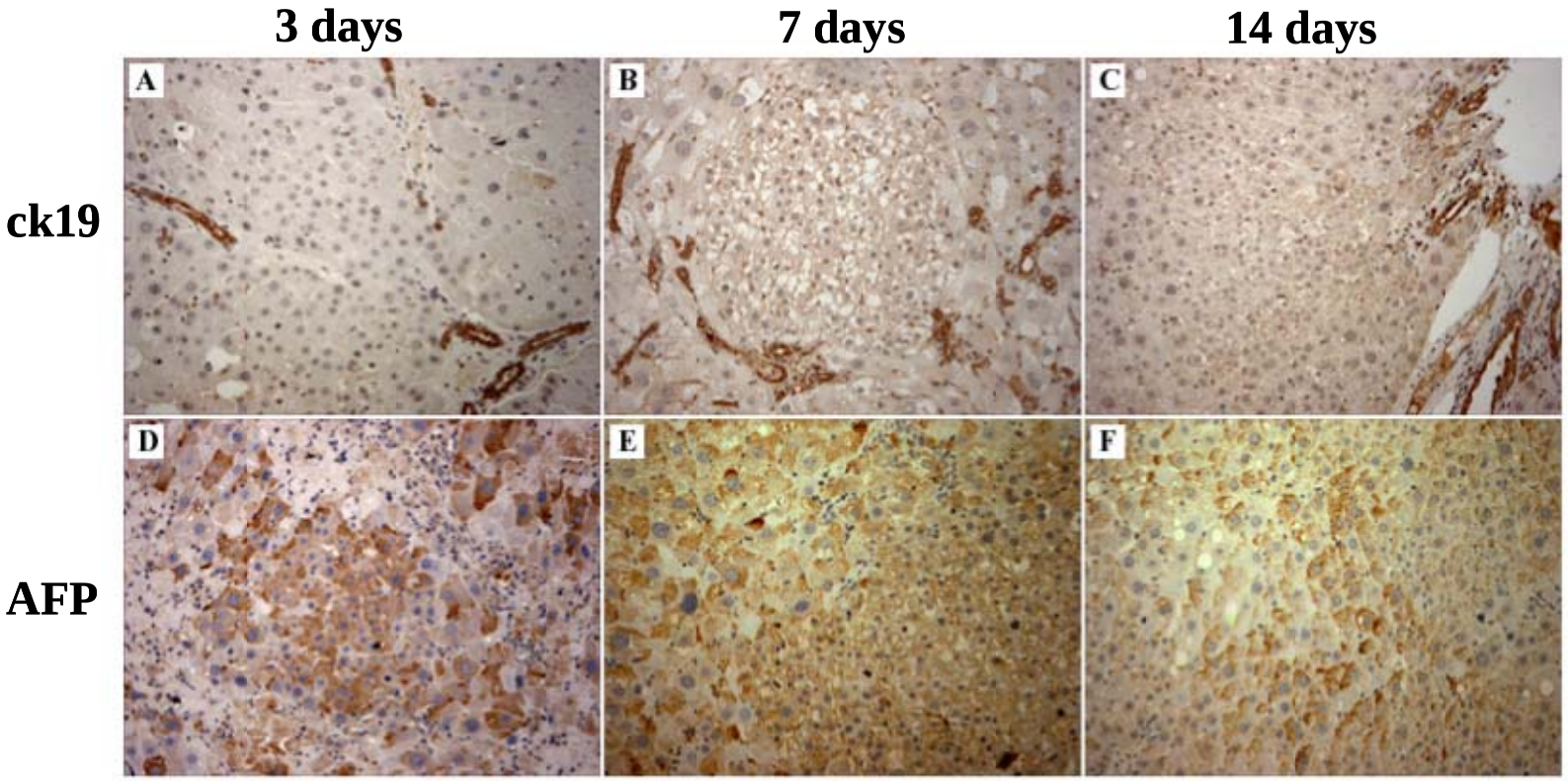
3 days
7 days
14 days
ck19
AFP
A
B
C
D
E
F

Table 3.3. *Number and Size of SHPC Clusters in Liver Sections from Ret/CCl_4-exposed Animals*

	7-days Post-CCl_4/PH		14-days Post-CCl_4/PH	
	Number of Clusters[1]	Size of Clusters[2]	Number of Clusters	Size of Clusters
RP	$82 \pm 2^{*}_{(n=3)}$	$4.8 \times 10^4 \pm 1.8 \times 10^{3\#}_{(n=100)}$	$95 \pm 14^{**}_{(n=5)}$	$8.7 \times 10^4 \pm 4.1 \times 10^{3\#\#}_{(n=100)}$
Ret/CCl_4	$93 \pm 20_{(n=5)}$	$7.9 \times 10^4 \pm 3.8 \times 10^3_{(n=100)}$	$132 \pm 4_{(n=2)}$	$8.7 \times 10^4 \pm 4.0 \times 10^3_{(n=100)}$

[1]Numbers of SHPC clusters represent mean ± standard error of the mean (n=number of animals/tissue sections analyzed). The number of SHPC clusters in each section was normalized to the cross-sectional area of the liver section analyzed.

[2]Size of clusters (given in μm^2) represents mean ± standard error of the mean (n=number of clusters analyzed per animal, between 3-5 animals analyzed per treatment group).

*P=0.621for RP versus Ret/CCl_4 at 7-days post-PH. **P=0.062 for RP versus Ret/CCl_4 at 14-days post-PH.

#P<0.0001 for RP versus Ret/CCl_4 at 7-days post-PH. ##P=0.903 for RP versus Ret/CCl_4 at 14-days post-PH.

Immunohistochemical analysis of carbon tetrachloride-treated retrorsine-exposed rat liver.

Previously it has been demonstrated that oval cells do not respond in significant numbers to surgical resection of the liver in retrorsine-exposed rats (39). In order to determine the magnitude of oval cell response to necrotic injury in retrorsine-exposed rats, liver tissue harvested at various times after CCl_4 injection was immunostained for the oval cell marker ck19. Significant numbers of ck19-postive cells are never observed in the parenchyma of Ret/CCl_4 rats at any time point after CCl_4 injection **(FIGURE 3.14A-C)**. At 3-days post-CCl_4, ck19-positive cells and biliary tracts are observed, but ck19-positive cells are never seen proximal to SHPC clusters **(FIGURE 3.14A)**. By 7-days and 14-days post-CCl_4 only the biliary tracts stain positive in Ret/CCl_4 animals **(FIGURE 3.14B-C)**. These observations suggest that oval cells do not significantly contribute to liver regeneration after CCl_4 exposure in retrorsine-exposed rats.

In RP rats, SHPCs express α-fetoprotein (AFP) until 20+ days after PH (72). In order to determine if SHPCs observed in Ret/CCl_4 rats exhibit similar phenotypic patterns as those observed in RP rats, liver tissues from Ret/CCl_4 rats at 3, 7, and 14-days post-injection were immunostained for AFP. SHPCs observed in Ret/CCl_4 rats were positive for AFP at these time points **(FIGURE 3.14D-F)**. However, hepatocytes (hepatocytic megalocytes) also exhibit AFP-positive staining in these animals **(FIGURE 3.14D-F)**. Expression of AFP by retrorsine-injured megalocytes may reflect the nature of the CCl_4 injury in these animals, consistent with previous findings in animals treated with CCl_4 (73).

Morphometric analysis of the small hepatocyte-like progenitor cell response in carbon tetrachloride-treated retrorsine-exposed rats.

To directly compare the magnitude of SHPC-mediated regenerative responses observed in Ret/CCl_4 rats with that of RP animals, morphometric analysis was performed on SHPC clusters observed in these animals. This analysis shows that the number of SHPC clusters in the livers of Ret/CCl_4 rats at 7-days post-CCl_4 is not significantly (P>0.05) different from the number of SHPC clusters observed in RP rats at this same time point **(TABLE 3.3)**. However, the size of SHPC clusters observed in Ret/CCl_4 rats at 7-days post-CCl_4 are 40% larger than those observed in RP rats **(TABLE 3.3)**. There is no significant difference (P>0.05) in the average number of cells present in the SHPC clusters of Ret/CCl_4 and RP rats (150 ± 10 in Ret/CCl_4 versus 142 ± 9 in RP). Thus, differences in the size of these clusters are due to variation in the size of the SHPCs composing these clusters. Morphologically, the SHPCs found in the livers of Ret/CCl_4 rats are highly vacuolated **(FIGURE 3.12)**. This feature of the cells is also observed in RP rats, but is much more pronounced in Ret/CCl_4 animals **(FIGURE 3.12)**. These results demonstrate that the SHPC-mediated regenerative response is not dampened by destruction of the pericentral region of the liver parenchyma, suggesting that the progenitor cells that give rise to SHPCs are not restricted the this zone of the liver.

CYTOKINE-DEPENDENT PRIMING OF SMALL HEPATOCYTE-LIKE PROGENITOR CELLS

Rationale

Cytokines (such as IL6, TNF-α) play an important role in the priming (activation) of both hepatocytes and oval cells for proliferation after liver injury or surgical resection (12, 21). However, the role that cytokines play in the activation of SHPCs has not been investigated. Therefore, we examined the possibility that cytokines are required for the

activation of SHPCs after injury by treating retrorsine-exposed rats with either a single dose or multiple doses (n=5) of the cytokine inhibitor dexamethasone (DEX). Other investigators established that DEX inhibits TNF-α and IL6 production in rat liver by interfering with the transcription of their respective genes (52, 74, 75). DEX has been used to block the activation of mature hepatocytes and oval cells after PH in the livers of F344 rats (52). Thus, if cytokine-priming is required for activation of the SHPC-mediated regenerative response, then treatment of retrorsine-exposed rats with DEX prior to PH should impair emergence and proliferation of SHPCs.

A single dexamethasone treatment dampens the small hepatocyte-like progenitor cell response after partial hepatectomy in retrorsine-exposed rats.

DRP (dexamethasone/retrorsine/PH) rats tolerate the experimental treatment protocol with minimal treatment-related mortality (90% surviving to 7 days). Following PH, DRP animals demonstrate weight gain comparable to that observed in RP and CP rats **(FIGURE 3.16A)**. The livers of CP rats rapidly recover tissue mass after PH, with complete regeneration by 14-days post-PH **(FIGURE 3.16B)**. RP rats also completely regenerate their livers after PH, but with a more protracted course. The liver weights of RP rats do not significantly increase during the first 14-days post-PH, but a progressive enlargement of liver size occurs from 14 to 30-days post-PH, with full restoration of liver mass by 30-days post-PH **(FIGURE 3.16B)**. CP rats rapidly restore normal liver/body weight ratios after PH (by 7 days), indicative of the robust regenerative activity in the livers of these animals **(FIGURE 3.16C)**. The restoration of normal liver/body weight ratio in RP rats occurs with a timing that reflects restoration of liver mass, with completion of this process by 30-days post-PH **(FIGURE 3.16C)**. In contrast, there is no appreciable gain of liver weight during the first 21-

FIGURE 3.16. *A single DEX treatment delays liver regeneration in retrorsine-exposed rats.* The effects of a single DEX dose on (A) average body weight, (B) average liver weight, and (C) average liver/body weight ratios are shown. All DRP animals received a single dose (2 mg/kg) of DEX 1 hour prior to PH. RP and CP animals did not receive DEX treatment. Each bar represents the mean calculated from all surviving animals (n=3-5) in the various experimental groups (± SEM). NS denotes no significant difference in DRP and RP weights.

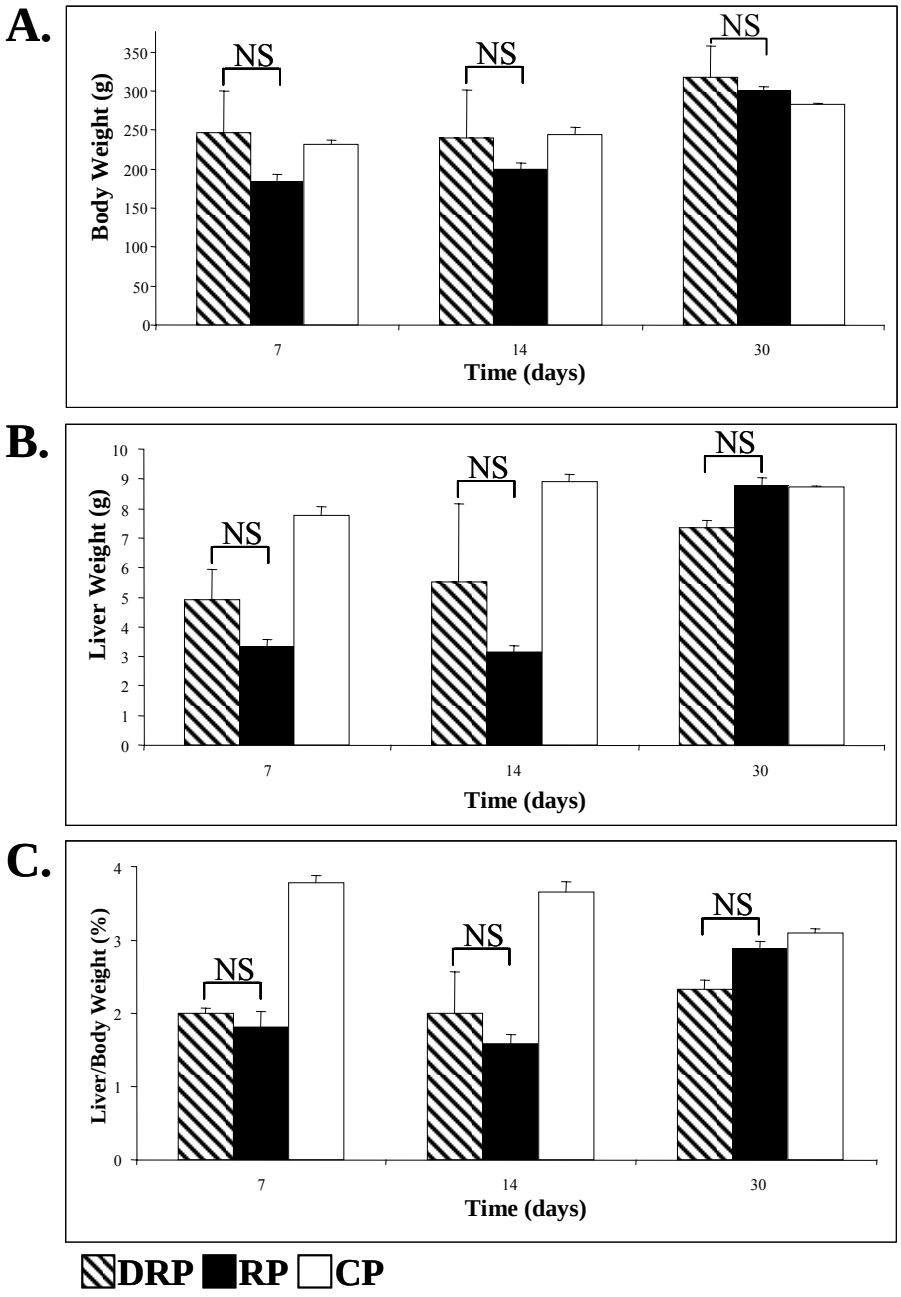
A.
Body Weight (g)
350
300
250
200
150
100
50
0
NS
NS
NS
7
14
30
Time (days)
B.
Liver Weight (g)
10
9
8
7
6
5
4
3
2
1
0
NS
NS
NS
7
14
30
Time (days)
C.
Liver/Body Weight (%)
4
3
2
1
0
NS
NS
NS
7
14
30
Time (days)
DRP
RP
CP

days post-PH among DRP rats, but an increase in liver weight is observed by 30-days post-PH **(FIGURE 3.16B)**. This observation suggests that a single dose of DEX dampens SHPC-mediated liver regeneration in retrorsine-treated rats. DRP rats do not achieve a normal liver/body weight ratio during the first 30-days after PH, but this measurement improves during the experimental period, consistent with an impaired regenerative response in these animals **(FIGURE 3.16C)**.

SHPCs are found among megalocytic hepatocytes at 7-days post-PH in DRP rats **(FIGURE 3.17E)**, but these regenerative SHPC clusters are 60% smaller (average cluster size of $1.92 \pm 0.44 \times 10^4$ μm^2, n=62, $P<0.0001$ for RP versus DRP at 7-days post-PH) than those observed in RP rats at this time point **(FIGURE 3.17 AND TABLE 3.4)**. During the subsequent time period (14 and 21-days post-PH), the SHPC clusters expand and eventually occupy approximately 50% of the liver parenchyma by 30-days post-PH. This observation is consistent with the partial normalization of liver/body weight ratios in these animals over this period of time. In comparison, liver tissue from RP rats (in the absence of DEX treatment) contain clusters of SHPCs at 7-days post-PH that progressively and rapidly expand from 14 to 21-days post-PH, eventually repopulating nearly the entire liver parenchyma by 30-days post-PH **(FIGURE 3.17)**. In DRP and RP rats, oval cell proliferation is minimal and limited to the periportal regions (39). In addition, SHPC clusters are never observed in CP animals (39).

Multiple dexamethasone treatments block the production of IL6 after partial hepatectomy.

To determine IL6 levels after PH, ELISA was performed on serum samples collected from CP, MDCP (multiple dexamethasone/control/PH), and MDRP (multiple dexamethasone/retrorsine/PH) animals at 1, 12, and 48-hours post-PH. Rats in the CP group

FIGURE 3.17. *A single DEX treatment dampens the SHPC response after PH in retrorsine- exposed rats.* H&E stained liver sections from retrorsine-exposed rats at (A) 7-days, (B) 14-days, (C) 21-days, and (D) 30-days post-PH are shown. Liver tissue from retrorsine-exposed rats treated with a single dose of DEX (1 hour prior to PH) at (E) 7-days, (F) 14-days, (G) 21-days, and (H) 30-days post-PH are shown. Arrows indicate SHPC clusters. (Original objective lens magnification 10x).

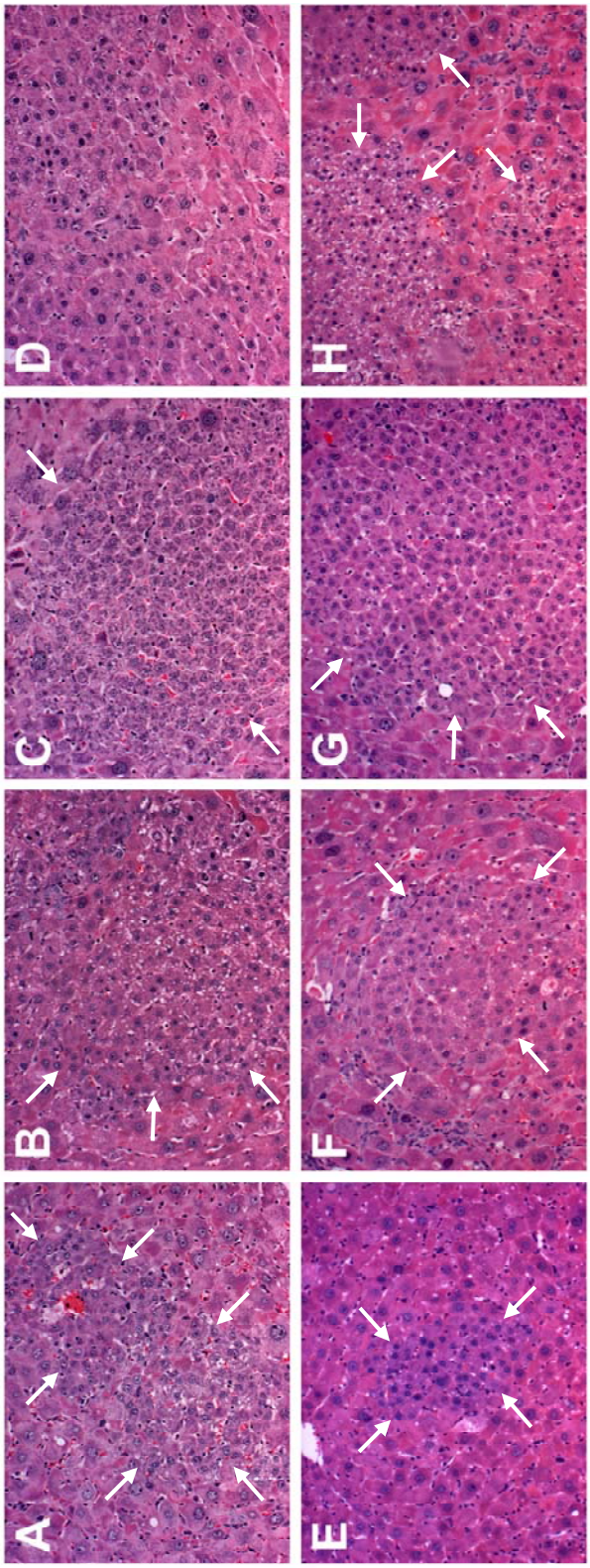
A
B
C
D
E
F
G
H

Table 3.4. *Number and Size of SHPC Clusters in Liver Sections from DEX-treated Retrorsine-exposed rats*

	7-days Post-PH		14-days Post-PH	
	Number of Clusters[1]	Size of Clusters[2]	Number of Clusters	Size of Clusters
RP	$80 \pm 11_{(n=3)}$	$4.8 \times 10^4 \pm 1.8 \times 10^3{}_{(n=100)}$	$79 \pm 8^{**}_{(n=5)}$	$8.7 \times 10^4 \pm 4.1 \times 10^3{}_{(n=100)}$
MDRP	$8 \pm 3^{*}_{(n=3)}$	$2.2 \times 10^4 \pm 1.6 \times 10^{3\#}{}_{(n=70)}$	$18 \pm 6^{***}_{(n=3)}$	$3.4 \times 10^4 \pm 3.2 \times 10^{3\#\#\#}{}_{(n=100)}$
MDRP/IL6	$22 \pm 7_{(n=3)}$	$2.3 \times 10^4 \pm 1.3 \times 10^{3\#\#}{}_{(n=100)}$	$49 \pm 7^{****}_{(n=6)}$	$7.1 \times 10^4 \pm 4.0 \times 10^{3\#\#\#\#}{}_{(n=100)}$

[1]Numbers of SHPC clusters represent mean ± standard error of the mean (n=number of animals/tissue sections analyzed). The number of SHPC clusters in each section was normalized to the cross-sectional area of the liver section analyzed.

[2]Size of clusters (given in μm^2) represents mean ± standard error of the mean (n=number of clusters analyzed per animal, between 3-5 animals analyzed per treatment group).

$^{*}P<0.0001$ for MDRP versus RP at 7-days post-PH. $^{**}P=0.0049$ for MDRP versus RP at 14-days post-PH. $^{***}P=0.208$ for MDRP 7-day post-PH versus MDRP at 14-days post-PH. $^{****}P=0.041$ for MDRP/IL6 versus RP at 14-days post-PH.

$^{\#}P<0.0001$ for MDRP versus RP at 14 days post-PH. $^{\#\#}P<0.0001$ for MDRP/IL6 versus MDRP at 14-days post-PH. $^{\#\#\#}P=0.0014$ for MDRP 7-days post-PH versus MDRP 14-days post-PH. $^{\#\#\#\#}P<0.0088$ for MDRP/IL6 versus RP at 14-days post-PH.

FIGURE 3.18. *Multiple DEX treatment effectively blocks the production of IL6 in retrorsine-exposed rats.* ELISA analysis demonstrates that multiple (n=5) DEX treatments results in the consistent blockade of IL6 production at 1, 12, and 48 hours after PH in both retrorsine-exposed and control rats. However, a consistent increase in IL6 levels is observed after PH in control animals that do not receive DEX treatment. Each bar represents the mean serum IL6 levels (pg/ml) calculated from of serum samples taken from (n=3-4) animals in the various experimental groups (± SEM). Large asterisk denotes presence of data but value too low to be visualized in graph (lowest value observable in graph 41 pg/ml). Small asterisks denote a statistically significant difference ($P<0.05$) among compared groups. NS denotes no statistically significant difference observed in compared values.

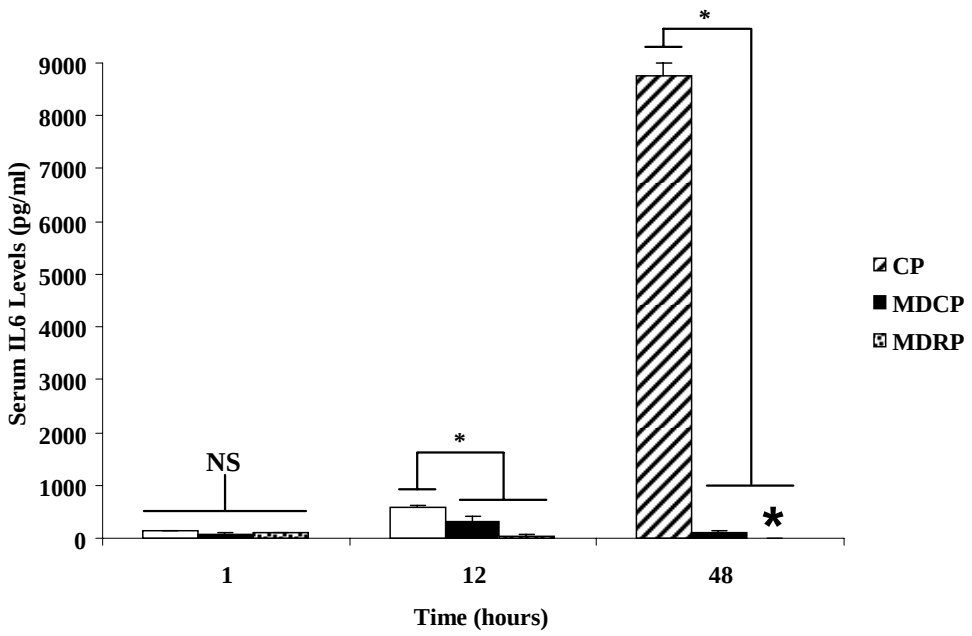
Serum IL6 Levels (pg/ml)
9000
8000
7000
6000
5000
4000
3000
2000
1000
0
NS
*
*
*
1
12
48
Time (hours)
CP
MDCP
MDRP

show a steady increase in IL6 levels over time after PH, reaching 8835 ± 299 pg/ml of IL6 at 48 hours after PH **(FIGURE 3.18)**. In contrast, negligible levels of IL6 were detected in MDCP and MDRP (P<0.05 at 12 and 24 hours for CP versus MDRP and MDCP) rats throughout the first 48-hours post-PH **(FIGURE 3.18)**. These data demonstrate that multiple DEX treatments effectively block the production of IL6 after PH.

Multiple dexamethasone treatments block the emergence and expansion of small hepatocyte-like progenitor cells after partial hepatectomy in retrorsine-exposed rats.

MDRP rats do not respond well to the experimental protocol, exhibiting signs of physical stress (lethargy, diarrhea) and high levels of post-operative mortality for the first 7-days following PH (22% surviving to 7 days) **(FIGURE 3.19)**. In addition, MDRP rats fail to gain weight during the course of 30-days post-PH **(FIGURE 3.20A)**, and there is no significant increase in liver mass in MDRP rats during the 30-day post-PH experimental period **(FIGURE 3.20B)**. In contrast, a slight recovery of liver weight is observed at 7-days post-PH in MDCP rats. These livers continue to increase in size through 14-days post-PH and are indistinguishable (P=0.167 for MDCP versus CP) from CP livers by the end of the experimental interval **(FIGURES 3.16B AND 3.20B)**. Similarly, the liver/body weight ratios of MDCP rats are consistently higher than those observed in MDRP (P<0.0001 for MDRP versus MDCP at 30-days post-PH) animals and reach CP levels by 30-days post-PH **(FIGURES 3.16C AND 3.20C)**. MDRP rats fail to reach CP liver/body weight ratios within the 30-days post-PH **(FIGURES 3.16C AND 3.20C)**, suggesting that the DEX-mediated blockade of IL6 significantly impairs liver regeneration by SHPCs in retrorsine-treated rats.

At 7-days after PH the livers of MDRP animals are characterized by megalocytic hepatocytes, rare small clusters of SHPCs, and sparse oval cells **(FIGURE 3.21 AND TABLE**

FIGURE 3.19. *Administration of IL6 improves survival of MDRP rats.* Retrorsine-exposed animals (n=9 at initiation of study) given multiple doses of DEX (blue line) exhibit high levels of mortality, whereas rats receiving a single intravenous dose (10 μg) of IL6 (red line) show increased survival (n=15 at initiation of study). Results presented are derived from a single 24 animal group receiving treatment concurrently, but are representative of trends observed throughout the study. (P=0.0057 by log-rank test).

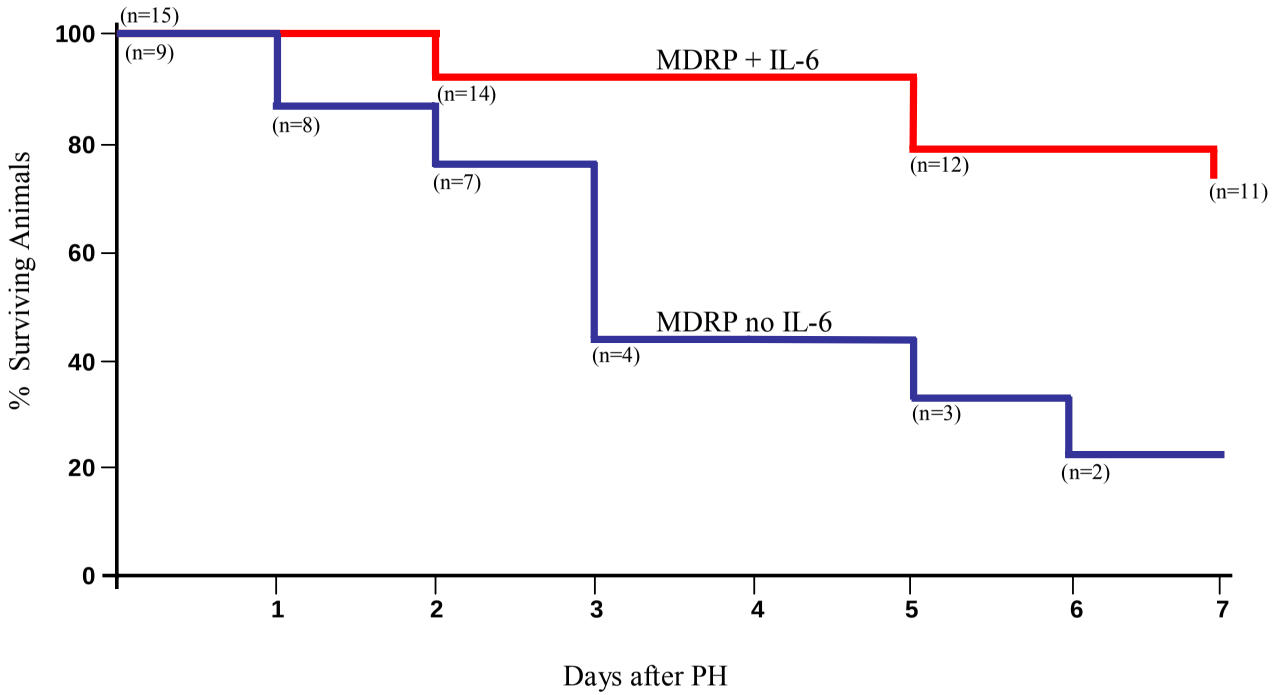
(n=15)
(n=9)
100
80
60
40
20
0
% Surviving Animals
MDRP + IL-6
(n=14)
(n=12)
(n=11)
(n=8)
(n=7)
MDRP no IL-6
(n=4)
(n=3)
(n=2)
1
2
3
4
5
6
7
Days after PH

3.4). The SHPC clusters expand in size modestly (32%) during the interval from 7-days to 14-days post-PH **(FIGURE 3.21 AND TABLE 3.4)**. Liver sections from MDRP animals that survive to 30-days post-PH contain SHPC clusters that are larger (average cluster size 7.1 x $10^4 \pm 7.3 \times 10^3$ μm^2 at 30-days post-PH, $P<0.0001$ for MDRP 30-days post-PH versus MDRP 14-days post-PH) than those observed at earlier time points, suggesting that some SHPC proliferation has occurred resulting in partial liver regeneration **(FIGURE 3.21)**. SHPC clusters in RP animals expand to completely regenerate the liver parenchyma by the end of the 30-day experimental period. Liver sections taken from CP, MDR (multiple dexamethasone/retrorsine), and MDCP animals do not exhibit SHPC clusters at any time during the experimental period **(FIGURE 3.21P-T)**.

At all time points examined, multiple DEX treatments suppressed SHPC emergence and expansion. At 7-days post-PH, RP animals contain 10-fold more SHPC clusters than MDRP rats (80 ± 11 SHPC clusters/liver section versus 8 ± 3 SHPC clusters/liver section) **(TABLE 3.4)**. The average number of SHPC clusters remains constant in RP animals at 14-days post-PH (79 ± 8 SHPC clusters/liver section), but the size of these clusters has nearly doubled. In contrast, MDRP animals show a marginal increase in the number (18 ± 6 SHPC clusters/liver section) and size of SHPC clusters at 14-days post-PH **(TABLE 3.4)**. At all time points analyzed MDRP animals contain the lowest average numbers of SHPC clusters. In addition, SHPC clusters observed in RP animals are substantially larger than those observed in MDRP animals at both 7 and 14-days post-PH (2.2-fold and 2.6-fold larger, respectively) **(TABLE 3.4)**.

IL6 administration rescues the SHPC regenerative response in retrorsine-exposed rats receiving multiple dexamethasone treatments.

MDRP/IL6 (multiple dexamethasone/retrorsine/PH/IL6) animals exhibit improved tolerance of the experimental protocol (73% surviving to seven days post-PH) compared to MDRP animals that do not receive IL6 **(FIGURE 3.19)**. Throughout the course of 30-days post-PH, the MDRP/IL6 rats consistently gain weight in manner comparable to that observed in CP and RP rats **(FIGURES 3.16A AND 3.20A)**. MDRP/IL6 animals also demonstrate increased liver mass and liver/body weight ratios, similar to those observed in RP animals **(FIGURES 3.16B-C AND 3.20B-C)**. Administration of IL6 to MDRP rats results in restoration of a robust SHPC response, suggesting that exogenous IL6 administration overcomes the DEX-mediated blockade of SHPC activation and expansion. The magnitude of the SHPC response in MDRP/IL6 animals is comparable to that observed in RP animals **(FIGURE 3.21)**. SHPC clusters emerge by day 7 and expand over time, reaching lobule size by 14-days post-PH. These expanding SHPC clusters merge to occupy the majority of the liver parenchyma by the end of the 30-day experimental period suggesting that regeneration of the liver in these animals is nearing completion.

The number of SHPC clusters present in MDRP/IL6 livers is not significantly different than the number found in MDRP animals at 7-days post-PH, and the size of the SHPC clusters is not significantly different between MDRP and MDRP/IL6 animals **(TABLE 3.4)**. However, by 14-days post-PH the number of SHPC clusters present in MDRP/IL6 animals is 2.7-fold higher than that observed in MDRP animals **(TABLE 3.4)**. Furthermore, there is a 300% increase in SHPC cluster size between 7 and 14-days post-PH in MDRP/IL6 and these clusters are only 18% smaller than those contained in RP animals at this time point suggesting that the regenerative responses observed in these two experimental groups is indistinguishable **(TABLE 3.4)**. In contrast, there is no significant increase in SHPC cluster

FIGURE 3.20. *Multiple DEX treatments block liver regeneration in retrorsine-exposed rats.* The effects of multiple doses of DEX on (A) average body weight, (B) average liver weight, and (C) average liver/body weight ratios are shown. All MDR (no PH), MDRP, MDRP/IL6, and MDCP animals received 5 doses of DEX (2 mg/kg each) at 1 day and 1 hour prior to PH, and then 1, 2, and 3 days after PH. Each bar represents the mean calculated from all surviving animals (n=3-6) in the various experimental groups (± SEM). Asterisks denotes significant differences in MDRP and MDRP/IL6 weights. NS denotes no significant difference in MDRP and MDRP/IL6 weights.

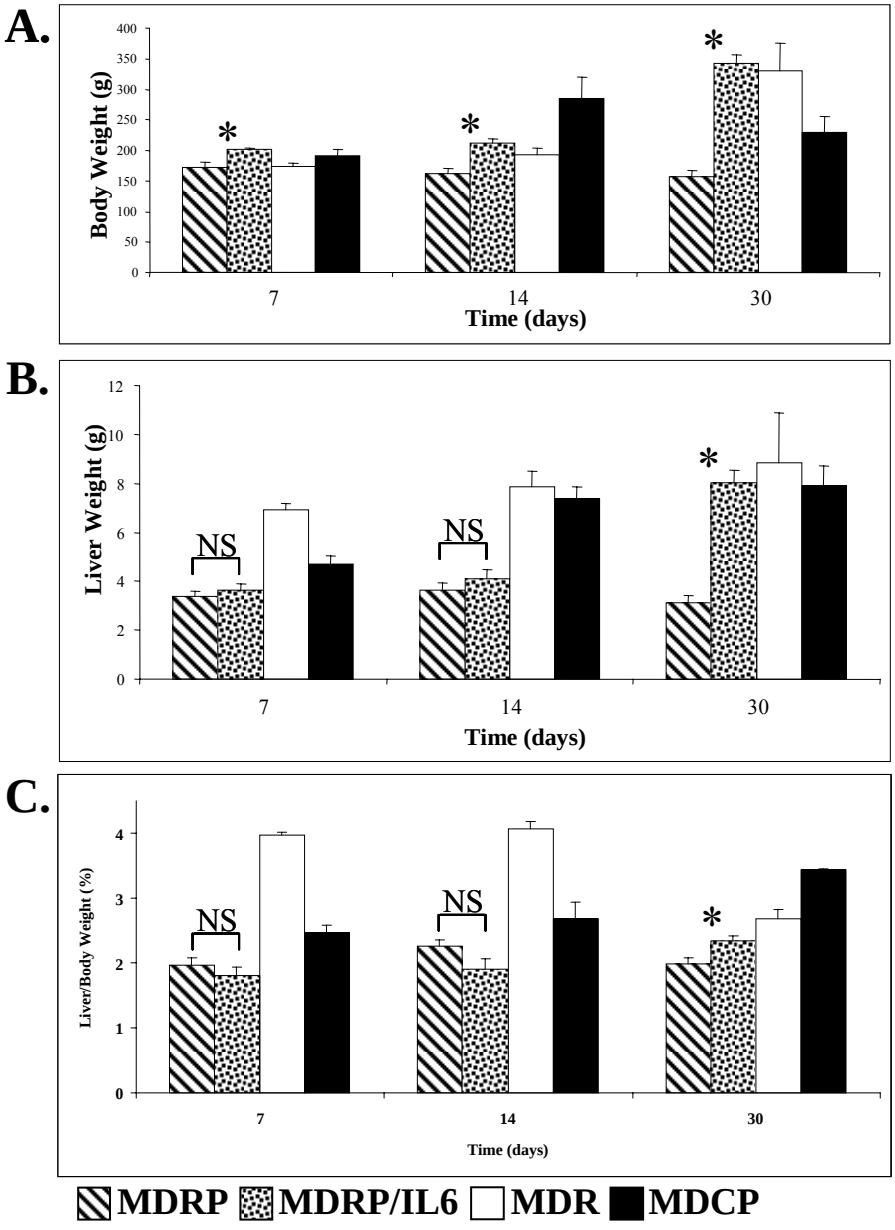
A.
Body Weight (g)
400
350
300
250
200
150
100
50
0
*
*
*
7
14
30
Time (days)
B.
Liver Weight (g)
12
10
8
6
4
2
0
NS
NS
*
7
14
30
Time (days)
C.
Liver/Body Weight (%)
4
3
2
1
0
NS
NS
*
7
14
30
Time (days)
MDRP
MDRP/IL6
MDR
MDCP

FIGURE 3.21. *IL6 administration restores the SHPC response to liver deficit in MDRP rats.* H&E stained liver sections from retrorsine-exposed animals at (A,B) 7-days, (C,D) 14-days, and (E) 30-days post-PH. H&E stained liver tissue from MDRP animals at (F,G) 7-days, (H,I) 14-days, and (J) 30-days post-PH. Liver tissue from MDRP/IL6 animals at 7-days (K,L), 14-days (M,N), and 30-days post-PH (O). Liver tissue from MDCP animals at 7-days (P), 14-days (Q), and 30-days post-PH (R). Liver tissue from MDR animals at 7-days (S) and 14-days (T) after DEX treatment. Arrows indicate SHPC clusters. (Original objective lens magnification 10x).

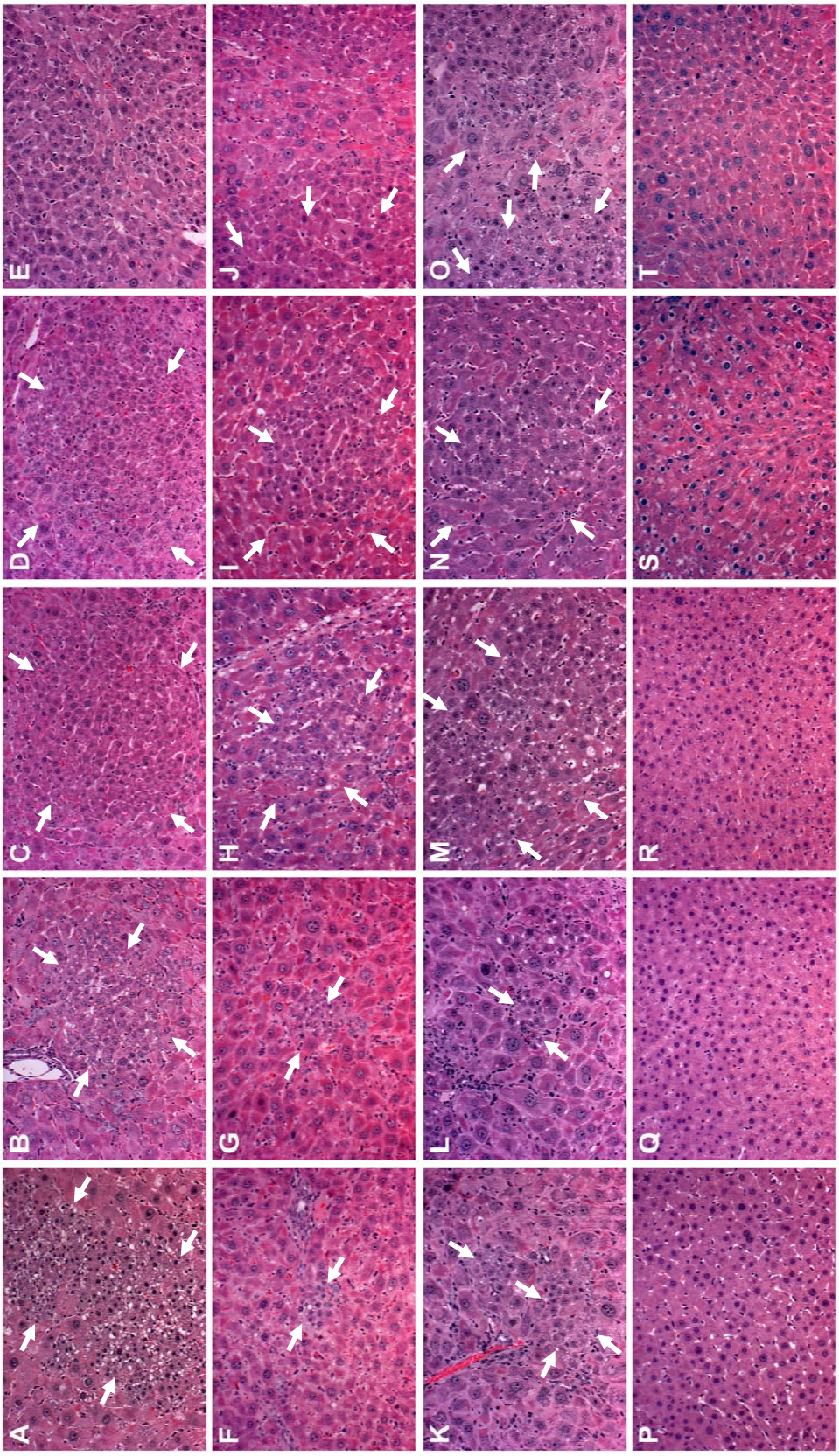
A
B
C
D
E
F
G
H
I
J
K
L
M
N
O
P
Q
R
S
T

size in MDRP animals during the 7 to 14-day post-PH interval and the SHPC clusters are significantly smaller than those in RP rats at 14-days post-PH suggesting that in the absence of cytokine priming SHPC-mediated liver regeneration does not occur **(TABLE 3.4)**.

IV. DISCUSSION

PYRROLIZIDINE ALKALOIDS

Pyrrolizidine alkaloids (PAs) are a family of naturally occurring toxins that are found worldwide in over 6000 plants of the three families, *Boraginaceae*, *Compositae*, and *Legumionsae* (76-78). PAs exert toxic effects on a variety of organ systems including the liver, blood vessels, pancreas, lungs, brain, kidneys, gastrointestinal tract, and bone marrow (77, 79, 80). However, toxicity varies dramatically among the 660 known PAs (76-79) and only a few PAs (i.e. lasiocarpine, retrorsine) have been used with any frequency in models of liver injury (39, 42, 44, 72, 81-84). The toxic effects of PAs are chronic and have been observed in the livers of animals more than one year after a single dose of PA (44). In the liver these effects include (but are not limited to) blockade of the cell cycle through DNA cross-linking and adduct formation, megalocytosis of hepatocytes, fibrosis, cirrhosis, as well as others (39, 41-44, 77, 79, 80, 82, 85-87). When treated with a PA and stimulated to proliferate, mature hepatocytes are incapable of dividing and instead undergo megalocytosis and subsequently apoptosis (39, 41, 77, 80-82). Thus, PAs are commonly employed in liver injury models as a means to block hepatocyte division, facilitating investigation of liver regeneration after injury by transplanted cells (hepatocytes and others) or other progenitor cell types (39, 62, 64, 81, 82).

PYRROLIZIDINE ALKALOIDS IN EXPERIMENTAL MODELS OF LIVER INJURY

One of the earliest studies to use a PA in a liver injury model was performed by Laconi *et al.* (82). In this investigation, F344 rats were exposed to the PA lasiocarpine in order to study the effects of transplanted mature hepatocytes on the development of chronic lesions in these animals (82). This study provided a strong framework for subsequent studies by the same group. Laconi *et al.* employed a similar liver injury model using the PA retrorsine to block hepatocyte proliferation to study the participation of transplanted hepatocytes in liver regeneration (81). In this model, F344 rats exposed to retrorsine were capable of regenerating their livers after PH if transplanted with an adequate number of normal hepatocytes (81). Since the publication of this study several investigators have used the retrorsine model of hepatocellular injury to study liver regeneration (39, 61, 62, 64). Perhaps the most significant finding of these studies was the discovery of the small hepatocyte-like progenitor cell by Gordon *et al.* (39). In this study Gordon *et al.* treated F344 rats with two doses of retrorsine and then stimulated hepatocyte proliferation through surgical PH (39). These investigators noted that the liver mass of these animals normalized by 30-days after PH, despite the absence of transplanted (exogenous) hepatocytes (39). This observation suggested that liver regeneration was not completely blocked by retrorsine treatment (39). However, histological examination of liver tissue from these retrorsine-exposed animals revealed the presence of clusters of proliferative cells beginning 1-3 days after PH (39). The cells contained in these clusters were histologically very similar to mature hepatocytes but were approximately one-third the size of mature hepatocytes. Based upon their morphologic characteristics, these cells were designated small hepatocyte-like progenitor cells (39). The SHPC clusters expanded through the subsequent interval, reaching

lobule size by 14-days after PH and ultimately differentiated into mature hepatocytes by 30-days after PH (39). Gordon *et al.* described the characteristics of SHPCs to include traits associated with mature hepatocytes, fetal hepatoblasts, and oval cells, suggesting that these cells may represent a distinct liver progenitor cell population (39). Subsequent studies by the same group bolstered this supposition by demonstrating that these cells are phenotypically less mature than fully differentiated mature hepatocytes and express cell markers in patterns not observed in any other known liver progenitor cell type (72). In addition, these studies demonstrated that SHPCs lack expression of CYP proteins that are induced by retrorsine (and/or required for its metabolism) providing a plausible mechanism for the retrorsine-resistance observed in these cells (72). The data from the studies performed by Gordon *et al.* combine to provide significant evidence that the SHPCs represent a distinct liver progenitor cell population. However, these investigators did not rule out the possibility that SHPCs are derived from a population of retrorsine-resistant mature hepatocytes or biliary epithelial cells (such as oval cells) (39, 72). To date the cellular origin of the SHPCs remains unknown. It is interesting to speculate that Laconi *et al.* did not observe SHPCs in the original retrorsine-based studies because their model provided the damaged liver with a primary cell population (transplanted hepatocytes) capable of restoring the lost tissue mass (81). In this environment, the hepatocyte-mediated cellular response would discourage the outgrowth of reserve (secondary) progenitor cells.

POTENTIAL SOURCES OF SHPCS

There are several potential sources of the SHPCs **(FIGURE 1.6)** (19). SHPCs may represent a transitional intermediate of proliferating/differentiating oval cells (19, 62).

FIGURE 4.1. *Liver progenitor cell responses after hepatotoxic injury in the presence of Retrorsine/2-AAF*. (A) In the normal liver the replacement of tissue mass lost to surgical resection or necrosis is accomplished through the proliferation and expansion of mature (fully differentiated) hepatocytes. Under these conditions reserve progenitor cell populations may be activated, but are never observed. (B) However, when the mitoinhibitory agent 2-AAF is used the proliferation of mature hepatocytes is blocked, and reserve progenitor cell populations (i.e. oval cells or SHPCs) are activated to restore the tissue mass. In the Retrorsine/2-AAF model, SHPCs are susceptible to 2-AAF poisoning and the liver mass is replaced through the proliferation and expansion of oval cells.

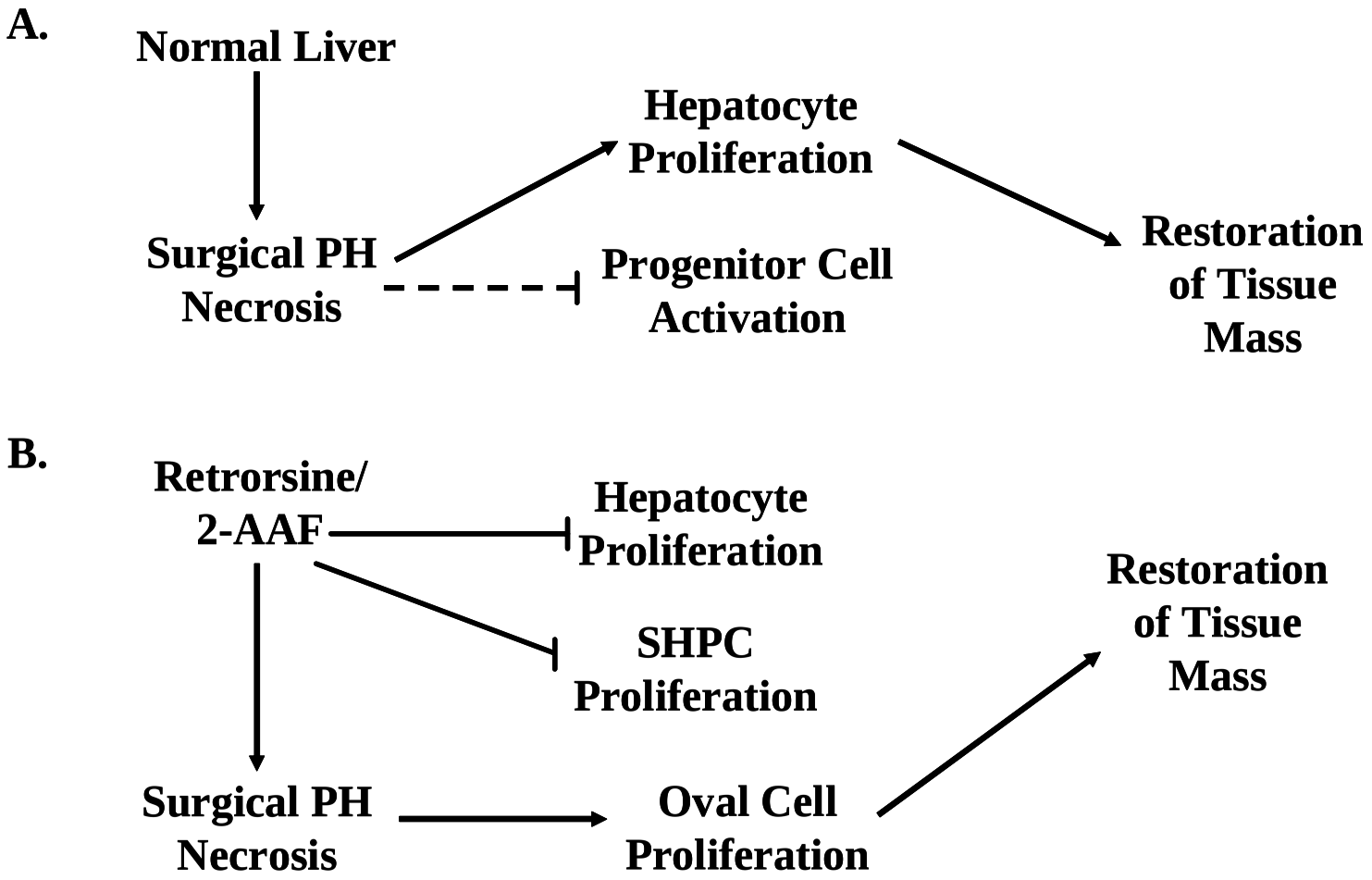
A.
Normal Liver
Hepatocyte Proliferation
Surgical PH Necrosis
Progenitor Cell Activation
Restoration of Tissue Mass
B.
Retrorsine/ 2-AAF
Hepatocyte Proliferation
SHPC Proliferation
Restoration of Tissue Mass
Surgical PH Necrosis
Oval Cell Proliferation

However, if SHPCs are the progeny of oval cells, the cellular mechanism for liver regeneration is distinct from that observed in most oval cell models of liver injury and regeneration. SHPCs may represent a population of retrorsine-resistant hepatocytes present in the liver parenchyma (61). This suggestion is consistent with the observation that SHPC clusters emerge in all three zones of the liver in RP rats (39). Alternatively, SHPCs may be a distinct progenitor cell population present in the liver parenchyma that is histologically indistinguishable from mature hepatocytes, but phenotypically less mature (19).

Oval cells as the progenitor of SHPCs

Over the past several years several investigators suggested that oval cells and SHPCs represent the same (or a closely related) cell populations (6). This idea was recently bolstered by studies performed in retrorsine-exposed mice (62). In this study Vig *et al.* utilized the hepatitis B surface antigen (HBsAg-tg) mouse model of chronic liver injury to investigate the contributions of various cell types to liver cell replacement. Using 3-dimensional mapping techniques, these investigators were are able to track oval cells streaming directly into AFP-positive "SHPC clusters" (62). Based upon this observation, Vig *et al.* concluded that oval cells can give rise to SHPCs (62). However, there are several significant differences between the liver injury model employed by Vig *et al.* and the retrorsine model of liver injury described by Gordon *et al.* (39). For example, the work by Gordon *et al.* was performed using F344 rats and an acute method of injury (such as surgical PH) resulting in the rapid activation of liver progenitor cells and subsequent regeneration of lost tissue mass (39). In contrast, the study by Vig *et al.* employed a mouse model of chronic liver injury where liver progenitor cells are in a continual state of proliferation (62). Based on the differences in the models used in these two studies it is difficult to accurately assess

whether or not the regenerative responses observed in the retrorsine-treated HBsAg-tg mice are identical to those observed in retrorsine-exposed F344 rats. Based on data from our studies and others (56, 88), it seems likely that the hepatocyte clusters observed by Vig *et al.* actually represent new hepatocyte progeny of oval cells rather than regenerative SHPCs.

Oval cells are known to proliferate robustly after PH in animals treated with the mito-inhibitory agent 2-AAF (6, 15, 19, 28, 49, 56). As such, oval cells are not susceptible to 2-AAF poisoning. Therefore, it would be expected that if SHPCs are the progeny of oval cells they too would be refractory to the toxic effects of 2-AAF (at least initially). However, data from our studies show that retrorsine-resistant SHPCs are susceptible to 2-AAF poisoning **(FIGURE 4.1)**. SHPCs are never observed in 2-AAF-treated retrorsine-exposed animals at any time after PH, but clustering of new hepatocytes is observed in these animals at 14-days post-PH **(FIGURE 3.2)**. This cellular response is identical to that observed in 2-AAF/PH animals (in the absence of retrorsine), suggesting that the presence of retrorsine has no effect on the oval cell-mediated response, but that the 2-AAF treatment blocks the outgrowth of SHPCs **(FIGURE 3.2)**. This suggestion is strengthened by results that treatment of rats with 2-AAF 7 days after initiation of the RP protocol (at a time when SHPCs are evident) results in a blockade of SHPC proliferation **(TABLE 3.1)**. This data directly demonstrates that SHPCs in early regenerative clusters are susceptible to 2-AAF poisoning, strongly suggesting that oval cells are not the progenitor cell of origin of the SHPCs. However, the current studies were performed using a high dose of 2-AAF and it has been demonstrated that oval cell regenerative responses vary based on the dose of 2-AAF administered (56, 89). Therefore it would be of some interest to study the effects of a low dose of 2-AAF on the

regeneration of liver in retrorsine-exposed rats as it is possible that a much lower dose of 2-AAF may allow for some SHPC proliferation and expansion.

Additional evidence that oval cells are not progenitors of SHPCs was generated using the biliary toxin DAPM **(FIGURE 1.5)** in conjunction with the RP protocol. Oval cells (or their progenitors) reside in the periportal region of the liver and may be directly derived from biliary epithelial cells. Previous studies have demonstrated that the elimination of bile ducts and the biliary epithelium through exposure to the biliary toxin DAPM results in the blockade of oval cell proliferation (60). The DAPM-mediated inhibition of oval cell proliferation is observed in animals treated with toxins known to elicit an oval cell response (such as 2-AAF) (60). Based on these observations, DAPM provides a powerful tool for investigation of the potential oval cell origins of the SHPCs. If SHPCs are derived from oval cells (or some other periportal cell) then one would not expect to observe these cells in animals treated with DAPM. In our studies, the destruction of the biliary epithelium and inhibition of oval cell proliferation by DAPM did not block the SHPC-mediated regenerative response in retrorsine-exposed rats **(FIGURE 3.9)**. The SHPC-mediated regenerative response observed in DAPM-treated retrorsine-exposed animals after PH was histologically indistinguishable from that of retrorsine-exposed animals in the absence of DAPM providing evidence that retrorsine-resistant SHPCs are also refractory to the effects of DAPM **(FIGURES 3.8 AND 4.3)**. Overall these results suggest that oval cells are not the progenitor cell of the SHPCs.

Retrorsine-resistant mature hepatocytes as the progenitor of SHPCs

Early characterization of the SHPCs demonstrated that these cells are phenotypically immature, expressing characteristics of fetal hepatoblasts and undifferentiated progenitor

FIGURE 4.2. *Liver progenitor cell responses after hepatotoxic injury in the presence of Retrorsine/DAPM.* (A) In the normal liver the replacement of tissue mass lost to surgical resection or necrosis is accomplished through the proliferation and expansion of mature (fully differentiated) hepatocytes. Under these conditions reserve progenitor cell populations may be activated, but are never observed. (B) When the mitoinhibitory agent retrorsine is used the proliferation of mature hepatocytes is blocked and reserve progenitor cell populations (i.e. oval cells or SHPCs) are activated to restore the tissue mass. In the retrorsine/DAPM model, oval cells are incapable of responding because bile ducts have been destroyed. As a result the liver mass is replaced through the proliferation and expansion of SHPCs.

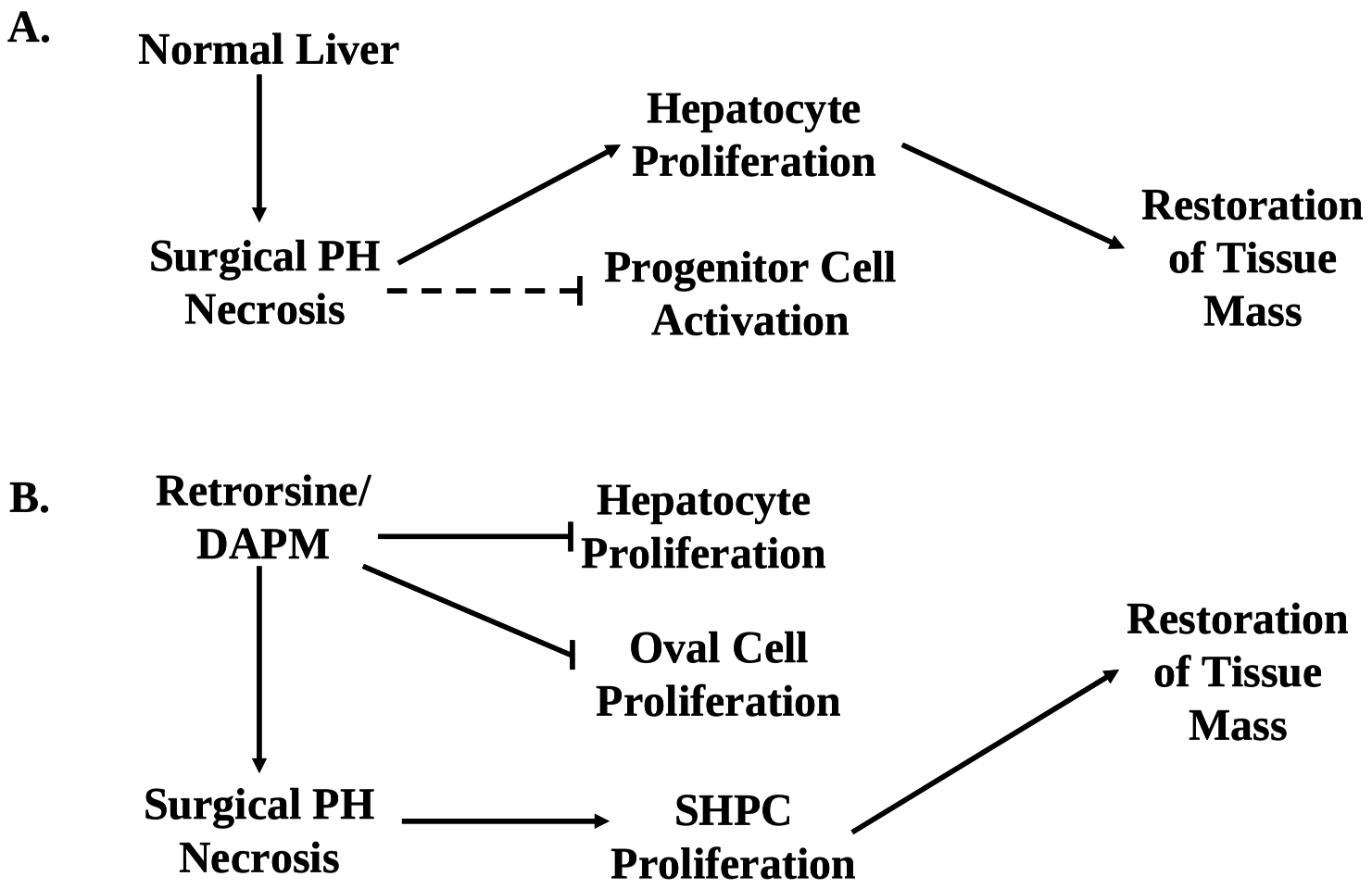
A.
Normal Liver
Hepatocyte Proliferation
Restoration of Tissue Mass
Surgical PH Necrosis
Progenitor Cell Activation
B.
Retrorsine/ DAPM
Hepatocyte Proliferation
Oval Cell Proliferation
Restoration of Tissue Mass
Surgical PH Necrosis
SHPC Proliferation

cells (such as oval cells), suggesting that it is unlikely that these cells represent a population of retrorsine-resistant mature (fully differentiated) hepatocytes present in the liver parenchyma.

Nevertheless, the possibility that SHPCs represent a subset of retrorsine-resistant mature hepatocytes was suggested by Gordon *et al.* (39), and more recently Avril *et al.* published evidence that SHPCs are derived from such a population of mature hepatocytes (61). Avril *et al*. employed a retroviral-based model to genetically label mature hepatocytes with the β-galactosidase gene in retrorsine-exposed Sprague-Dawley rats before PH to examine the contribution of genetically labeled mature hepatocytes to the formation of SHPC clusters (61). The authors observed that after retroviral infection 4% of hepatocytes were positive for β-galactosidase at the time of PH (61). Several weeks (26 days) later, the authors noted that a significant number (4.6%) of SHPC clusters were positive for β-galactosidase (61). These results suggest that some of the mature hepatocytes originally labeled with β-galactosidase were retrorsine-resistant and contributed to the formation of SHPCs in this model (19, 61). However, there are potential problems with the findings of this study. For example, it was not stated how many biliary cells were labeled with β-galactosidase which leaves open the possibility that oval cells or some other biliary epithelial cell contributed to the formation of SHPCs (19). In addition, the model utilized by Avril *et al.* was not capable of addressing the possibility that a progenitor cell population present in the liver parenchyma could potentially be the source of the SHPCs.

SHPCs: A distinct parenchymal progenitor cell population?

Given the evidence suggests that SHPCs do not originate from known liver progenitor cell populations (mature hepatocytes or oval cells), the possibility remains that these cells

represent a distinct progenitor cell population, composed of cells that are histologically similar to mature hepatocytes but phenotypically less mature, and sited in the liver parenchyma. This is based on several lines of evidence. First, when bile ducts are destroyed through the use of the toxin DAPM the regenerative response from oval cells is eliminated, but SHPCs respond **(FIGURE 3.8)**. Second, data from several studies demonstrates that extrahepatic cell types (such as hematopoietic cells) do not significantly contribute to the formation of new hepatocytes (90-95), providing strong evidence that extrahepatic cells are not likely to be contributing substantially to SHPC cluster formation. Finally, there is evidence of a population of AFP-positive cells in the normal liver parenchyma **(FIGURE 4.3)** (96). SHPCs are AFP-positive at emergence and throughout expansion in RP rats (72). Thus, the AFP-positive parenchymal cells observed in normal liver may represent the progenitors of the SHPCs. However, detailed studies to address this possibility have not been carried out.

TISSUE NICHE OF THE SHPCS

In the original SHPC studies by Gordon *et al.*, SHPC clusters were found in all zones of the hepatic lobule: 31% of SHPC clusters arise in the periportal zone, 26% of clusters are localized to the pericentral zone, and the majority (43%) are found midlobular (39). These observations suggest that the progenitor cell that gives rise to SHPCs may be located throughout the liver parenchyma, but the specific tissue niche of the SHPCs has not been identified. Are the SHPCs localized to a specific zone of the liver or are they found throughout the entire parenchyma? This important question can be addressed using liver zone-specific necrotizing agents (such as CCl_4 and allyl alcohol). In the current study we

FIGURE 4.3. *AFP-positive parenchymal cells in normal liver*. Panels A-B and C-D represent typical AFP immunostains obtained from two separate 13-week-old animals, respectively. AFP-positive staining in the normal liver parenchyma was observed in 6 separate animals. Black arrows denote AFP-positive cells. (Original objective lens magnification 20x, original objective lens magnification for insets 40x).

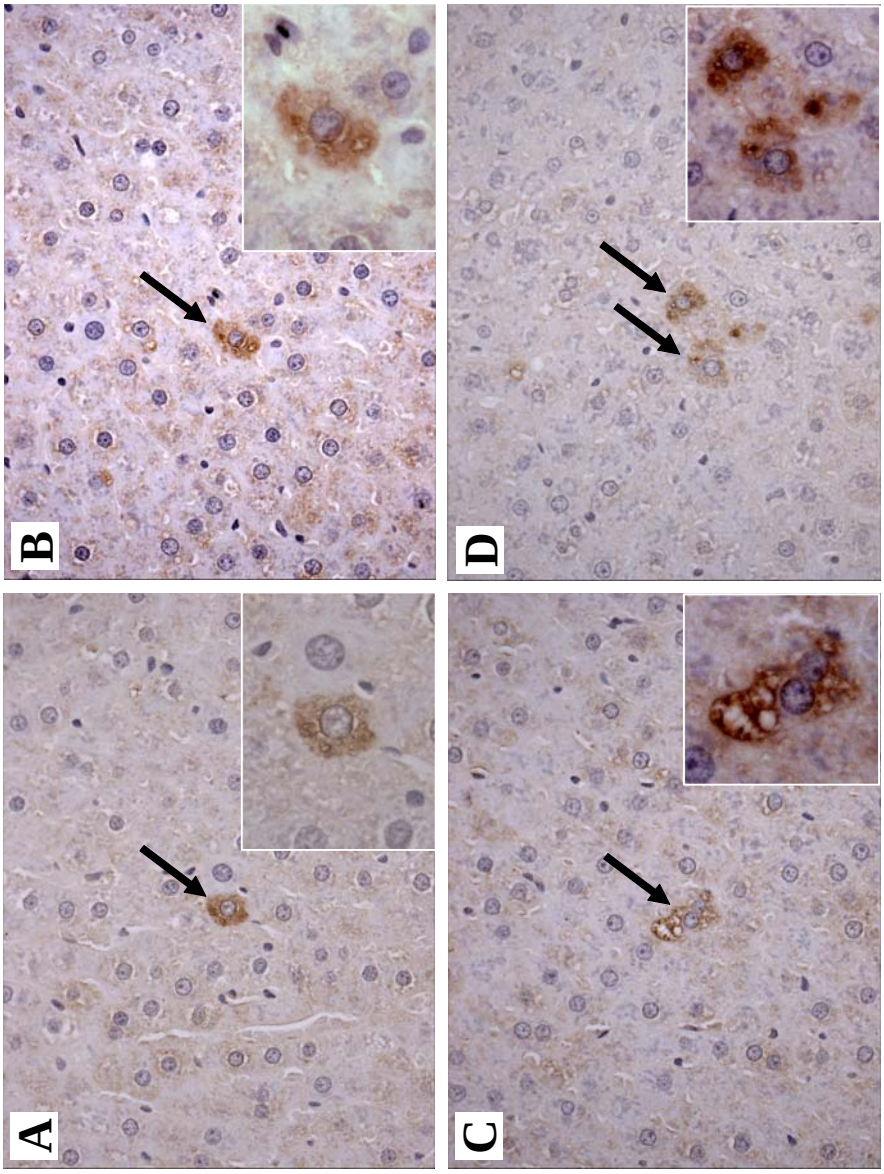
B
D
A
C

have attempted to identify the potential parenchymal location of the SHPCs (or their progenitor) using these necrotizing agents. In these investigations retrorsine-exposed rats were treated with either CCl_4 or ally alcohol, necrotizing agents specific for the pericentral and periportal zones of the parenchyma, respectively. It would be expected that if progenitor cell of origin of the SHPCs is localized to one of these zones then the targeted destruction of that zone would result in a dampened or blocked SHPC regenerative response.

In our studies the destruction of the pericentral zone of the parenchyma by CCl_4 did not result in a dampened SHPC-regenerative response in these animals **(FIGURE 3.13)**. In fact, there were no observable differences in the size or number of SHPC clusters in CCl_4-treated animals (versus retrorsine-exposed rat liver after PH) **(TABLE 3.3-3.4)**. These data suggest that the progenitor cell of the SHPCs is not restricted to this region of the parenchyma. Though it has been published that treatment with the necrotic agent allyl alcohol results in the targeted destruction of the periportal region of the parenchyma (50, 97), our attempts to utilize this agent proved to be unsuccessful at the reported dose of 37 mg/kg. At no time after allyl alcohol injection was necrosis observed. However, increasing the dose to 64 mg/kg resulted in the expected level (>60%) of necrosis **(FIGURE 4.4)**, but also caused 90% mortality in animals treated. In the future, the determination of a well-tolerated yet effective dose of allyl alcohol will be extremely important in the determination of the niche of the SHPCs.

CYTOKINE-MEDIATED ACTIVATION OF SHPCS

The molecular mechanisms for hepatocyte activation and proliferation have been elucidated in some detail. Differentiated hepatocytes are typically refractory to stimulation

FIGURE 4.4. *The effects of allyl alcohol in F344 rat liver.* The dose of allyl alcohol reported in the literature to cause >60% necrosis (37 mg/kg) did not result in any observable damage at (A) 48 hours, (B) 3 days, or (C) 7-days post-administration of allyl alchol in F344 rats. Increasing the allyl alcohol dose to 64 mg/kg produced the expected level of necrosis at (D-E) 24 hours post-administration. However, this dose also resulted in 90% mortality of the animals treated.

C
B
A
E
D

by growth factors, and require a priming stimulus in order to proliferate in response to damage (98). In rats, infusion of various growth factors (including EGF, TGFα, HGF, or combinations of these) into the liver does not result in DNA synthesis by hepatocytes, unless this growth factor infusion is preceded by a priming stimulus (such as 30% PH) (98). The signaling molecules responsible for hepatocyte priming have been shown to be specific cytokines that activate NF-κB (99), including TNF-α and IL6 (13, 14, 100-104). Liver regeneration after PH is severely impaired when TNF-α signaling is eliminated using neutralizing antibodies in rats (13) or in TNF receptor I (TNFR-I) knockout mice (102-104). The downstream effector of TNF-α signaling is IL6 (103), and liver regeneration after PH is impaired in IL6 knockout mice (14, 105) in a manner similar to that observed in TNFR-I knockout mice. In both of these models, administration of exogenous IL6 rescues the regenerative response (14, 105). These observations combine to suggest that the priming and activation of mature hepatocytes in response to liver deficit (i.e. PH) is a cytokine-mediated process that specifically requires IL6 and TNF-α (14, 101, 103-105).

Under certain pathological conditions mature hepatocytes are unable to divide in response to liver injury (loss of cell number), resulting in the activation of reserve (stem-like) progenitor cell populations which proliferate to regenerate the liver tissue (6). Oval cells represent an undifferentiated progenitor cell population that is activated to proliferate in liver injury models that combine a proliferative stimulus (like PH) with chemical agents (like 2-acetylaminofluorene) that inhibit the proliferation of hepatocytes (21). The emergence of the oval cell population occurs approximately 36-48 hours after PH in the 2-AAF/PH model (31, 32), in a delayed response to the lack of hepatocyte reaction to liver deficit. Analogous to mature hepatocytes, the oval cell reaction requires a cytokine-mediated priming stimulus

(52). Blockade of cytokine release after PH in rats treated with 2-AAF leads to inhibition of oval cell activation, but this inhibition can be overcome through the administration of exogenous IL6 (52, 53). Thus, liver regeneration by hepatocytes and oval cells represent different cellular reactions to liver injury, but require similar cytokines and growth factors. SHPCs represent a second population of reserve progenitor cells, which proliferate after PH to repopulate the damaged livers of rats exposed to the pyrrolizidine alkaloid retrorsine (39). Though the nature of the signaling molecules and events that are responsible for the activation of SHPCs in this form of liver injury have not been studied in detail, results from the current study suggest that these cells are also activated in a cytokine-dependent manner (**FIGURES 3.15-3.20**). Administration of the cytokine inhibitor DEX to retrorsine-injured rats prior to PH blocks the emergence of SHPCs in a dose-dependent manner. A single administration of DEX dampens the magnitude of SHPC response, resulting in a delayed regenerative reaction, while multiple doses of DEX (prior to and following PH) produces a near complete inhibition of SHPC emergence. These observations suggest a role for cytokine priming in the activation and emergence of this reserve progenitor cell population. In fact, the SHPC response was restored by the administration of a single dose of recombinant IL6 protein at the time of PH, suggesting strongly that the emergence of SHPCs after PH in retrorsine-injured rats requires cytokine priming, and that IL6 directly mediates this cellular reaction. Thus, SHPCs represent a third population of progenitor cells that can be activated under specific conditions to regenerate the liver through a unique cellular reaction that is mediated through a common signaling pathway that specifically requires IL6.

The molecular mechanism of IL6-mediated hepatocyte activation in normal liver regeneration has been extensively studied using knockout mice (9). After PH, serum

concentrations of TNF-α increase resulting in an upregulation of NF-κB (9). In turn NF-κB activates transcription of IL6 which then binds to the IL6 receptor (IL6-R) and interacts with gp130 resulting in the activation of the Janus kinase (JAK) ultimately priming the hepatocytes for proliferation (9). JAK activates cell proliferation through either (i) the mitogen-activated protein kinase (MAPK) pathway, or (ii) the signal transducer and activator of transcription 3 (STAT3) pathway (9). It is intriguing to speculate that this represents the sequence of molecular events occurring in the activation of SHPCs after PH in retrorsine-injured liver. However, it is impossible to directly investigate the early molecular events during SHPC activation due to our current inability to effectively identify these cells until several days after PH (39). One attractive experimental possibility is to utilize IL6-deficient mice in conjunction with retrorsine injury and regeneration after PH to more precisely dissect the involvement of IL6 in SHPC activation. However, mice do not display the same form of liver injury in response to retrorsine as that observed in rat, and SHPCs have not been observed in any mouse model of acute liver injury.

HIERARCHICAL RESPONSE TO LIVER INJURY

The mammalian liver possesses tremendous flexibility in its capacity to respond to injury and loss of cell numbers (function). At least three different cell populations have been implicated in liver regeneration: (i) differentiated hepatocytes (in otherwise normal liver), (ii) SHPCs (observed in retrorsine-exposed rats), and (iii) oval cells (observed in numerous models of liver injury). Given multiple sources of regenerative cells and the observed differences in timing of activation of these cell populations in response to liver deficit, it is intriguing to speculate that there is a hierarchy of cellular responses in liver regeneration and

FIGURE 4.5. *A proposed model of hierarchical responses to injury in rat liver.* After injury the primary response of the liver is mediated by the (A) mature (fully differentiated) hepatocytes. Reserve progenitor cell populations may be activated under these circumstances, but are never observed. When mature hepatocytes are incapable of proliferating due to exposure to chemical agents such as (B) 2-AAF or (C) retrorsine reserve progenitor cell populations are activated to proliferate and restore tissue mass. The responding cell population is dependent on the type of damage that has occurred. When animals are exposed to (B) 2-AAF, the mature hepatocytes and SHPCs are damaged and incapable of proliferating in response to surgical resection or necrosis. As a result the oval cells proliferate and replace the damaged liver tissue. Likewise, when animals are exposed to (C) retrorsine, the mature hepatocytes are damaged and oval cells do not respond in response to liver injury. Therefore, the liver is completely regenerated through the outgrowth and expansion of SHPCs.

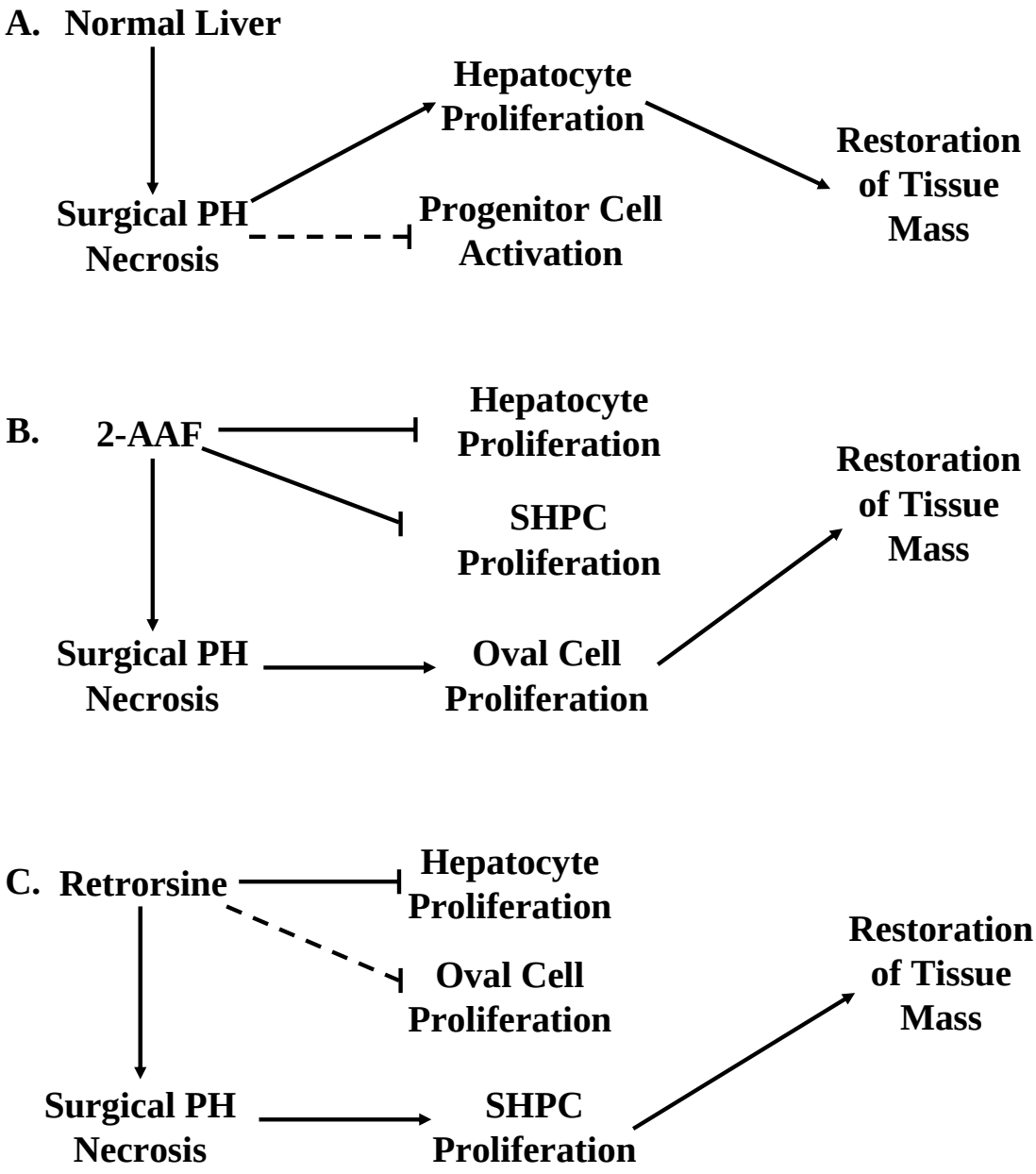
A. Normal Liver
Hepatocyte Proliferation
Restoration of Tissue Mass
Surgical PH Necrosis
Progenitor Cell Activation
B. 2-AAF
Hepatocyte Proliferation
SHPC Proliferation
Restoration of Tissue Mass
Surgical PH Necrosis
Oval Cell Proliferation
C. Retrorsine
Hepatocyte Proliferation
Oval Cell Proliferation
Restoration of Tissue Mass
Surgical PH Necrosis
SHPC Proliferation

that the nature of the regenerative cell population is determined by (a) the presence or absence of liver injury, (b) the type and extent of injury, and (c) the capacity of each cell population to respond **(FIGURE 4.5)**. In this model, activation and proliferation of mature hepatocytes represents the primary (preferential) cellular response, and the activation, emergence, and proliferation of reserve progenitor cell populations (SHPCs or oval cells) represent secondary cellular responses, occurring only when the primary response is blocked or impaired **(FIGURE 4.5)**. The results of the current investigation combined with previous studies from the literature (52, 100, 106, 107), suggest that IL6 may be a common signaling molecule that functions to regulate the liver's response to injury. There may be redundancy in the cellular reactions to liver injury, but a common regulatory pathway that directs the process of regeneration. Thus, following a signal for liver regeneration, all possible progenitor cell populations may be concurrently primed for activation (IL6-mediated), but that the secondary reserve progenitor cell responses do not manifest unless the primary (hepatocyte-mediated) response fails. However, the controlling factors in the termination of each of these regenerative responses are likely to vary. For example, an increase in TGFβ expression is known to signal the termination of hepatocyte division but oval cells are refractory to increases in the expression of this protein (108, 109). These findings provide strong evidence that a hierarchy does exist in progenitor cell response of the liver and that mechanisms regulating these responses vary appropriately. In the future studies must be performed to determine the factors controlling SHPC proliferation as well as those involved in the control of oval cells. A better understanding of the signals required to activate liver progenitor cells for proliferation may provide the key to modulating these responses in the clinical treatment of liver disease.

SUMMARY AND IMPACT

The overall goals of this dissertation were to (i) to characterize the SHPC responses in both hepatotoxic and necrotic models of liver injury, (ii) to determine the progenitor cell of origin of the SHPC, and (iii) to determine the factors involved in the activation of SHPCs for proliferation after liver injury. The results of the studies described herein demonstrate that SHPCs contribute to the restoration of liver mass after both hepatotoxic and necrotic methods of injury. Although the current study does not definitively determine the progenitor cell of origin of SHPCs, the results generated provide strong evidence that these cells are not the progeny of other known liver progenitor cell populations, such as oval cells. In addition, these studies provide significant new evidence that SHPCs are most likely derived from a population of cells located in the liver parenchyma that may be histologically similar to mature (fully differentiated) hepatocytes but phenotypically distinct. Finally, the observations from this investigation strongly suggest that SHPCs are activated for proliferation in a cytokine-mediated manner, providing evidence that cytokines (specifically IL6) may represent the master regulatory molecules in the activation of progenitor cell responses after injury in the adult liver. However, further analysis must be performed before the mechanisms governing the activation of specific liver progenitor cell populations are completely understood. In addition, it is essential that future studies be conducted using the periportal-specific necrotic agent allyl alcohol. Such studies will provide additional and important data about the specific tissue niche of the SHPCs. Furthermore, studies should also be performed utilizing laser capture microdissection (LCM) to collect SHPCs for molecular analysis. Although previous studies have been conducted utilizing LCM technology, a more detailed analysis of the changes in protein and gene expression observed

in the SHPCs during the regenerative interval following liver injury may provide additional insight into the differences between SHPCs and other known liver progenitor cells. Finally, studies should be carried out to determine the molecular signals governing growth suppression of SHPCs. TGFβ is an important regulator of liver regeneration by mature hepatocytes, providing the signal for cessation of proliferation. In a similar manner, TGFβ may be involved in suppression of SHPC proliferation as liver regeneration is completed in retrorsine-exposed rats. Studies addressing this possibility would further our understanding of the mechanisms governing SHPC proliferation.

V. BIBLIOGRAPHY

1. Desment, V. J. Organizational principles. *In:* I. M. Arias, J. L. Boyer, N. Fausto, W. B. Jakoby, D. A. Schachter, and D. A. Shafritz (eds.), The Liver: Biology and Pathobiology, Third edition, pp. 3-14. New York: Raven Press, 1994.

2. Campbell, N. A. Biology, Fourth edition, p. 1206. New York: Benjamin/Cummings Publishing, 1996.

3. Guyton, A. C. Anatomy and Physiology, p. 869. Philadelphia: Saunders College, 1985.

4. Popper, H. and Schaffner, F. Liver: Structure and Function, p. 777. New York: McGraw-Hill, 1957.

5. Fausto, N. Liver regeneration. J Hepatol, *32:* 19-31, 2000.

6. Fausto, N. Liver regeneration and repair: hepatocytes, progenitor cells, and stem cells. Hepatology, *39:* 1477-1487, 2004.

7. Fausto, N., Campbell, J. S., and Riehle, K. J. Liver regeneration. Hepatology, *43:* S45-53, 2006.

8. Michalopoulos, G. K. and DeFrances, M. C. Liver regeneration. Science, *276:* 60-66, 1997.

9. Taub, R. Liver regeneration: From myth to mechanism. Nat Rev Mol Cell Biol, *5:* 836-847, 2004.

10. Higgins, G. M. and Anderson, R. M. Experimental pathology of the liver. I. Restoration of the liver of the white rat following partial surgical removal. Arch Pathol, *12:* 186-202, 1931.

11. Diehl, A. Cytokine regulation of liver regeneration. *In:* W. E. Fleig (ed.), Normal and Malignant Liver Cell Growth, pp. 47-55. Dordrecht: Kluwer Academic Publishers, 1999.

12. Fausto, N., Laird, A. D., and Webber, E. M. Liver regeneration. 2. Role of growth factors and cytokines in hepatic regeneration. FASEB J, *9:* 1527-1536, 1995.

13. Akerman, P., Cote, P., Yang, S. Q., McClain, C., Nelson, S., Bagby, G. J., and Diehl, A. M. Antibodies to tumor necrosis factor-alpha inhibit liver regeneration after partial hepatectomy. Am J Physiol, *263:* G579-585, 1992.

14. Cressman, D. E., Greenbaum, L. E., DeAngelis, R. A., Ciliberto, G., Furth, E. E., Poli, V., and Taub, R. Liver failure and defective hepatocyte regeneration in interleukin-6-deficient mice. Science, *274:* 1379-1383, 1996.

15. Fausto, N. and Campbell, J. S. The role of hepatocytes and oval cells in liver regeneration and repopulation. Mech Dev, *120:* 117-130, 2003.

16. Fabrikant, J. I. Size of proliferating pools in regenerating liver. Exp Cell Res, *55:* 277-279, 1969.

17. Overturf, K., al-Dhalimy, M., Ou, C. N., Finegold, M., and Grompe, M. Serial transplantation reveals the stem-cell-like regenerative potential of adult mouse hepatocytes. Am J Pathol, *151:* 1273-1280, 1997.

18. Dabeva, M. D., Alpini, G., Hurston, E., and Shafritz, D. A. Models for hepatic progenitor cell activation. Proc Soc Exp Biol Med, *204:* 242-252, 1993.

19. Coleman, W. B. and Best, D. H. Cellular responses in experimental liver injury: possible cellular origins of regenerative stem-like progenitor cells. Hepatology, *41:* 1173-1176, 2005.

20. Coleman, W. B. and Grisham, J. W. Epithelial stem-like cells of the rodent liver. *In:* A. J. Strain and A. M. Diehl (eds.), Liver Growth and Repair, pp. 50-99. London: Chapman and Hall, 1998.

21. Lowes, K. N., Croager, E. J., Olynyk, J. K., Abraham, L. J., and Yeoh, G. C. Oval cell-mediated liver regeneration: Role of cytokines and growth factors. J Gastroenterol Hepatol, *18:* 4-12, 2003.

22. Inaoka, Y. Significance of the so-called oval cell proliferation during azo-dye hepatocarcinogenesis. Gann, *58:* 355-366, 1967.

23. Ogawa, K., Minase, T., and Onhoe, T. Demonstration of glucose 6-phosphatase activity in the oval cells of rat liver and the significance of the oval cells in azo dye carcinogenesis. Cancer Res, *34:* 3379-3386, 1974.

24. Higashi, K., Denda, A., Higashi, T., and Hiai, H. Genetic resistance to chemical hepatocarcinogenesis in the DRH rat strain. Comp Med, *54:* 373-377, 2004.

25. Zeng, Z. Z., Higashi, S., Kitayama, W., Denda, A., Yan, Y., Matsuo, K., Konishi, Y., Hiai, H., and Higashi, K. Genetic resistance to chemical carcinogen-induced preneoplastic hepatic lesions in DRH strain rats. Cancer Res, *60:* 2876-2881, 2000.

26. Shinozuka, H., Lombardi, B., Sell, S., and Iammarino, R. M. Early histological and functional alterations of ethionine liver carcinogenesis in rats fed a choline-deficient diet. Cancer Res, *38:* 1092-1098, 1978.

27. Akhurst, B., Croager, E. J., Farley-Roche, C. A., Ong, J. K., Dumble, M. L., Knight, B., and Yeoh, G. C. A modified choline-deficient, ethionine-supplemented diet protocol effectively induces oval cells in mouse liver. Hepatology, *34:* 519-522, 2001.

28. Sell, S., Leffert, H. L., Shinozuka, H., Lombardi, B., and Gochman, N. Rapid development of large numbers of alpha-fetoprotein-containing "oval" cells in the liver of rats fed N-2-fluorenylacetamide in a choline-devoid diet. Gann, *72:* 479-487, 1981.

29. Sell, S., Osborn, K., and Leffert, H. L. Autoradiography of "oval cells" appearing rapidly in the livers of rats fed N-2-fluorenylacetamide in a choline devoid diet. Carcinogenesis, *2:* 7-14, 1981.

30. Solt, D. and Farber, E. New principle for the analysis of chemical carcinogenesis. Nature, *263:* 701-703, 1976.

31. Evarts, R. P., Nagy, P., Nakatsukasa, H., Marsden, E., and Thorgeirsson, S. S. In vivo differentiation of rat liver oval cells into hepatocytes. Cancer Res, *49:* 1541-1547, 1989.

32. Sarraf, C., Lalani, E. N., Golding, M., Anilkumar, T. V., Poulsom, R., and Alison, M. Cell behavior in the acetylaminofluorene-treated regenerating rat liver. Light and electron microscopic observations. Am J Pathol, *145:* 1114-1126, 1994.

33. Verna, L., Whysner, J., and Williams, G. M. 2-Acetylaminofluorene mechanistic data and risk assessment: DNA reactivity, enhanced cell proliferation and tumor initiation. Pharmacol Ther, *71:* 83-105, 1996.

34. Bisgaard, H. C., Nagy, P., Santoni-Rugiu, E., and Thorgeirsson, S. S. Proliferation, apoptosis, and induction of hepatic transcription factors are characteristics of the early response of biliary epithelial (oval) cells to chemical carcinogens. Hepatology, *23:* 62-70, 1996.

35. Evarts, R. P., Hu, Z., Omori, N., Omori, M., Marsden, E. R., and Thorgeirsson, S. S. Precursor-product relationship between oval cells and hepatocytes: Comparison between tritiated thymidine and bromodeoxyuridine as tracers. Carcinogenesis, *17:* 2143-2151, 1996.

36. Evarts, R. P., Nagy, P., Marsden, E., and Thorgeirsson, S. S. A precursor-product relationship exists between oval cells and hepatocytes in rat liver. Carcinogenesis, *8:* 1737-1740, 1987.

37. Lemire, J. M., Shiojiri, N., and Fausto, N. Oval cell proliferation and the origin of small hepatocytes in liver injury induced by D-galactosamine. Am J Pathol, *139:* 535-552, 1991.

38. Lesch, R., Reutter, W., Keppler, D., and Decker, K. Liver restitution after acute galactosamine hepatitis: Autoradiographic and biochemical studies in rats. Exp Mol Pathol, *12:* 58-69, 1970.

39. Gordon, G. J., Coleman, W. B., Hixson, D. C., and Grisham, J. W. Liver regeneration in rats with retrorsine-induced hepatocellular injury proceeds through a novel cellular response. Am J Pathol, *156:* 607-619, 2000.

40. Factor, V. M., Radaeva, S. A., and Thorgeirsson, S. S. Origin and fate of oval cells in dipin-induced hepatocarcinogenesis in the mouse. Am J Pathol, *145:* 409-422, 1994.

41. Jago, M. V. The development of the hepatic megalocytosis of chronic pyrrolizidine alkaloid poisoning. Am J Pathol, *56:* 405-421, 1969.

42. Schoental, R. and Magee, P. N. Further observations on the subacute and chronic liver changes in rats after a single dose of various pyrrolizidine (Senecio) alkaloids. J Pathol Bacteriol, *78:* 471-482, 1959.

43. Schoental, R. Toxicology and carcinogenic action of pyrrolizidine alkaloids. Cancer Res, *28:* 2237-2246, 1968.

44. Schoental, R. and Magee, P. N. Chronic liver changes in rats after a single dose of lasiocarpine, a pyrrolizidine (senecio) alkaloid. J. Pathol. Bacteriol., *74:* 305-319, 1957.

45. Fausto, N. Liver stem cells. The Liver: Biology and Pathobiology. *In:* I. M. Arias, J. L. Boyer, N. Fausto, W. B. Jakoby, D. Shachter, and D. A. Shafritz (eds.), The Liver: Biology and Pathobiology, Third edition, pp. 1501-1518. New York: Raven Press, 1994.

46. Orkin, S. H. Hematopoietic stem cells: Molecular diversification and developmental interrelationships. *In:* D. R. Marshak, R. L. Gardner, and D. Gottlieb (eds.), Stem Cell Biology, pp. 515-536. Cold Spring Harbor, NY: Cold Spring Harbor Press, 2001.

47. Winton, D. J. Stem cells in epithelium of the small intestine and colon. *In:* D. R. Marshak, R. L. Gardner, and D. Gottlieb (eds.), Stem Cell Biology, pp. 515-536. Cold Spring Harbor, NY: Cold Spring Harbor Press, 2001.

48. Coleman, W. B., Grisham, J. W., and Malouf, N. N. Adult liver stem cells. *In:* K. Turksen (ed.), Adult Stem Cells, pp. 101-148. Totowa, NJ: Humana Press, 2004.

49. Sell, S. Distribution of alpha-fetoprotein- and albumin-containing cells in the livers of Fischer rats fed four cycles of N-2-fluorenylacetamide. Cancer Res, *38:* 3107-3113, 1978.

50. Petersen, B. E., Zajac, V. F., and Michalopoulos, G. K. Hepatic oval cell activation in response to injury following chemically induced periportal or pericentral damage in rats. Hepatology, *27:* 1030-1038, 1998.

51. Matthews, V. B., Klinken, E., and Yeoh, G. C. Direct effects of interleukin-6 on liver progenitor oval cells in culture. Wound Repair Regen, *12:* 650-656, 2004.

52. Nagy, P., Kiss, A., Schnur, J., and Thorgeirsson, S. S. Dexamethasone inhibits the proliferation of hepatocytes and oval cells but not bile duct cells in rat liver. Hepatology, *28:* 423-429, 1998.

53. Knight, B., Yeoh, G. C., Husk, K. L., Ly, T., Abraham, L. J., Yu, C., Rhim, J. A., and Fausto, N. Impaired preneoplastic changes and liver tumor formation in tumor necrosis factor receptor type 1 knockout mice. J Exp Med, *192:* 1809-1818, 2000.

54. Nagy, P., Bisgaard, H. C., and Thorgeirsson, S. S. Expression of hepatic transcription factors during liver development and oval cell differentiation. J Cell Biol, *126:* 223-233, 1994.

55. Nagy, P., Teramoto, T., Factor, V. M., Sanchez, A., Schnur, J., Paku, S., and Thorgeirsson, S. S. Reconstitution of liver mass via cellular hypertrophy in the rat. Hepatology, *33:* 339-345, 2001.

56. Paku, S., Nagy, P., Kopper, L., and Thorgeirsson, S. S. 2-acetylaminofluorene dose-dependent differentiation of rat oval cells into hepatocytes: confocal and electron microscopic studies. Hepatology, *39:* 1353-1361, 2004.

57. Paku, S., Schnur, J., Nagy, P., and Thorgeirsson, S. S. Origin and structural evolution of the early proliferating oval cells in rat liver. Am J Pathol, *158:* 1313-1323, 2001.

58. Omori, N., Omori, M., Evarts, R. P., Teramoto, T., Miller, M. J., Hoang, T. N., and Thorgeirsson, S. S. Partial cloning of rat CD34 cDNA and expression during stem cell-dependent liver regeneration in the adult rat. Hepatology, *26:* 720-727, 1997.

59. Petersen, B. E., Goff, J. P., Greenberger, J. S., and Michalopoulos, G. K. Hepatic oval cells express the hematopoietic stem cell marker Thy-1 in the rat. Hepatology, *27:* 433-445, 1998.

60. Petersen, B. E., Zajac, V. F., and Michalopoulos, G. K. Bile ductular damage induced by methylene dianiline inhibits oval cell activation. Am J Pathol, *151:* 905-909, 1997.

61. Avril, A., Pichard, V., Bralet, M. P., and Ferry, N. Mature hepatocytes are the source of small hepatocyte-like progenitor cells in the retrorsine model of liver injury. J Hepatol, *41:* 737-743, 2004.

62. Vig, P., Russo, F. P., Edwards, R. J., Tadrous, P. J., Wright, N. A., Thomas, H. C., Alison, M. R., and Forbes, S. J. The sources of parenchymal regeneration after chronic hepatocellular liver injury in mice. Hepatology, *43:* 316-324, 2006.

63. Gordon, G. J., Coleman, W. B., and Grisham, J. W. Bax-mediated apoptosis in the livers of rats after partial hepatectomy in the retrorsine model of hepatocellular injury. Hepatology, *32:* 312-320, 2000.

64. Michalopoulos, G. K., Barua, L., and Bowen, W. C. Transdifferentiation of rat hepatocytes into biliary cells after bile duct ligation and toxic biliary injury. Hepatology, *41:* 535-544, 2005.

65. Gordon, G. J., Coleman, W. B., and Grisham, J. W. Induction of cytochrome P450 enzymes in the livers of rats treated with the pyrrolizidine alkaloid retrorsine. Exp Mol Pathol, *69:* 17-26, 2000.

66. Tateishi, T., Nakura, H., Asoh, M., Watanabe, M., Tanaka, M., Kumai, T., and Kobayashi, S. Multiple cytochrome P-450 subfamilies are co-induced with P-glycoprotein by both phenothiazine and 2-acetylaminofluorene in rats. Cancer Lett, *138:* 73-79, 1999.

67. Novikoff, P. M., Yam, A., and Oikawa, I. Blast-like cell compartment in carcinogen-induced proliferating bile ductules. Am J Pathol, *148:* 1473-1492, 1996.

68. Qin, A. L., Zhou, X. Q., Zhang, W., Yu, H., and Xie, Q. Characterization and enrichment of hepatic progenitor cells in adult rat liver. World J Gastroenterol, *10:* 1480-1486, 2004.

69. Paku, S., Dezso, K., Kopper, L., and Nagy, P. Immunohistochemical analysis of cytokeratin 7 expression in resting and proliferating biliary structures of rat liver. Hepatology, *42:* 863-870, 2005.

70. Corcelle, V., Stieger, B., Gjinovci, A., Wollheim, C. B., and Gauthier, B. R. Characterization of two distinct liver progenitor cell subpopulations of hematopoietic and hepatic origins. Exp Cell Res, *312:* 2826-2836, 2006.

71. Czaja, M. J. Liver regeneration following hepatic injury. *In:* A. J. Strain and A. M. Diehl (eds.), Liver Growth and Repair, pp. 28-49. New York: Chapman and Hall, 1998.

72. Gordon, G. J., Coleman, W. B., and Grisham, J. W. Temporal analysis of hepatocyte differentiation by small hepatocyte-like progenitor cells during liver regeneration in retrorsine-exposed rats. Am J Pathol, *157:* 771-786, 2000.

73. Panduro, A., Shalaby, F., Biempica, L., and Shafritz, D. A. Changes in albumin, alpha-fetoprotein and collagen gene transcription in CCl_4-induced hepatic fibrosis. Hepatology, *8:* 259-266, 1988.

74. Kubo, Y., Yasunaga, M., Masuhara, M., Terai, S., Nakamura, T., and Okita, K. Hepatocyte proliferation induced in rats by lead nitrate is suppressed by several tumor necrosis factor alpha inhibitors. Hepatology, *23:* 104-114, 1996.

75. Ledda-Columbano, G. M., Columbano, A., Cannas, A., Simbula, G., Okita, K., Kayano, K., Kubo, Y., Katyal, S. L., and Shinozuka, H. Dexamethasone inhibits induction of liver tumor necrosis factor-alpha mRNA and liver growth induced by lead nitrate and ethylene dibromide. Am J Pathol, *145:* 951-958, 1994.

76. Roeder, E. Medicinal plants in China containing pyrrolizidine alkaloids. Pharmazie, *55:* 711-726, 2000.

77. Fu, P. P., Xia, Q., Lin, G., and Chou, M. W. Pyrrolizidine alkaloids--genotoxicity, metabolism enzymes, metabolic activation, and mechanisms. Drug Metab Rev, *36:* 1-55, 2004.

78. Stegelmeier, B. L., Edgar, J. A., Colegate, S. M., Gardner, D. R., Schoch, T. K., Coulombe, R. A., and Molyneux, R. J. Pyrrolizidine alkaloid plants, metabolism and toxicity. J Nat Toxins, *8:* 95-116, 1999.

79. Mattocks, A. R. Chemistry and Toxicology of Pyrrolizidine Alkaloids. London: Academic Press, 1986.

80. McLean, E. K. The toxic actions of pyrrolizidine (senecio) alkaloids. Pharmacol Rev, *22:* 429-483, 1970.

81. Laconi, E., Oren, R., Mukhopadhyay, D. K., Hurston, E., Laconi, S., Pani, P., Dabeva, M. D., and Shafritz, D. A. Long-term, near-total liver replacement by transplantation of isolated hepatocytes in rats treated with retrorsine. Am J Pathol, *153:* 319-329, 1998.

82. Laconi, E., Sarma, D. S., and Pani, P. Transplantation of normal hepatocytes modulates the development of chronic liver lesions induced by a pyrrolizidine alkaloid, lasiocarpine. Carcinogenesis, *16:* 139-142, 1995.

83. Laconi, S., Curreli, F., Diana, S., Pasciu, D., De Filippo, G., Sarma, D. S., Pani, P., and Laconi, E. Liver regeneration in response to partial hepatectomy in rats treated with retrorsine: A kinetic study. J Hepatol, *31:* 1069-1074, 1999.

84. Laconi, S., Pillai, S., Porcu, P. P., Shafritz, D. A., Pani, P., and Laconi, E. Massive liver replacement by transplanted hepatocytes in the absence of exogenous growth stimuli in rats treated with retrorsine. Am J Pathol, *158:* 771-777, 2001.

85. Bull, L. B. and Dick, A. T. The chronic pathological effects on the liver of the rat of the pyrrolizidine alkaloids heliotrine, lasiocarpine, and their N-oxides. J Pathol Bacteriol, *78:* 483-502, 1959.

86. Peterson, J. E. Effects of the pyrrolizidine alkaloid, lasiocarpine N-oxide, on nuclear and cell division in the liver rats. J Pathol Bacteriol, *89:* 153-171, 1965.

87. Reddy, J. K., Rao, M. S., and Jago, M. V. Rapid development of hyperplastic nodules and cirrhosis in the liver of rats treated concurrently with thioacetamide and the pyrrolizidine alkaloid lasiocarpine. Int J Cancer, *17:* 621-625, 1976.

88. Best, D. H. and Coleman, W. B. Treatment with 2-AAF blocks the small hepatocyte-like progenitor cell response in retrorsine-exposed rats. J Hepatol*:* (in press), 2007.

89. Alison, M., Golding, M., Lalani, E. N., Nagy, P., Thorgeirsson, S., and Sarraf, C. Wholesale hepatocytic differentiation in the rat from ductular oval cells, the progeny of biliary stem cells. J Hepatol, *26:* 343-352, 1997.

90. Thorgeirsson, S. S. and Grisham, J. W. Hematopoietic cells as hepatocyte stem cells: A critical review of the evidence. Hepatology, *43:* 2-8, 2006.

91. Wang, X., Montini, E., Al-Dhalimy, M., Lagasse, E., Finegold, M., and Grompe, M. Kinetics of liver repopulation after bone marrow transplantation. Am J Pathol, *161:* 565-574, 2002.

92. Camargo, F. D., Finegold, M., and Goodell, M. A. Hematopoietic myelomonocytic cells are the major source of hepatocyte fusion partners. J Clin Invest, *113:* 1266-1270, 2004.

93. Lagasse, E., Connors, H., Al-Dhalimy, M., Reitsma, M., Dohse, M., Osborne, L., Wang, X., Finegold, M., Weissman, I. L., and Grompe, M. Purified hematopoietic stem cells can differentiate into hepatocytes in vivo. Nat Med, *6:* 1229-1234, 2000.

94. Mallet, V. O., Mitchell, C., Mezey, E., Fabre, M., Guidotti, J. E., Renia, L., Coulombel, L., Kahn, A., and Gilgenkrantz, H. Bone marrow transplantation in mice leads to a minor population of hepatocytes that can be selectively amplified in vivo. Hepatology, *35:* 799-804, 2002.

95. Wagers, A. J., Sherwood, R. I., Christensen, J. L., and Weissman, I. L. Little evidence for developmental plasticity of adult hematopoietic stem cells. Science, *297:* 2256-2259, 2002.

96. Lemire, J. M. and Fausto, N. Multiple alpha-fetoprotein RNAs in adult rat liver: cell type-specific expression and differential regulation. Cancer Res, *51:* 4656-4664, 1991.

97. Yavorkovsky, L., Lai, E., Ilic, Z., and Sell, S. Participation of small intraportal stem cells in the restitutive response of the liver to periportal necrosis induced by allyl alcohol. Hepatology, *21:* 1702-1712, 1995.

98. Webber, E. M., Godowski, P. J., and Fausto, N. In vivo response of hepatocytes to growth factors requires an initial priming stimulus. Hepatology, *19:* 489-497, 1994.

99. Wuestefeld, T., Klein, C., Streetz, K. L., Betz, U., Lauber, J., Buer, J., Manns, M. P., Muller, W., and Trautwein, C. Interleukin-6/glycoprotein 130-dependent pathways are protective during liver regeneration. J Biol Chem, *278:* 11281-11288, 2003.

100. Blindenbacher, A., Wang, X., Langer, I., Savino, R., Terracciano, L., and Heim, M. H. Interleukin 6 is important for survival after partial hepatectomy in mice. Hepatology, *38:* 674-682, 2003.

101. Webber, E. M., Bruix, J., Pierce, R. H., and Fausto, N. Tumor necrosis factor primes hepatocytes for DNA replication in the rat. Hepatology, *28:* 1226-1234, 1998.

102. Yamada, Y. and Fausto, N. Deficient liver regeneration after carbon tetrachloride injury in mice lacking type 1 but not type 2 tumor necrosis factor receptor. Am J Pathol, *152:* 1577-1589, 1998.

103. Yamada, Y., Kirillova, I., Peschon, J. J., and Fausto, N. Initiation of liver growth by tumor necrosis factor: Deficient liver regeneration in mice lacking type I tumor necrosis factor receptor. Proc Natl Acad Sci U S A, *94:* 1441-1446, 1997.

104. Yamada, Y., Webber, E. M., Kirillova, I., Peschon, J. J., and Fausto, N. Analysis of liver regeneration in mice lacking type 1 or type 2 tumor necrosis factor receptor: requirement for type 1 but not type 2 receptor. Hepatology, *28:* 959-970, 1998.

105. Sakamoto, T., Liu, Z., Murase, N., Ezure, T., Yokomuro, S., Poli, V., and Demetris, A. J. Mitosis and apoptosis in the liver of interleukin-6-deficient mice after partial hepatectomy. Hepatology, *29:* 403-411, 1999.

106. Galun, E., Zeira, E., Pappo, O., Peters, M., and Rose-John, S. Liver regeneration induced by a designer human IL-6/sIL-6R fusion protein reverses severe hepatocellular injury. Faseb J, *14:* 1979-1987, 2000.

107. Camargo, C. A., Jr., Madden, J. F., Gao, W., Selvan, R. S., and Clavien, P. A. Interleukin-6 protects liver against warm ischemia/reperfusion injury and promotes hepatocyte proliferation in the rodent. Hepatology, *26:* 1513-1520, 1997.

108. Braun, L., Gruppuso, P., Mikumo, R., and Fausto, N. Transforming growth factor beta 1 in liver carcinogenesis: messenger RNA expression and growth effects. Cell Growth Differ, *1:* 103-111, 1990.

109. Nguyen, L. N., Furuya, M. H., Wolfraim, L. A., Nguyen, A. P., Holdren, M. S., Campbell, J. S., Knight, B., Yeoh, G. C., Fausto, N., and Parks, W. T. Transforming growth factor-beta differentially regulates oval cell and hepatocyte proliferation. Hepatology, *45:* 31-41, 2007.